THE UNIVERSITY OF MICHIGAN

INDUSTRY PROGRAM OF THE COLLEGE OF ENGINEERING

KINETICS OF THE NON-ISOTHERMAL PYROLYSIS OF PROPANE

Lester S. Kershenbaum

A dissertation submitted in partial fulfillment
of the requirements for the degree of
Doctor of Philosophy in the
University of Michigan
Department of Chemical and Metallurgical Engineering
1964

December, 1964

IP-687

ACKNOWLEDGEMENTS

The author wishes to express his appreciation to all those persons who have aided in this investigation. In particular, he wishes to acknowledge the guidance and encouragement of Professor Joseph J. Martin who suggested the topic of this research and served as chairman of the doctoral committee. The interest and suggestions of Professors R. B. Bernstein, R. H. Kadlec, G. Parravano, R. C. Taylor and J. L. York were also appreciated.

The author wishes to thank the Procter and Gamble Company, the Horace H. Rackham School of Graduate Studies and the National Science Foundation who made this work possible through their financial assistance.

Special thanks are due to Mr. Frank Drogosz and his staff in the Instrumental Analysis Laboratory for performing the sample analysis and to Mr. Grant Fisher and Professor R. H. Kadlec for helping the author to master the use of the analog computer.

Finally, the author would like to express his thanks to his wife for typing the first draft of this manuscript and to the Industry Program of the College of Engineering for preparing the manuscript in its final form.

TABLE OF CONTENTS

TABLE OF CONTENTS (CONT'D)

LIST OF TABLES

LIST OF FIGURES

LIST OF FIGURES (CONT'D)

LIST OF APPENDICES

ABSTRACT

The purpose of this research was to study the kinetics of the pyrolysis of propane at high temperatures (800° - 1000°C). At these temperatures, the rates of the various reactions are so high that a batch or even an isothermal flow experiment is impossible. Since the rate constants are temperature dependent, a method was devised which analyzed the data resulting from non-isothermal, non-isobaric, flow experiments.

The reaction gases flowed through the annulus of a ceramic reactor which was contained in an electric furnace; temperatures were measured by a movable thermocouple located in the central tube of the reactor. To keep the conversions low so that the initial stages of decomposition could be studied, the feed gas was diluted with varying amounts of nitrogen. The reactor exit gas was analyzed by mass spectrometry.

The major products of propane decomposition were found to be propylene, hydrogen, ethylene and methane, and could be represented stoichiometrically by

$$C_3H_8 \rightarrow C_3H_6 + H_2$$

$$C_3H_8 \rightarrow C_2H_4 + CH_4$$

although the reactions are actually free radical in nature. The secondary and minor products found were acetylene, methylacetylene, ethane, butane and carbon.

The overall disappearance of propane and the two major reactions above were found experimentally to be of the first order.

The rate constants were evaluated in each case, assuming an Arrhenius-type temperature dependence, $k = Ae^{-E/RT}$, where A is the pre-exponential factor in (sec^{-1}) and E is the activation energy in (K cal/g-mole). Over this temperature range, the overall propane decomposition is represented by $k = (2.40 \times 10^{11}) \exp(-52.1/RT)$; the formation of propylene and hydrogen by $k_1 = (9.26 \times 10^{10}) \exp(-51.7/RT)$; and the formation of ethylene and methane by $k_2 = (1.52 \times 10^{11}) \exp(-52.5/RT)$.

At the highest temperatures, the rate constants for propane disappearance decreased relative to the Arrhenius plot. A series of independent experimental runs was then made to show that this decrease resulted from inhibition of the reaction by propylene —— one of the reaction products.

Finally, a program was devised which could use results of this study to predict conversions and product distributions over a wide range of experimental conditions.

I. INTRODUCTION

A. Objectives of the Research

The main object of this work was to obtain rate constants for the primary reactions involved in the pyrolysis of propane at high temperatures (800° - 1000°F). Although the kinetics of the decomposition of many hydrocarbons have been studied under varied conditions, at these high temperatures little more than product distributions have been obtained. While this information is valuable in designing plants (to produce ethylene and acetylene from paraffins), no insight can be gained about the primary kinetics.

The term "primary reactions" as used above might be, to some extent, a misnomer; for it has been shown fairly conclusively that these reactions are free radical in nature, and hence, the true primary reaction products are free radicals (methyl, ethyl, etc.). However, it is still convenient to refer arbitrarily to the first stable products formed in pyrolysis (i.e., those present at the lowest measurable conversions) as the "primary products of reaction."

At these high temperatures, the rate of reaction is extremely fast; furthermore, the products of reaction themselves decompose under these conditions, tending to mask the primary kinetics. Conversions, therefore, were kept low through the use of a steady state flow system, where residence times can be shorter than in batch systems. Furthermore, the concentration of the reaction products was minimized by diluting the feed gas with nitrogen to about 5 per cent propane. The extent of this dilution was limited though, because the higher the concentration of diluent and the lower the conversion, the more difficult becomes the exit gas analysis.

Since all rate constants are strongly dependent upon temperature, it is most convenient to conduct kinetic experiments isothermally. However, because of the low residence times required, the heating up and cooling down times in this system are far from negligible and a non-isothermal experiment results. Some previous workers have attempted to choose an "equivalent, average temperature," but this procedure leads to far from satisfactory results. The only alternative is to measure the gas temperature profile throughout the reactor, and devise some method of treating the data to yield the desired rate constants. Such was the method used in this study; the gas was passed, at high velocities, through an annular reactor in an electrically heated furnace. The temperature was measured throughout the reactor with a movable thermocouple.

The calculations required in obtaining kinetic data from nonisothermal experiments become quite complicated, and a digital computer was employed extensively in processing the data. Once the rate constants were obtained, the kinetic model was programmed on an analog computer; it was then possible to test the consistency of the data, and to predict product distributions, conversions, etc., for any arbitrary set of conditions. This is extremely valuable if similar studies are made for the other low hydrocarbons which are products of propane pyrolysis. Then the entire series could be studied simultaneously; i.e., product distributions could be predicted not only for the simple case of low conversions, but also for the more complicated cases of consecutive reactions where reaction products themselves react further. This could be useful for industrial

operations wishing to optimize production of ethylene (or acetylene, or propylene) from paraffins.

The experimental program was carried out in several stages. First, the primary products of reaction were determined; then the orders of reaction were obtained for each of the reactions involved, and finally the rate constants (with an Arrhenius temperature dependence) were calculated. Although an investigation of the mechanisms involved in these reactions was not a major aim of this work, some runs were made along these lines. However, no attempt was made to discover the actual mechanisms involved; rather this phase of the work was designed to see if the results obtained were consistent with the current free radical theories of hydrocarbon pyrolysis.

Several experiments were run with the addition of propylene (a known free radical inhibitor) in varying concentrations to the propane feed gas. The results obtained were then compared with the available data in the field of hydrocarbon pyrolysis mechanisms.

B. Literature Survey

There is much published information in the literature dealing with the thermal decomposition of hydrocarbons in general, and propane in particular. While there has been a good deal of kinetic work done with propane at lower temperatures (500° - 600°C), none has been done in the temperature range of this study (800° - 1000°C). At high temperatures, some product distribution data are available from commercial plants producing acetylene and olefins from paraffins, but no kinetics are discussed. The difficulty in controlling the extent of the reaction at higher temperatures has, most likely, been the reason for the

unavailability of kinetic data before this time. Low temperature work has also been done on the kinetics of propylene pyrolysis, and there has been considerable research devoted to possible mechanisms for all of these reactions at lower temperatures (500° - 600°C). A brief review of the literature is presented below; comparisons of the literature with the results of this work will be given, whenever applicable, in the section discussing the experimental results.

The data available on product distributions over a wide range of temperatures (500° - 900°C) all agree that the main reaction products are methane, ethylene, propylene and hydrogen. Most of these data are from commercial and pilot plant processes for producing ethylene, acetylene, and/or aromatics from paraffins. High temperature, non-catalytic processes are described by Akin, Reid and Schrader;[1] Farnsworth, et al.;[16] Linden and Peck;[33] Schutt;[56] Bixler and Coberly;[5] Eastwood and Potas;[13] and Reid and Linden.[49] Some of the earliest work in this area was done by Pease[44] and Frey and Smith[19] at lower temperatures (500° - 600°C) and gives product distributions in that range.

There is not as much agreement among the authors regarding minor and secondary products of reaction, probably because the extent of reaction has a strong influence on their formation and subsequent decomposition. Most of the sources above used a pure hydrocarbon feed and relatively long residence times (on the order of seconds), to maximize conversion to useful products. Some secondary products found were ethane, butane, butylene, butadiene, acetylene and benzene. Akin et al.,[1] and Farnsworth et al.[16] note that acetylene formation is not appreciable

(because of thermodynamic considerations) below 1100°C. Akin et al.[1] and Pretsch[48] are the only researchers to detect the presence of methylacetylene, C_3H_4, as a secondary reaction product. Eastwood and Potas[13] used, as their reactor, a non-catalytic pebble heater, while Calderbank et al.[10] and Deansley and Watkins[11] ran autothermic cracking units, i.e., those in which the hydrocarbon feed is mixed with air. The heat of reaction is thereby supplied by the partial combustion of the hydrocarbon.

There has been, on the other hand, considerable work done on the kinetics of propane pyrolysis at lower temperatures (500° - 600°C). The results of earliest researchers are reviewed in books by Dunsten[12] and Egloff.[14] Most workers have found the reactions to be homogeneous and of the first order, although recent mechanism studies seem to indicate otherwise. Arrhenius rate constants have been obtained in this temperature range for the overall decomposition of propane by Hepp and Frey,[23] Marek and McCleur,[34] Paul and Marek,[42] Peard et al.,[43] Laidler et al.,[29] and Steacie and Puddington.[58] Most of these workers ran their experiments at low conversions to minimize the complications of consecutive reactions. None of them, however, attempted to give rate expressions for the individual reactions other than saying that the two major reactions,

$$C_3H_8 \rightarrow C_2H_4 + CH_4$$

$$C_3H_8 \rightarrow C_3H_6 + H_2 \quad ,$$

were of approximately equal importance. Others who studied the kinetics of propane pyrolysis, but did not arrive at rate expressions were Kinney and Crowley,[26] Blackmore and Hinshelwood,[6] Martin et al.,[35] and Stubbs et al.[59]

An enormous amount of work has been done in the past on possible mechanisms for the pyrolysis of propane and hydrocarbons in general. Indeed, so many problems and inconsistencies remain that present-day chemists are still in conflict over the true mechanisms involved. All of the experimental work has been done at moderately low temperatures (500° - 600°C), to facilitate observation of the initial stages of reaction. The earliest research on free radical mechanisms was done by Rice and Herzfeld,(50) Rice and Polly,(51) Rice and Polly,(52) Rice and Teller,(53) Hobbs and Hinshelwood,(24) Steacie and Parlee,(57) and Kossiakoff and Rice.(28) Eltenton(15) attempted to study reaction mechanisms by detecting reaction intermediates with a mass spectrometer. Experiments with addition of free radical chain inhibitors have been performed by Partington,(41) Wojciechowski and Laidler,(65) Stubbs et al.,(59) and Laidler et al.(29) Because inhibitors only reduced the rate of reaction and did not stop it entirely, some researchers felt that the mechanism consisted of two segments: one free radical and one molecular (see Peard et al.(43) and Stubbs et al.(59)). Subsequent work with radioactive isotopes tends to contradict that possibility; discussion of these experiments has been presented by Voevodsky,(64) Poltorak and Voevodskii,(46) Medvedeva et al.,(36) Medvedeva et al.,(37) Neiman,(40) and Rice and Varnerin.(54)

The role of the surface in these reactions and the subsequent effect upon the mechanism have been studied recently by Voevodsky,(64) Martin et al.,(35) and Poltorak et al.(47) However, the question of a completely homogeneous mechanism versus a partly homogeneous, partly heterogeneous mechanism has yet to be settled satisfactorily.

Some work has been done on the various equilibria associated with propane decomposition. Among these are the papers of Frey and Huppke,[18] Kistiakowsky and Nickle,[27] Myers and Watson,[39] and Pretsch.[48] These works, along with tabulated thermodynamic data published by the API[55] and ASTM,[3] give important equilibrium constants and free energies for many relevant systems.

The pyrolysis of propylene has likewise been studied at moderate temperatures (600° - 800°C) in order to obtain product distributions and kinetic data. Tropsch, Parrish and Egloff[63] give some product distributions, and Szwarc[60] calculates the rate expressions for low conversions. Ingold and Stubbs,[25] and Laidler and Wojciechowski[30] hypothesize mechanisms to substantiate their observations that the order of reaction is 1.0 and 1.5, respectively.

Shock waves have been used by Miller[38] and Greene et al.[22] to study the pyrolysis of hydrocarbons, but no work seems to have been done with propane as the starting material.

II. THEORY

A. General Introduction

When hydrocarbons are thermally decomposed at high temperatures, they usually split into lower hydrocarbons, carbon and/or hydrogen; there is a tendency, in addition, towards polymerization into higher hydrocarbons, especially if the starting material is an olefin.

Past work has shown that, over a wide range of conditions, the main reaction products of propane pyrolysis are methane, ethylene, propylene and hydrogen. Although it is well known that these are not molecular reactions but free radical in nature, it is convenient to stoichiometrically represent them as

$$C_3H_8 \rightarrow C_3H_6 + H_2$$
$$C_3H_8 \rightarrow C_2H_4 + CH_4$$

Since the products are apt to decompose further, it would be helpful to define the "primary" products as the first products formed. As mentioned earlier, in this case the first materials formed are free radicals, and they react to form all subsequent products. Thus, for convenience, the definition of primary products arbitrarily becomes "those stable products present in appreciable quantities at the lowest attainable conversions."

B. Thermodynamic Considerations

All chemical reactions are limited from thermodynamic and equilibrium considerations; it is therefore important to investigate the thermodynamics of a system before studying the kinetics of the corresponding reactions. The main equilibria pertinent to this study are:

$$C_3H_8 \rightleftharpoons C_3H_6 + H_2 \quad (1)$$

$$C_3H_8 \rightleftharpoons C_2H_4 + CH_4 \quad (2)$$

$$C_2H_4 \rightleftharpoons C_2H_2 + H_2 \quad (3)$$

$$C_3H_6 \rightleftharpoons C_3H_4 + H_2 \quad (4)$$

Equations (1) and (2) stoichiometrically represent the decomposition of propane, while (3) and (4) represent possible further decomposition of the reaction products, ethylene and propylene. The equilibrium constants were calculated from the thermodynamic data of the API Research Project #4(55) listed below in Table I; they are plotted against reciprocal temperature in Figure 1.

TABLE I

THERMODYNAMIC DATA FOR HYDROCARBONS AT 1200°K

	ΔH_f° [Kcal/g-mole]	ΔF_f° [Kcal/g-mole]	ΔS_f° [cal/g-mole-°K]
H_2	0	0	0
CH_4	-21.79	9.85	-26.37
C_2H_6	-25.64	36.45	-51.74
C_3H_8	-31.16	61.01	-76.81
C_4H_{10}	-37.46	84.85	-101.92
C_2H_4	8.88	32.09	-19.34
C_3H_6	-0.32	52.15	-43.72
$1\text{-}C_4H_8$	-6.26	76.74	-69.17
C_2H_2	53.00	38.09	+12.42
C_3H_4	41.19	56.46	-12.72

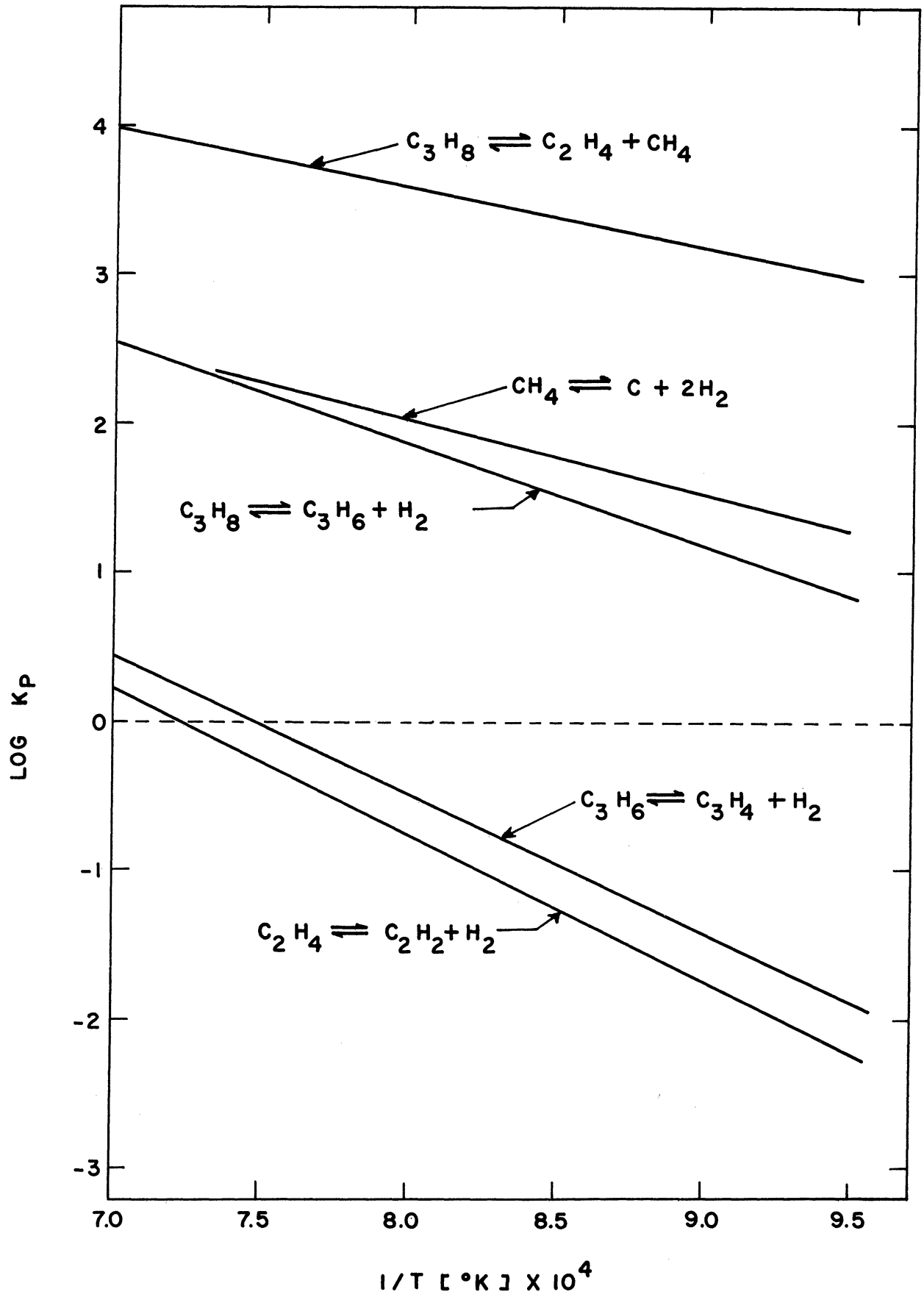

Figure 1. Equilibrium Constants [Atm] for Several Reactions.

From Figure 1 it can be seen that there is little tendency for the reaction products of propane to recombine above about 800°C. (This fact is proven quantitatively in Appendix C.) On the other hand, reaction products ethylene and propylene do not tend to undergo further decomposition below about 1000°C. Equilibrium considerations, of course, only place limits on the extent of each reaction; the amounts of the actual products formed will depend upon the kinetics of the reactions.

C. Steps in the Experimental Program

The theoretical bases for this study will be developed in the forthcoming sections. In order to tie the theory in with the experimental aspect of the work, a brief description of the experimental program now follows.

In all runs, the feed (hydrocarbon diluted with nitrogen) is passed through the heated reactor at high linear velocities. The inlet is near room temperature and the exit gas is quenched close to room temperature by a cold air blast. The temperature throughout the length of the reactor is measured by a thermocouple which is slowly driven through the reactor. A typical temperature profile is shown in Figure 2.

Because of the high reaction rates at these elevated temperatures, the residence times must be kept short in order to prevent complete decomposition. Mechanical and heat transfer limitations therefore make it impossible to approach a square temperature profile, i.e., one with instantaneous heating and cooling. The assumption of an average, equivalent temperature has been made by some researchers in the past, but this usually yields unsatisfactory results. (Although obtaining a truly equivalent temperature is possible, it is a complicated, trial and error process and is outlined in Appendix D.)

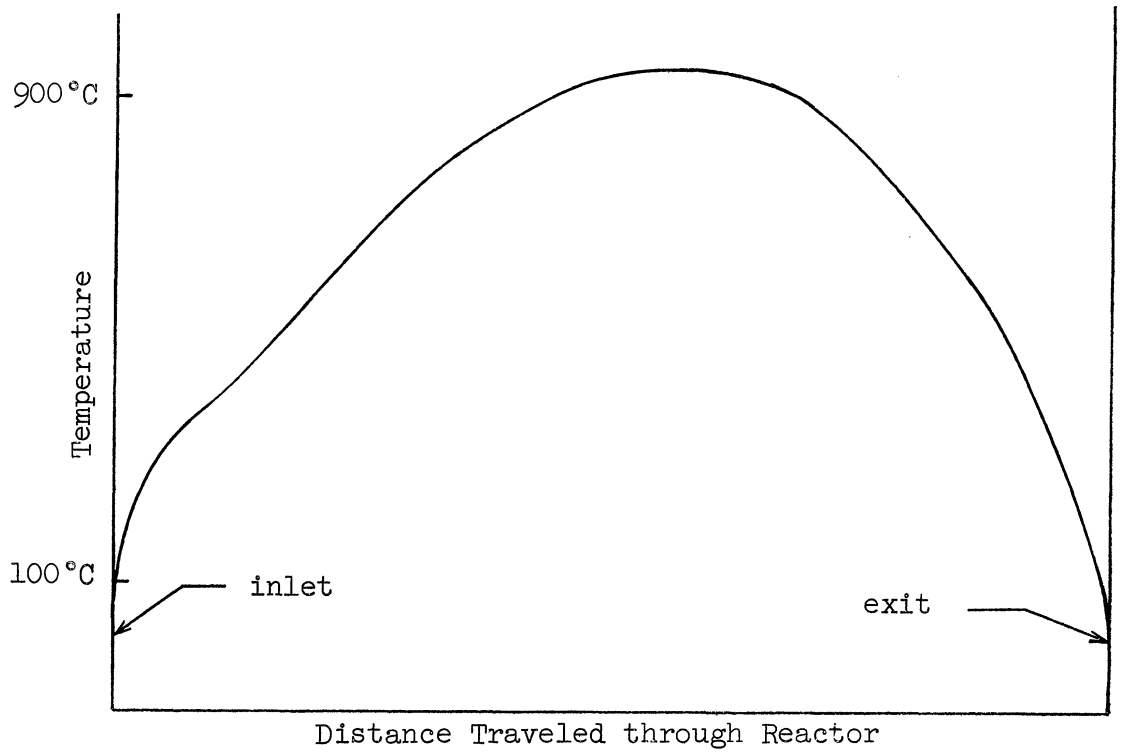

Figure 2. Typical Temperature Profile.

Although isothermal kinetic experiments are convenient (obtaining the kinetic parameters becomes relatively simple), it is possible to obtain the same results -- but not as easily -- from non-isothermal experiments. In this work, no attempt was made to alter the shape of the temperature profile; rather, the existing profile was accurately measured and used in the determination of rate constants as outlined below.

On this basis, experimental runs could be made to yield a) data on product distribution and differentiation between primary and secondary products; b) information about the orders of the various reactions involved; c) the rate constants for each of these reactions once the order of reaction is known.

D. Product Distribution

The primary reaction products have been defined above as those products present in appreciable quantities at the lowest conversions of feed. To determine which products are primary, a set of runs can be made in which the temperature profile and total flow rate are kept constant. Varying the mole fraction of propane in the feed should cause a change in the overall propane conversion. If the percentage conversion to each product is then plotted against the overall propane conversion, those products present at the lowest conversions (or after extrapolation to zero conversion) are the primary reaction products.

E. Determination of Orders of Reaction

The order of a chemical reaction can be calculated theoretically when a mechanism for the reaction is hypothesized. This is especially true in free radical, hydrocarbon pyrolysis, where slight changes in a mechanism theory will alter the calculated order of reaction. (This will be illustrated later, and in greater detail in Appendix H.) Usually, a mechanism is chosen which will explain any puzzling experimental results.

The question of how to determine empirically the orders of reaction in a non-isothermal experiment thus arises. The procedure is quite similar to that of an isothermal experiment and is outlined below.

For an irreversible reaction,

$$C_3H_8 \longrightarrow \text{Products},$$

which takes place in a flow reactor, the overall rate can be expressed as

$$-\frac{dm}{dV} = kC^n \qquad (5)$$

where

m is the flow rate of propane (g-moles/sec)

V is the reactor volume (liters)

n is the order of reaction

C is the concentration of propane (g-moles/liter)

k is the rate constant ($\text{liter}^{n-1}/\text{g-mole}^{n-1} \cdot \text{sec}$)

If an Arrhenius type rate constant is assumed, in a non-isothermal reactor,

$$-\frac{dm}{dV} = Ae^{-E/RT(\ell)}C^n \tag{6}$$

where

A is the pre-exponential factor ($\text{liter}^{n-1}/\text{g-mole}^{n-1} \cdot \text{sec}$)

E is the activation energy (Kcal/g-mole)

$T(\ell)$ is the temperature profile (°K)

R is the gas constant (Kcal/g-mole·°K)

At pressures near atmospheric, the ideal gas law can be used to express the concentration C as

$$C = \frac{xP(\ell)}{RT(\ell)} \tag{7}$$

where

x is the mole fraction of propane

$P(\ell)$ is the pressure profile (mm Hg)

R is the gas constant $\left(\frac{\text{liter-mm Hg}}{\text{g-mole}\cdot{}^\circ\text{K}}\right)$

Then, in a reactor with constant cross-section,

$$dV = sd\ell \tag{8}$$

where

s is the cross-sectional area (meters^2)

ℓ is the reactor length (mm) to give volume in liters

Substituting (7) and (8) in (6)

$$-\frac{dm}{sd\ell} = Ae^{-E/RT(\ell)} \left[\frac{xP(\ell)}{RT(\ell)}\right]^n \qquad (9)$$

For small conversions of propane, the mole fraction x will not change appreciably throughout the reactor; the arithmetic average $\bar{x}$ can be used upon integration to yield

$$\Delta m = \bar{x}^n \left[\frac{sA}{R^n} \int_o^L e^{-E/RT(\ell)} \left(\frac{P(\ell)}{T(\ell)}\right)^n d\ell\right] \qquad (10)$$

Note that for a set of runs at identical temperature profiles and flow rates (and hence pressure profiles) the entire term within the brackets in Equation (10) is a constant.

Then, a logarithmic plot of Δm (which is actually the rate of propane disappearance) versus the average propane mole fraction should yield a straight line of slope n,

$$\text{Log } (\Delta m) = n \text{ Log } (\bar{x}) + \text{Log (Const.)} \qquad (11)$$

The same analysis applies just as easily to any of the individual reactions in the decomposition of propane. In that case the rate of reaction can be expressed as

$$\frac{dm_1}{dV} = kC^{n_1} \qquad (12)$$

where, now, m_1 is the flow rate (g-moles/sec) of any of the reaction products. The identical analysis leads, instead, to Equation (13),

$$\text{Log } (\Delta m_1) = n_1 \text{ Log } (\bar{x}) + \text{Log (Const.)} \qquad (13)$$

where Δm_1 is simply the rate of formation of that reaction product.

It is interesting to note that such a procedure for obtaining reaction orders corresponds exactly to the procedure in an isothermal experiment. There, the common method of obtaining reaction orders is to plot (for a series of runs at the same temperature) the logarithm of the reactant concentration versus the logarithm of the rate of reaction. The slope of the resulting line is the order of reaction. One would have expected this method to apply to the non-isothermal case as well, since the identical temperature profiles were achieved for the entire series of runs.

Discussions of similar derivations for order of reaction determination have been presented by Lee and Oliver[31] and Towell.[61]

F. Evaluation of Rate Constants in Non-Isothermal Experiments

Once the order of reaction is known, some stoichiometric relationship must be postulated to obtain the rate constant. Assuming an irreversible decomposition

$$A \rightarrow B + C$$

the rate of decomposition of A has been expressed by Equation (9) above

$$-\frac{dm}{sd\ell} = Ae^{-E/RT(\ell)} \left[\frac{xP(\ell)}{RT(\ell)}\right]^n \qquad (9)$$

Now, if F and N_o are the initial feed rates (g-moles/sec) of propane and nitrogen, respectively, and z is the fractional conversion of propane, then at any point in the reactor,

$$m = F(1-z)$$

and

$$dm = -F\,dz \qquad (14)$$

Because of the stoichiometry of the reaction (1 mole reactant $\rightarrow$ 2 moles product) the mole fraction, x, of propane is

$$x = \frac{F(1-z)}{F(1+z) + N_o} \tag{15}$$

Substituting (14) and (15) in Equation (9)

$$\frac{F}{s}\frac{dz}{d\ell} = Ae^{-E/RT(\ell)} \left[\frac{P(\ell)}{RT(\ell)}\right]^n \left[\frac{1-z}{1 + N_o/F + z}\right]^n$$

or

$$\frac{F}{s}\left[\frac{1 + N_o/F + z}{1 - z}\right]^n dz = \frac{A}{R^n} e^{-E/RT(\ell)} \left[\frac{P(\ell)}{T(\ell)}\right]^n d\ell \tag{16}$$

Equation (16) can be integrated along the length of the reactor from 0 to L and from conversions 0 to z_e to yield

$$\frac{F}{s}\int_o^{z_e} \left[\frac{1 + N_o/F + z}{1 - z}\right]^n dz = \frac{A}{R^n}\int_o^L e^{-E/RT(\ell)} \left[\frac{P(\ell)}{T(\ell)}\right]^n d\ell \tag{17}$$

or

$$A = \frac{\frac{FR^n}{s}\int_o^{z_e} \left[\frac{1 + N_o/F + z}{1 - z}\right]^n dz}{\int_o^L e^{-E/RT(\ell)} \left[\frac{P(\ell)}{T(\ell)}\right]^n d\ell} = \varphi(E) \tag{18}$$

Since the temperature and pressure profiles, $T(\ell)$ and $P(\ell)$ will be known graphically, the lower integral in Equation (18) will have to be evaluated by some numerical method; calculations showed that Simpson's rule was more than satisfactory and the data did not warrant a more sophisticated treatment.

The upper integral in Equation (18) can likewise be handled by Simpson's rule. However, when n is either an integer or half-integer,

that integral can be evaluated algebraically. The integrations are performed using formulae #39, 41, 113 and 115 of Peirces' Tables.(45)

For values of $n = 1$, 2, and 1.5 the results are

$$\int_0^{z_e} \frac{1 + N_o/F + z}{1 - z}\, dz = -z_e - \left(2 + \frac{N_o}{F}\right) \mathrm{Ln}\,(1 - z_e) \qquad (19)$$

$$\int_0^{z_e} \left(\frac{1 + N_o/F + z}{1 - z}\right)^2 dz = \frac{(1 + N_o/F + z_e)^2}{1 - z_e} + 2\left[z_e + \left(2 + \frac{N_o}{F}\right) \mathrm{Ln}(1 - z_e)\right] - \left(1 + \frac{N_o}{F}\right)^2 \qquad (20)$$

$$\int_0^{z_e} \left(\frac{1 + N_o/F + z}{1 - z}\right)^{1.5} = \frac{2(1 + N_o/F + z_e)^{1.5}}{\sqrt{1 - z_e}} + 3\sqrt{(1 + N_o/F + z_e)(1 - z_e)} - 3\left(2 + \frac{N_o}{F}\right) \mathrm{Tan}^{-1}\sqrt{\frac{1 + N_o/F + z_e}{1 - z_e}} - 2\left(1 + \frac{N_o}{F}\right)^{1.5} - 3\sqrt{1 + N_o/F} + 3\left(2 + \frac{N_o}{F}\right) \mathrm{Tan}^{-1}\sqrt{1 + \frac{N_o}{F}} \qquad (21)$$

Although Equations (19) - (21) apply to almost all the important orders of reaction, it will be more general to refer to Equation (18) in integral form. Since the actual calculations were performed on a digital computer, no inconvenience was encountered by evaluating both integrals of Equation (18) numerically.

Returning to Equation (18), it is noted that L and s are the dimensions of the reactor and F, N_o, z, $T(\ell)$ and $P(\ell)$ are experimental data. Therefore, once the order of reaction n has been determined as outlined in Section II-E, the pre-exponential factor, A, is merely a function of the activation energy, E.

A similar equation results if, rather than the overall propane decomposition rate constant, one of the individual rate constants is desired. For instance, consider the simultaneous decomposition of A by two parallel reactions:

$$A \xrightarrow{k_1} B + C$$

$$A \xrightarrow{k_2} D + E$$

where the orders of reaction have been determined to be n_1 and n_2. If the total conversion of A is denoted by z, the conversion to B is βz and the conversion to D is δz, where β and δ are fractions whose sum is unity. Then, the Arrhenius parameters for the individual reactions become

$$A_1 = \frac{\frac{FR^{n_1}}{s}\beta \int_o^{z_e} \left[\frac{1 + N_o/F + z}{1 - z}\right]^{n_1} dz}{\int_o^L e^{-E_1/RT(\ell)} \left[\frac{P(\ell)}{T(\ell)}\right]^{n_1} d\ell} \tag{22}$$

$$A_2 = \frac{\frac{FR^{n_2}}{s}\delta \int_o^{z_e} \left[\frac{1 + N_o/F + z}{1 - z}\right]^{n_2} dz}{\int_o^L e^{-E_2/RT(\ell)} \left[\frac{P(\ell)}{T(\ell)}\right]^{n_2} d\ell} \tag{23}$$

The expressions reduce to this relatively simple form because both of the parallel reactions have one reactant yielding two products. Derivations of similar expressions in the more general cases will be found in Appendix F.

G. Determination of the "Best Values" of the Rate Constants

1. The Pairing Method

The remaining task is to obtain the rate constants for the overall decomposition from Equation (18) or for any of the individual

reactions from Equations (22) or (23). It is obvious that no single set of data will be sufficient to solve Equation (18) for the kinetic parameters A and E.

$$A = \frac{\frac{FR^n}{s}\int_0^{z_e}\left[\frac{1 + N_o/F + z}{1 - z}\right]^n dz}{\int_0^L e^{-E/RT(\ell)}\left[\frac{P(\ell)}{T(\ell)}\right]^n d\ell} = \varphi(E) \qquad (18)$$

A first thought would be to use the data of two distinct experimental runs to solve the two resulting equations simultaneously for A and E. Since the equations are explicit in A, it is relatively simple to select a series of values for E and solve for A in each of the cases, although the numerical integration requires the use of a digital computer. The solution is obtained when for a certain E, the value of A for both runs is identical. Practically, this is best done by plotting $A = \varphi(E)$ for both of the runs and noting the point of intersection. Conveniently, the functional relationship is such that a plot of log A versus E is always a fairly good straight line; this permits the determination of the exact point of intersection analytically. Runs (1) and (2) in Figure 3 are a typical illustration of this method.

Unfortunately, when two other runs are paired, substantially different values of A and E result. Thus, it becomes important to devise some method of obtaining the best value of A and E for all the runs.

Towell[61] developed the following method for treating the data. A pair of runs is used to calculate the kinetic parameters for

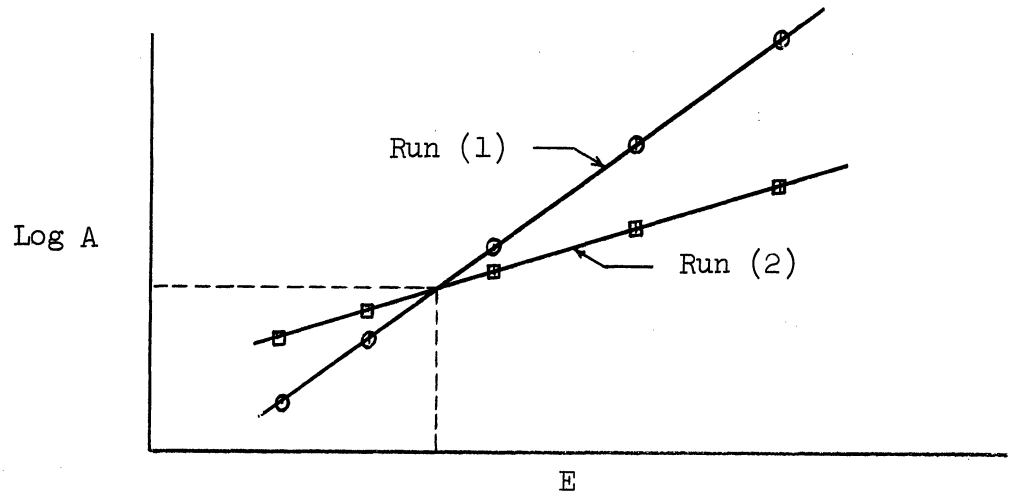

Figure 3. Pairing Method Illustration.

that pair. Then, for every run, the maximum rate constant,

$$k_{max} = Ae^{-E/RT_{max}} \tag{24}$$

is calculated. The calculated values of k_{max} for each run are used in an Arrhenius plot of log k_{max} versus $1/T_{max}$ as illustrated schematically in Figure 4.

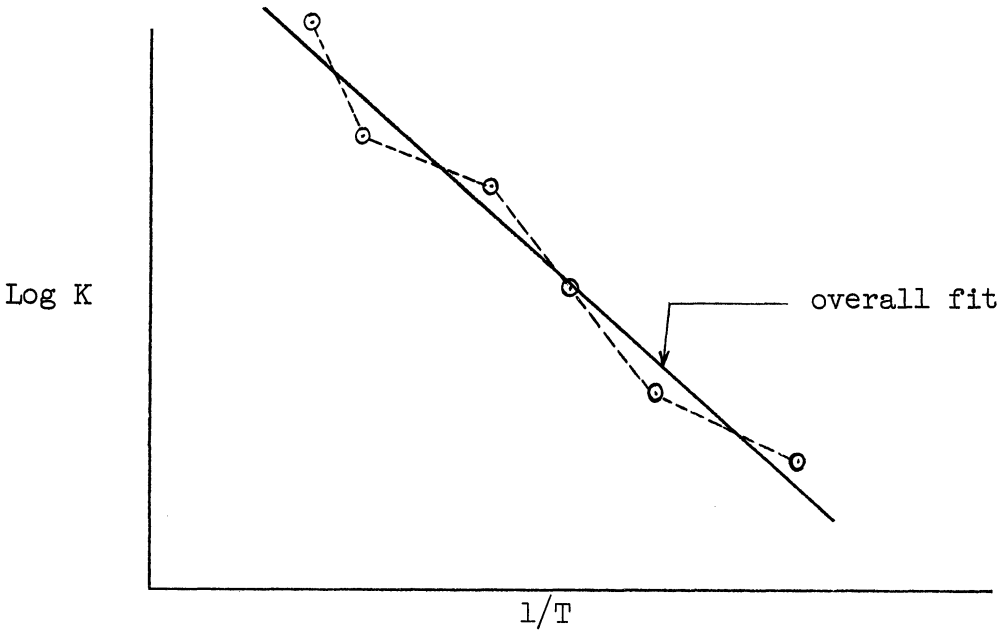

Figure 4. Data Smoothing in the Pairing Method.

Note that although the values of E (slopes of the connecting lines) and A (intercepts of the lines) differ considerably from pair to pair, the overall fit represents the data quite well. The slope and intercepts of the line which is a least squares fit of the data will yield the "best" values of E and A, respectively.

Unfortunately, there is one very serious drawback to this method: depending upon how the points (data runs) are paired, different values of the kinetic parameters can result. Figure 5 illustrates schematically the reason for this discrepancy.

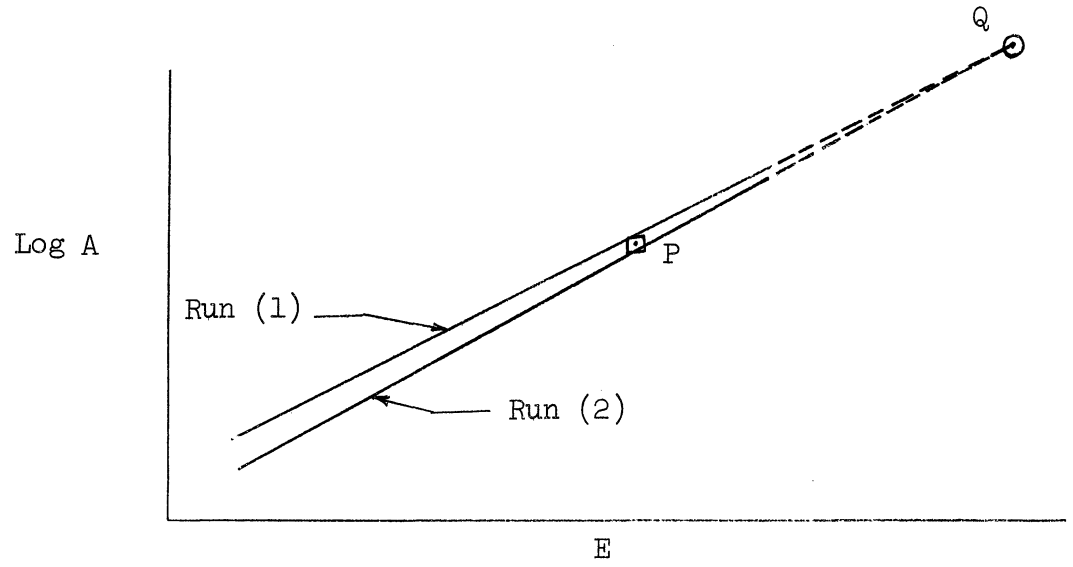

Figure 5. Errors Introduced by the Pairing Method.

Suppose a pairing between two runs which were made under similar conditions of temperature and pressure. Now Equation (18) above represents a functional relationship between A and E for a given set of conditions (F, N_o, $P(\ell)$, $T(\ell)$, etc.). If one attempts to solve Equation (18) simultaneously for two runs which do not differ greatly, the resulting functions should be quite similar. Thus, in Figure 5, if the point P

represents the "true" value of E and A, the functions obtained from Runs (1) and (2) are both satisfied (within the limits of experimental error) by the true value. However, if the two are paired, the intersection point, Q, is considerably in error. Thus, depending upon how the paired runs are chosen, there can be much variation in the final average values of E and A.

It should be possible, it was reasoned, to find the best values of the kinetic parameters in a one-step treatment of the data -- rather than by pairing them two runs at a time and smoothing those results. Four possible methods were found, two acceptable and two unacceptable. These methods will be outlined briefly here, and the complete derivations can be found in Appendix G.

2. Use of Steepest Descent Method

A straightforward direct attack on the problem at once presents itself. Each experimental run generates a functional relationship from Equation (18). If there are N such runs,

$$\begin{aligned} A &= \varphi_1(E) \\ A &= \varphi_2(E) \\ &\cdot \quad\quad \cdot \\ &\cdot \quad\quad \cdot \\ &\cdot \quad\quad \cdot \\ A &= \varphi_N(E) \end{aligned} \tag{25}$$

The best values for A and E are those for which the sum of the squares of deviations from Equation (25) over all the runs is a minimum. In mathematical notation, it is desired to find the values of A and E such that

$$\Delta = \sum_{i=1}^{N} [\varphi_i(E) - A]^2 \tag{26}$$

is a minimum. This, of course, requires a two-dimensional search over a matrix of possible A and E values. The method of steepest descent works well in this type of problem. A trial point (E_1, A_1) is chosen and Δ_1 is computed from Equation (26). The variables E and A are then changed by a small amount to (E_2, A_2) and Δ_2 is computed. When several such changes are made around the initial trial point, it is possible to note the direction in which to move to decrease Δ most rapidly. Thus, arriving at the next trial point, the process is repeated again and again until the minimum Δ is reached.

Although this is an efficient search technique, the Equations (25) are so complicated that this method takes an excessive amount of time, even on a digital computer. Another method of solution is therefore sought.

3. Center of Gravity Method

The next three possible solutions are based upon the observed fact that when any of Equations (25) is plotted as log A versus E, a very good straight line results. This phenomenon (known as the Compensation Effect) has been observed in several instances in the past and is discussed in Appendix L. Figure 6 shows five straight lines which could represent five experimental runs in the form of Equations (25).

The center of gravity method states that the best values of E and A is that point in Figure 6, for which the sum of the squares of the distances to all the intersection points is a minimum. This turns out to be simply the center of gravity of the intersection points. If there are N runs, there will be $\frac{N(N-1)}{2}$ intersection points. It is shown in Appendix G that if the solution of Equation (18) for the i-th

run is put in the form

$$\text{Log } A = u_i + v_i E \tag{27}$$

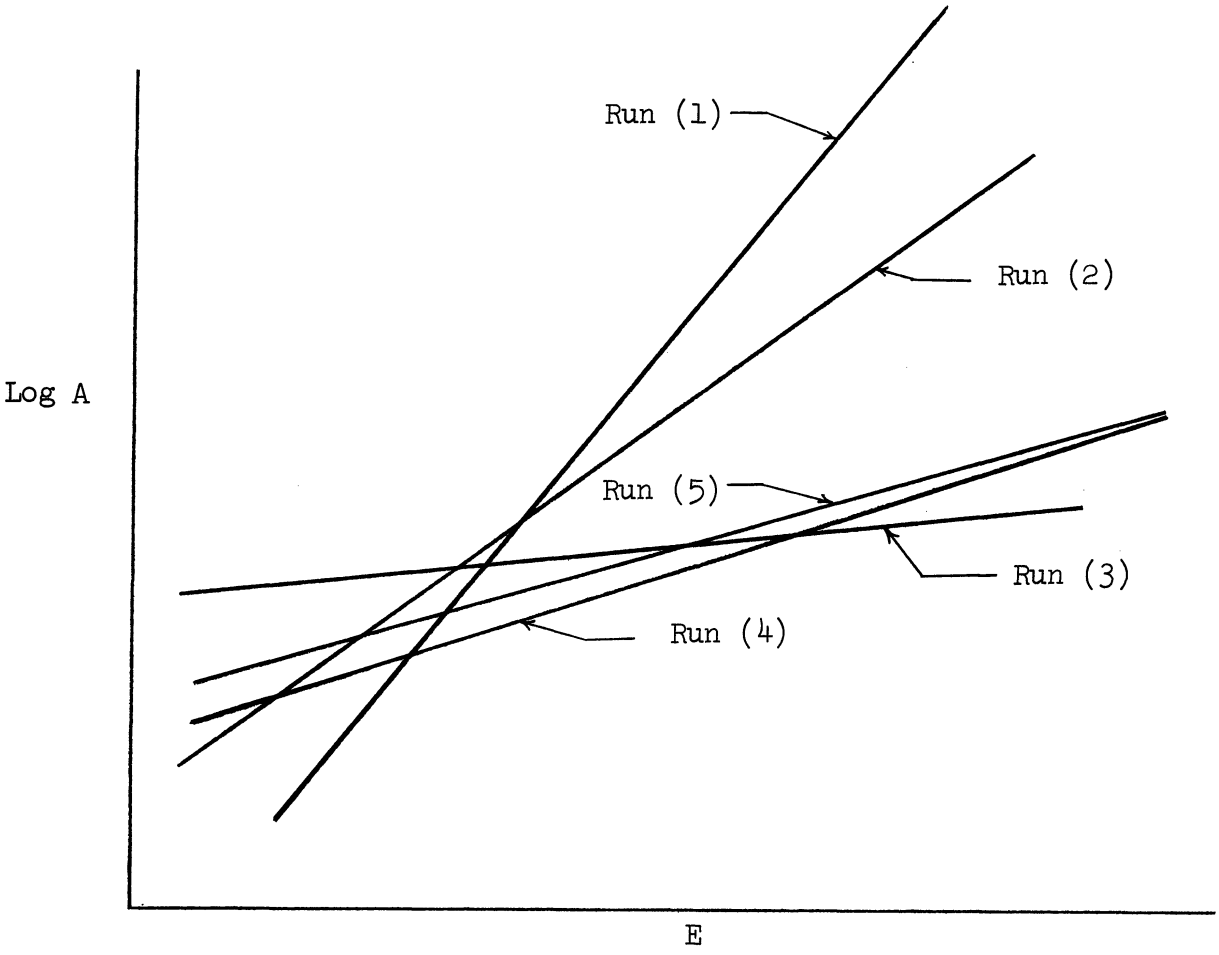

Figure 6. Alternate Solution Methods.

the "best values" for A and E by this method are given by

$$\text{Log } A = \frac{2}{N(N-1)} \sum_{i=1}^{N} \sum_{j=i+1}^{N} \frac{v_j u_i - v_i u_j}{v_j - v_i} \tag{28}$$

$$E = \frac{2}{N(N-1)} \sum_{i=1}^{N} \sum_{j=i+1}^{N} \frac{u_i - u_j}{v_j - v_i} \tag{29}$$

Unfortunately, this method likewise proves unsatisfactory, because it does not eliminate the chief defect of the pairing method

outlined above. Two runs made under similar experimental conditions will be close to parallel as (4) and (5) are in Figure 6. This will weight the average very strongly in the direction of the ultimate intersection of those lines.

4. Minimum Distance Method

A more successful averaging technique is the determination of the point in Figure 6 such that the sum of the squares of the distances to each of the lines is a minimum. This method eliminates the problem associated with nearly parallel lines. Again, if the data of each run are represented in the form of Equation (27), the best values for A and E can be expressed by

$$\text{Log } A = \frac{1}{D_1}\left[\sum_{i=1}^{N}\frac{v_i^2}{v_i^2+1}\sum_{i=1}^{N}\frac{u_i}{v_i^2+1} - \sum_{i=1}^{N}\frac{v_i}{v_i^2+1}\sum_{i=1}^{N}\frac{u_i v_i}{v_i^2+1}\right] \tag{30}$$

$$E = \frac{1}{D_1}\left[\sum_{i=1}^{N}\frac{v_i}{v_i^2+1}\sum_{i=1}^{N}\frac{u_i}{v_i^2+1} - \sum_{i=1}^{N}\frac{u_i v_i}{v_i^2+1}\sum_{i=1}^{N}\frac{1}{v_i^2+1}\right] \tag{31}$$

where

$$D_1 = \sum_{i=1}^{N}\frac{v_i^2}{v_i^2+1}\sum_{i=1}^{N}\frac{1}{v_i^2+1} - \left(\sum_{i=1}^{N}\frac{v_i}{v_i^2+1}\right)^2 \tag{32}$$

The derivations of these relationships are given in Appendix G. This method gave excellent results with all kinds of test data and would have been used if the next method -- Overall Least Squares Analysis -- had not been developed.

5. Overall Least Squares Method

The ultimate in smoothing the data comes with a least squares analysis of all the runs simultaneously. Equation (27), which represents

the experimental results of any single run, can be transposed to yield

$$u_i = \text{Log } A + (-E)\, v_i \tag{33}$$

A series of equations similar to (33) can be written for each run. A least squares analysis can now be performed on $u = \psi(v)$ to yield the best fit through choice of constants A and (-E).

The results (as developed in Appendix G) are:

$$\text{Log } A = \frac{1}{D_2}\left[\sum_{i=1}^{N} u_i \sum_{i=1}^{N} v_i^2 - \sum_{i=1}^{N} u_i v_i \sum_{i=1}^{N} v_i \right] \tag{34}$$

$$E = \frac{1}{D_2}\left[\sum_{i=1}^{N} u_i \sum_{i=1}^{N} v_i - N \sum_{i=1}^{N} u_i v_i \right] \tag{35}$$

where

$$D_2 = N \sum_{i=1}^{N} v_i^2 - \left(\sum_{i=1}^{N} v_i \right)^2 \tag{36}$$

This was the method finally used to calculate the "best" values of E and A for the entire set of data. As might have been expected, the results always agreed very closely with those obtained by the Minimum Distance Method (Number 4 above); there were, however, enormous deviations when compared with results from the Center of Gravity Method (Number 3 above).

All of the preceding discussion was developed for determination of the kinetic parameters for a single reaction, e.g., the overall decomposition of propane. The same derivations apply to any of the individual reactions involved in the overall decomposition, since those data can be put in exactly the same form as that of the overall decomposition. This had been noted before when Equation (18) (for the overall decomposition) was compared with Equations (22) and (23) (for the individual, parallel reactions). A more detailed discussion is presented in Appendix F.

H. Mechanisms

Although the postulation or the determination of mechanisms was not an objective of this work, no kinetic study can be complete without some reference to the mechanisms of reaction. Hydrocarbon pyrolysis was thought to be a simple, molecular reaction until Rice and Herzfeld[50] brought forth their theory of free radical chain reactions. The Rice-Herzfeld mechanism is treated in detail in the current books on Chemical Kinetics, (e.g., Frost and Pearson,[20] Benson,[4] etc.) usually using the decomposition of ethane as a prototype; therefore, only a brief outline of the essential points will be presented here. Some applications have been made to the decomposition of propane, and those will be discussed in somewhat greater detail.

In essence, the Rice-Herzfeld mechanism parallels other kinds of chain reaction mechanisms in that it consists of three steps: chain initiation, chain propagation, and chain termination. In the initiation step, by the breaking of a carbon-to-carbon bond, the reactant is split into two free radicals (either identical or different, depending upon the reactant). The propagation step consists of the decomposition of free radicals to stable molecules plus other free radicals, and reactions between free radicals and stable molecules to yield other free radicals and stable molecules. In the termination step, two radicals combine, producing one or more stable species.

For example, in the case of ethane, some of the main free radical reactions are:

Initiation: $C_2H_6 \rightarrow CH_3 + CH_3$

Propagation: $CH_3 + C_2H_6 \rightarrow CH_4 + C_2H_5$

$C_2H_5 \rightarrow C_2H_4 + H$

$H + C_2H_6 \rightarrow H_2 + C_2H_5$

Termination: $2C_2H_5 \rightarrow C_2H_6 + C_2H_4$

However, there are many more reactions that are of lesser importance which account for some of the minor products of reaction found in the decomposition.

The hypothesis of the Rice-Herzfeld mechanism did not solve all of the difficulties. When free-radical inhibitors such as nitric oxide and propylene are added to the reacting hydrocarbon, the rate of reaction diminishes to some finite, non-zero level. This has led many researchers (e.g., Peard et al.[43] and Stubbs et al.[59]) to believe that, in fact, the decomposition consisted of two mechanisms, one free radical and one molecular. More recent studies with radioactive isotope labeling have disproven that hypothesis, and will be discussed below.

The decomposition of propane, because of its more complex mechanisms, has not been studied nearly as extensively as that of ethane. It is only very recently (1962), that Laidler, Sagert and Wojciechowski[29] have formulated the free radical steps as follows:

Initiation:	C_3H_8	$\rightarrow$	$CH_3 + C_2H_5$	(I)
Propagation:	$C_2H_5 + C_3H_8$	$\rightarrow$	$C_2H_6 + C_3H_7$	(II)
	$H + C_3H_8$	$\rightarrow$	$C_3H_7 + H_2$	(III)
	$CH_3 + C_3H_8$	$\rightarrow$	$C_3H_7 + CH_4$	(IV)
	C_3H_7	$\rightarrow$	$CH_3 + C_2H_4$	(V)
	C_3H_7	$\rightarrow$	$H + C_3H_6$	(VI)
Termination:	$C_3H_7 + CH_3$	$\rightarrow$	$CH_4 + C_3H_6$	(VII)
OR	$2CH_3$	$\rightarrow$	C_2H_6	(VIII)

It has been shown[21] that for free radical reactions, the overall order of reaction is theoretically determined once the mechanisms for the individual steps are hypothesized. In fact, the overall order

of reaction is a function only of the radical initiation and radical termination steps. A table exhibiting this functional dependence is found in Appendix H. Reaction (VII) above leads to first order kinetics; chain termination through step (VIII), on the other hand, leads to 1.5 order kinetics. These derivations are presented in detail in Appendix H. The experimental work of Laidler et al.[29] shows that the overall reaction is first order at high pressures and low temperatures, and 1.5 order at low pressures and high temperatures.

The most recent mechanism studies predict orders of reaction between 1.0 and 1.5, and the older and more empirical work seems to agree, in general. Reference will only be made to those workers who were concerned with primary kinetics and the initial stages of reaction. Stubbs et al.[59] found wide variations in their experimental determination of the overall order of reaction for propane. The average order was approximately 1.5. Blackmore and Hinshelwood[6] studied the entire series of lower paraffins and found them to be of the first order. Medvedeva et al.[36] found that for propane decomposition, the reactions were first order initially, but only for the smallest conversions, inhibition effects then becoming important. Martin et al.,[35] working with propane at approximately 550°C found that, depending upon the extent of reaction, the order varies between 1.2 and 1.3. However, they offer no mechanism to explain their experimental results.

In order to gain further insight into hydrocarbon pyrolysis, many workers studied the inhibition of these reactions by free radical inhibitors, like C_3H_6 and NO. As mentioned above, although the inhibitors reduced the rate considerably, they did not eliminate it

completely. A very early theory on radical inhibition was given by Rice and Polly.[51] They noted two different kinds of free radical inhibitors: a) those which react with the existing free radicals to yield non-reactive stable molecules (e.g., nitric oxide) and b) those which form free radicals themselves, which are not as efficient chain carriers as were the original free radicals (e.g., propylene).

More recent work has attempted to outline the steps in the inhibited reactions. For the inhibition of ethane decomposition by nitric oxide, Wojciechowski and Laidler[65] give:

Initiation: $C_2H_6 + NO \rightarrow C_2H_5 + HNO$

Propagation: $C_2H_5 \rightarrow C_2H_4 + H$

$H + C_2H_6 \rightarrow C_2H_5 + H_2$

$H + NO \rightleftharpoons HNO$

Termination: $C_2H_5 + HNO \rightarrow C_2H_6 + NO$

OR $H + HNO \rightarrow H_2 + NO$

For the inhibition of hydrocarbon decomposition, in general, by propylene, Laidler and Wojciechowski[30] propose that if R is any of the free radicals of the hydrocarbon pyrolysis, the inhibition is represented by

$$C_3H_6 + R \rightarrow C_3H_5 + RH$$

and

$$C_3H_5 + H \rightarrow C_3H_6$$

The fact that inhibitors do not reduce the reaction rate to zero can still be made consistent with a completely free radical mechanism and no molecular decomposition. The role of the surface in these reactions is basic to such an explanation, and current researchers are not at all in agreement on that role.

All workers have found that, from an overall point of view, the pyrolysis is homogeneous. Recent workers disagree, however, as to whether certain of the free radical reactions take place at the reactor walls. Poltorak et al.[47] and Voevodsky[64] believe that the free radical chain propagation is indeed homogeneous, but the initiation and/or termination can be heterogeneous. They have designed experiments to detect this dual nature, but their results have not been universally confirmed. Martin et al.[35] have done similar work and their results seem to show that the surface plays no important part in any of the free radical reactions. However, if it can be assumed that the radical initiation and/or termination reactions are heterogeneous, it is possible to explain the strange behavior of inhibited decomposition without hypothesizing a residual molecular reaction. Free radicals are produced by irreversible reactions (in the initiation step) and by reversible reactions (in the propagation). If the initiation is heterogeneous, there is an initially high reaction rate because radicals are formed at the active surface sites. Upon addition of an inhibitor, those active sites are eliminated; the reaction will then continue only by means of the radicals produced homogeneously (in the propagation reactions). Thus, the rate will drop from its initially high one, but will not be stopped completely because of the continued reversible formation of radicals in the gas; and this is, in fact, observed experimentally.

At this point, it is fairly obvious that many of the problems in the mechanisms for hydrocarbon pyrolysis have yet to be solved. The situation is optimistic, however, in the light of current work being done using radioactive isotope tracers in studying reaction intermediates.

Neiman[40] gives a detailed description of how to use isotopes to determine the mechanisms and intermediates in kinetic experiments. Most of the work has been done with the simplest member of the series -- the decomposition of ethane. Rice and Varnerin[54] study the pyrolysis of C_2D_6 and Poltorak and Voevodskii[46] introduce molecular D_2 with the reactant and study the kinetics with and without free radical inhibitors. Basic to this work is the fact that the free radicals will readily exchange H for D, while stable molecules will not. Medvedeva et al.[36] did some tracer work on propane decomposition and introduced ethylene made with carbon-14. They were primarily concerned with the mechanisms of the secondary reactions. More recently[37] they extended their method and introduced radioactive propylene into the propane feed.

While these methods have not yet been perfected, they should soon be able to eliminate much of the confusion present in Rice-Herzfeld mechanisms in general and hydrocarbon pyrolysis in particular.

The equipment used in this study was not sensitive enough to verify any of the above theories, nor was it designed to do so. However, a series of runs was made in which small amounts of propylene were added to the propane feed. If, for these runs, the temperature profile, total flow rate, and mole fraction propane in the feed are held constant, the effect of the free radical inhibitor, propylene, can be studied. Analysis of the results is simplified if the experimental conditions are chosen such that the decomposition rate of the propylene is negligible. Since propylene requires higher temperatures for decomposition and is in much lower concentration than propane, these conditions are not difficult to achieve.

Further discussion on mechanisms is found in the section on experimental results.

III. EXPERIMENTAL APPARATUS AND TECHNIQUES

A. Apparatus

A schematic diagram of the experimental apparatus is shown in Figure 7. The reactant gases and nitrogen diluent were metered from cylinders into a ceramic reactor which was contained inside the electrically heated furnace. Power input to the furnace was controlled manually with a variac connected to a 220 volt supply. Temperature was measured with a thermocouple which was continuously driven along the length of the reactor. Pressures were measured with mercury and water manometers. Upon leaving the furnace, the gas was quickly cooled to room temperature with an air blast. For each run, a sample of the reactor exit gas stream was taken. A vacuum pump was used to prevent contamination in the sample tube. The gas then passed through a saturator and wet test meter (for overall volumetric flow measurement) before being vented.

The gases used in this work were obtained from The Matheson Company, Inc. Prepurified grade nitrogen (99.996% minimum purity, with a typical oxygen content of 8 ppm) was used as the diluent; the oxygen content had to be kept low because oxygen is a known accelerator of hydrocarbon pyrolysis. The propane used was instrument grade (99.5% minimum purity) and the propylene, C.P. grade (99.0% minimum purity); both hydrocarbons were products of the Phillips Petroleum Company.

The gases were fed from the cylinders at a constant pressure of about 20 p.s.i.g. by Matheson Number 1 single stage regulators.

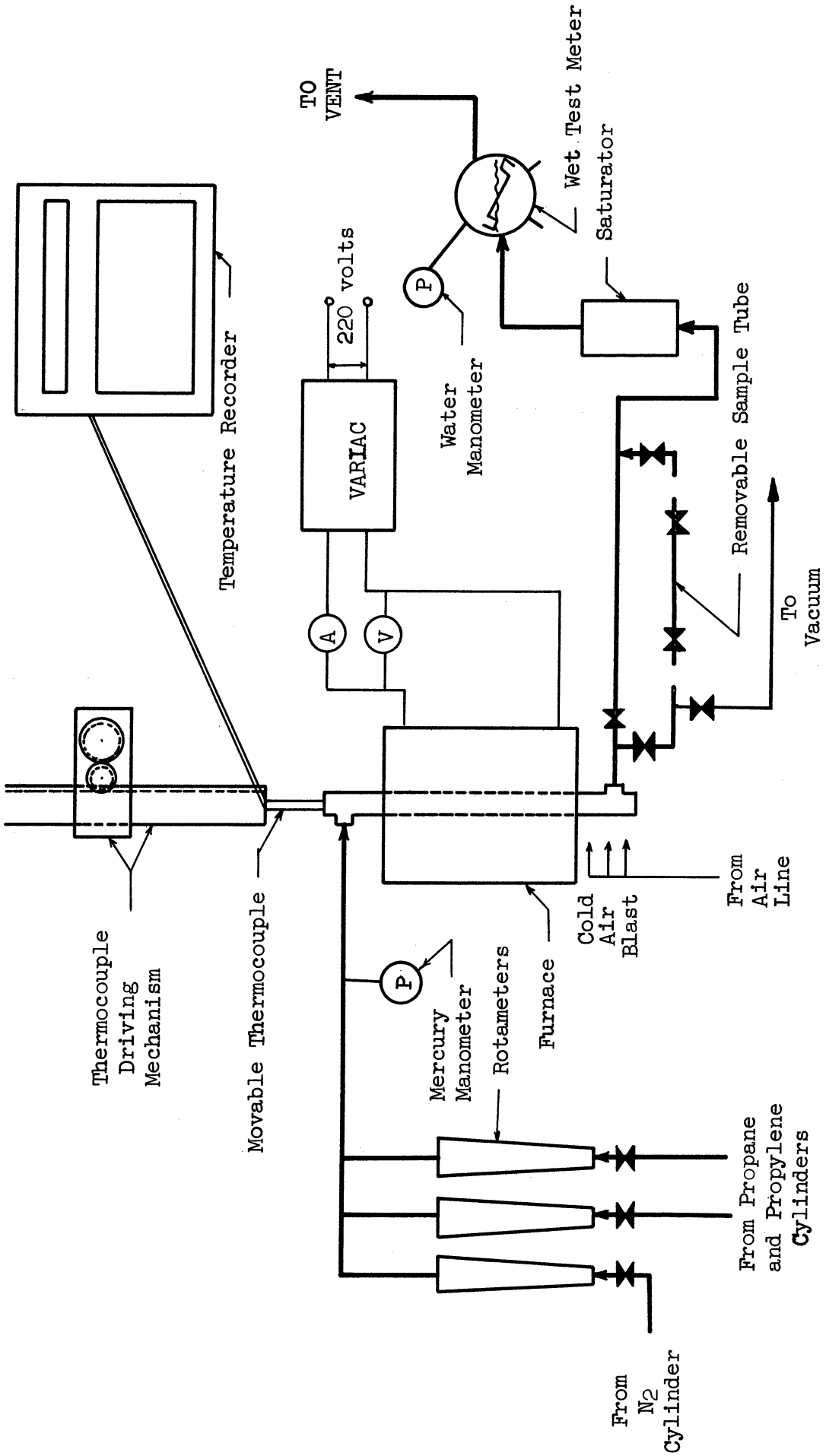

Figure 7. Schematic Diagram of Apparatus.

The gas flow rates were measured with Fischer and Porter rotameters of various sizes (FP 1/4 20-5; FP 1/8 16-5; FP 1/16 20-4; FP 1/16 08-4), and were controlled manually with 1/8 inch needle valves. The gas flowed through 1/4 inch and 3/8 inch copper tubing with brass compression fittings.

The electric furnace used in this study was the one built by G. D. Towell for his work at The University of Michigan. The alundum muffle was obtained from the Norton Compnay and was 1-1/2 inch bore with 1/4 inch walls of type RA139 material. The platinum wire for the windings was 0.020 inches in diameter and 50 feet long. The furnace was designed to operate up to 1600°C and the watt density on the winding at 1500 watts power input was 40 watts/sq.in. The winding was all in one piece and the turns were placed closer together at the ends to compensate for the large end heat losses. Double lead in wires for the power supply were used to prevent overheating in the passage through the insulation. The platinum winding was cemented to the muffle with Norton RA1139 cement. Norton Bubble Type alumina was used as the high temperature insulation close to the muffle. Johns Manville Superex (a silica type insulation) blocks were used for the lower temperature insulation. The whole furnace was contained in a light sheet steel rectangular box.

A diagram of the furnace is shown in Figure 8, and further details of construction may be found in Towell's Ph.D. thesis.[61]

The reactor used was an annular one, with both surfaces made from Vitreous Refractory Mullite ($Al_6Si_2O_{13}$) and obtained from

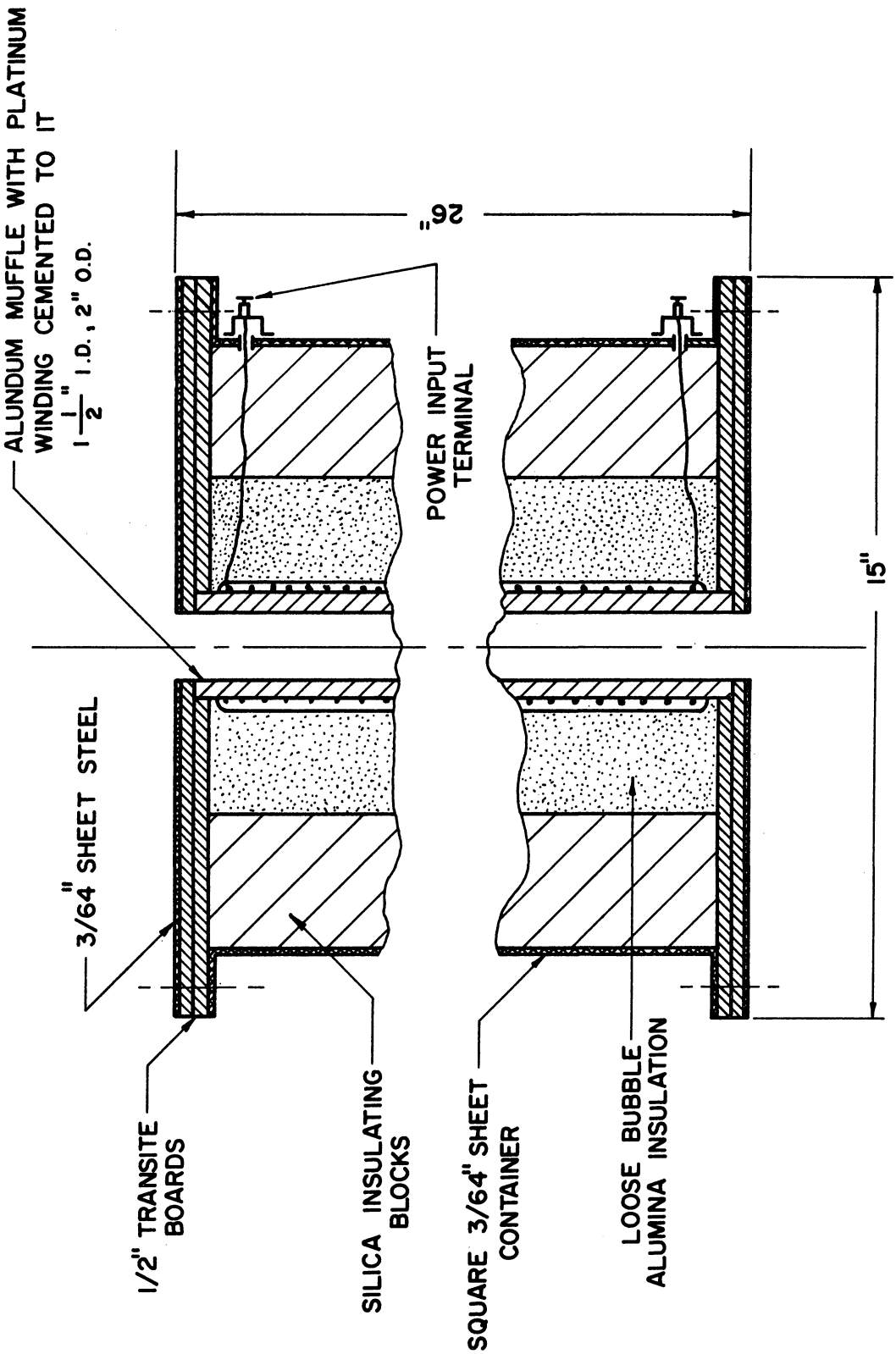

Figure 8. Furnace Details.

McDanel Refractory Porcelain Company. The I. D. of the outer tube was 1/4 inch and the O. D. of the inner tube was 7/32 inch as shown in Figure 9. Several runs were made with an inner tube O. D. of 3/16 inch to test the homogeneity of the reactions. The gas flowed through the annulus and the thermocouple traveled up and down the reactor's central tube.

Twenty-four gage (20 mils) chromel-p and alumel thermocouple wire was obtained from Hoskins Manufacturing Company; the type used was laboratory grade (3G178). The thermocouple wires were insulated by a thin, mullite tube at the bead end and were connected at the other end to a Brown Recorder (Model number 153X11P-X-28).

The driving mechanism, shown in Figure 10, continuously moved the thermocouple up and down the reactor. It consisted of a 1/2 r.p.m. reversible, synchronous motor and a set of gears which were used to change the thermocouple drive speed. The brass gears were products of the Boston Gear Company. The drive speed could be varied by as much as a factor of 4 (from 3.26 to 0.82 inches/minute) by changing the gears used. Six possible combinations were available, the diameters of the paired gears being (in eights of an inch): 5-10; 6-9; 7-8; 8-7; 9-6; 10-5. The thermocouple was attached to 4 feet of the rack corresponding to those gears (catalogue listing: Y24).

The drive was designed to switch the direction of the motor when the thermocouple reached either the top or the bottom of the reactor. Depending upon the steepness of the temperature profile of any particular run, the drive speed was increased or decreased

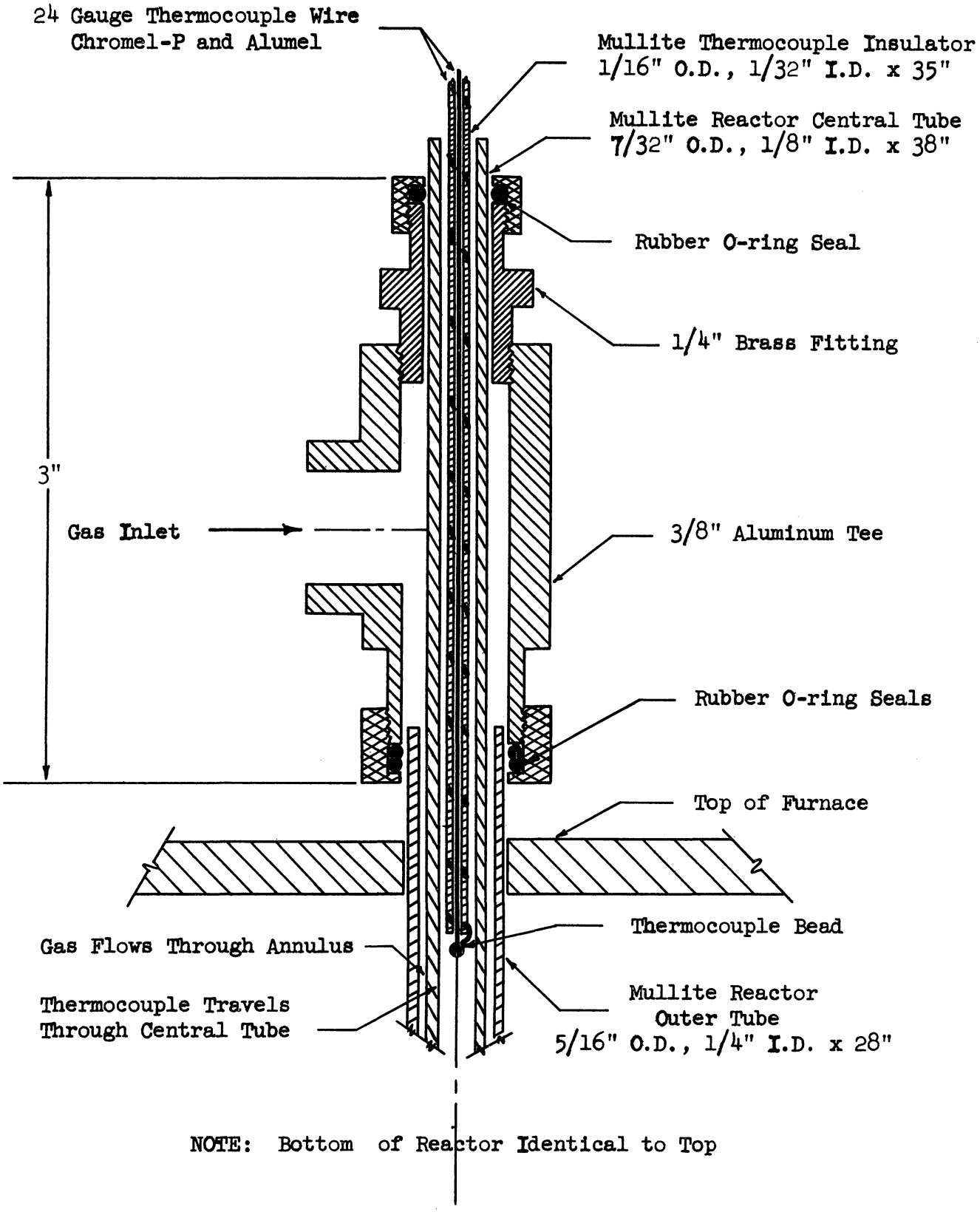

Figure 9. Details of Reactor and Thermocouple.

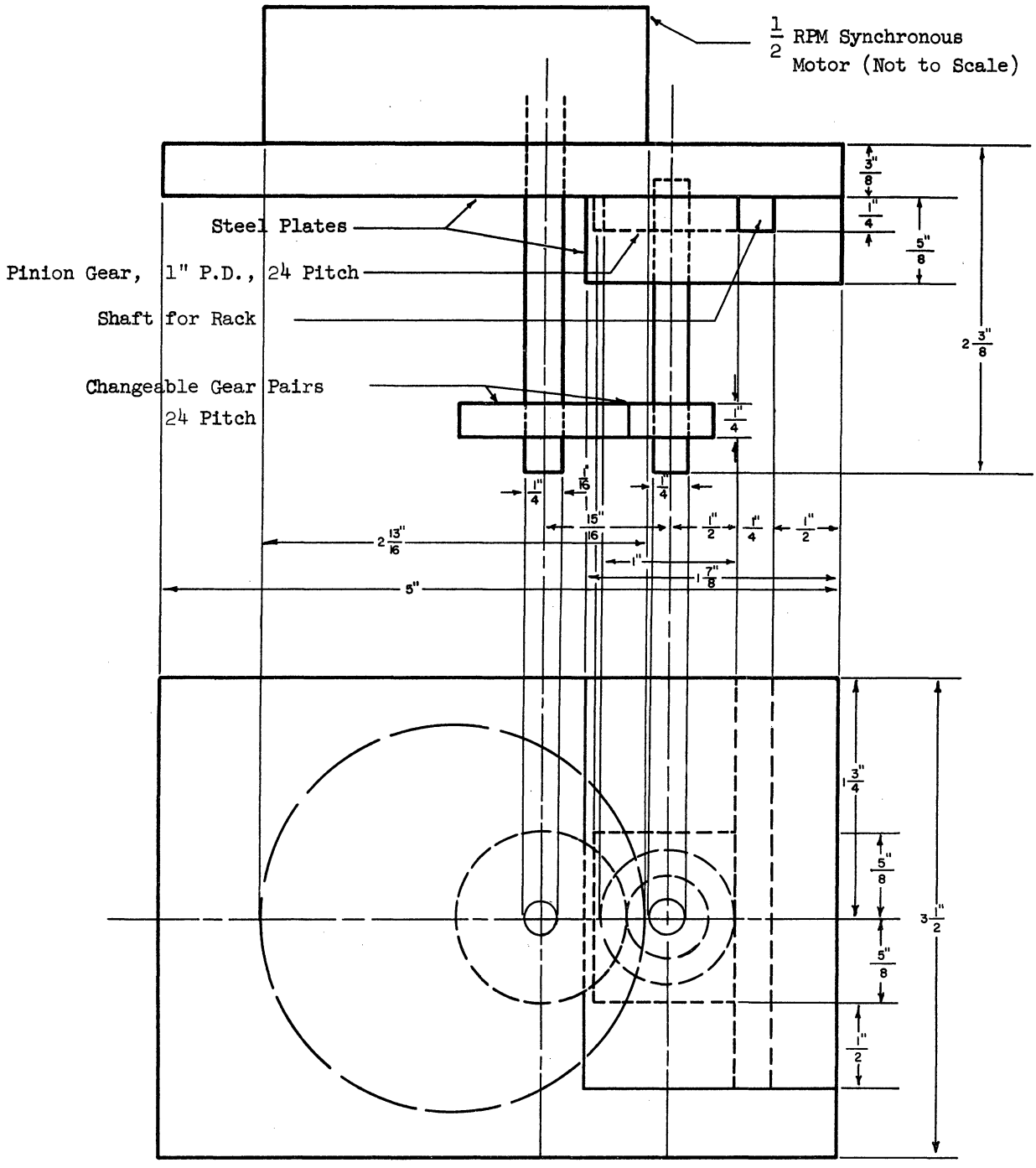

Figure 10. Details of Thermocouple Driving Mechanism.

to give easily readable temperature profiles on the recorder chart. The thermocouple measured the gas temperature from the inlet to the reactor (at room temperature) down to the point where the exit gas has been cooled close to room temperature by the air blast. Thus, there is no need to assume an instantaneous or linear heating and cooling; gas temperatures are measured to below the point where the reactions become negligible (see thermodynamic data, Figure 1).

B. Experimental Techniques

The furnace was allowed to heat up slowly overnight to prevent damage caused by thermal shock. The feed rates of the hydrocarbons and nitrogen diluents were adjusted manually and measured with the rotameters. The maximum temperature could be controlled crudely by changing the power input through the variac. The thermocouple drive mechanism was started and the temperature profiles recorded. Steady state conditions were achieved when successive temperature profiles (representing approximately 45 minutes total traversing time for most runs) were identical.

At that time, the experimental conditions were recorded and a gas sample was taken for analysis. The sample tube, by then, had been evacuated, placed in the line, and flushed with the exit gas stream. (The sample tubes were straight bore with constant diameter throughout, so that flushing would leave no stagnant areas.) The gas stream was diverted from the by-pass line and a sample was obtained.

The experimental parameters which were recorded were:

a) nitrogen and hydrocarbon feed rates

b) reactor inlet pressure

c) reactor exit pressure

d) atmospheric pressure

e) reactor temperature profile

f) room temperature

g) furnace power input (voltage, current and variac setting)

h) total exit gas volumetric flow rate

i) thermocouple drive speed

j) exit gas composition (by mass spec analysis)

The experimental conditions (namely, nitrogen and hydrocarbon feed rates, and the furnace power input) were then changed for the next run, and the parameters were allowed to reach the steady state again. After an entire series of runs, the power was turned off and air was passed through to burn any carbon deposits and to help cool the reactor seals.

The exit gas samples were analyzed primarily on a mass spectrometer (Consolidated Engineering Corporation Type 21-103B). The mass spectrometer can not give quantitative analysis unless the cracking pattern for each of the pure components of the mixture is available. The cracking pattern gives the relative amount of ions present at each mass-to-charge ratio when the sample is cracked. These data are published,[2] but since the patterns vary from

machine to machine (and even on the same machine from day to day), it is best to run a standard of each of the pure components before performing an unknown analysis. Once M standards have been run (if there are M compounds in the mixture), the sensitivity of each pure compound can be calculated for each of M mass-to-charge ratios. (The sensitivity is the intensity of ions present at any mass-to-charge ratio per unit of sample pressure, and usually measured in divisions/micron.)

Then, when the intensity of the unknown sample is read at each of the M mass-to-charge ratio peaks, a set of M simultaneous equations in M unknowns (the partial pressure of each of the M components) can be set up as follows:

$$\begin{aligned} \sigma_{1,1}\mu_1 &+ \sigma_{1,2}\mu_2 + \dots + \sigma_{1,M}\mu_M = I_1 \\ &\vdots \\ \sigma_{M,1}\mu_1 &+ \sigma_{M,2}\mu_2 + \dots + \sigma_{M,M}\mu_M = I_M \end{aligned} \tag{37}$$

where $\sigma_{i,j}$ is the sensitivity at the i-th mass-to-charge ratio of the j-th component

μ_j is the unknown partial pressure of the j-th component

I_i is the intensity of the unknown at the i-th mass-to-charge ratio

The solution of these M equations in M unknowns was obtained through the use of a digital computer. The partial pressures,

$\mu_1 \ldots \mu_M$, are proportional to the mole fractions of each of the M components.

Numerous checks are available to test the accuracy of the obtained results. First, the sum of all the partial pressures should add up to the measured total pressure of the unknown sample. Secondly, the known sensitivities and the calculated partial pressures can be used to check the intensities of peaks other than the M peaks used in solving Equations (37).

If the calculated intensity for any of the peaks does not check with the measured intensity for the unknown sample, it is very possible that there is another component present which has not been considered. By this method the presence of methylacetylene (C_3H_4) was detected in the pyrolysis of propane, although it had not been anticipated among the M components. It was also possible to confirm that the material was indeed methylacetylene and not allene (both are C_3H_4).

Finally, a standard known mixture was prepared and analyzed with the mass spectrometer to test the instrument's accuracy. Some independent checks were also made using a dual column gas chromatography unit.

C. Some Preliminary Problems Solved

A major problem which had to be solved before any useful data could be obtained was whether the thermocouple (located at the center of the reactor) was reading the true temperature of the gas

(flowing through the annulus). Theoretical considerations of fluid dynamics and heat transfer might have been used to settle the question, but instead, the problem was solved experimentally.

A thin thermocouple was cemented with Sauereisen (a high temperature ceramic paste) in a fixed position through the rubber seals into the annulus of the reactor. The depth of the thermocouple into the reactor was noted, and the movable thermocouple was placed in the corresponding position of the central tube. The thermocouples were placed (as nearly as could be estimated) at the maximum temperature point in the profile. The reason for this was to keep the temperature error at a minimum if the two thermocouples were not lined up exactly. The temperature profile is flattest near the maximum (cf., Figure 2).

Over a wide range of conditions of temperatures and flow rates, the two thermocouples agreed to within 3°C. It was thereby concluded that the central thermocouple could indeed be used to give the true gas temperature.

A second question raised was the effect of any radial velocity profile and longitudinal diffusion as the gas flowed through the reactor. If any radial velocity profiles were present (as they would be in laminar flow), the gas flowing close to the walls would have a larger residence time and hence higher conversion than the gas in the middle of the annulus. In this work, however, Reynolds numbers were approximately 4000 and plug flow conditions could be assumed.

The problem of longitudinal diffusion presents somewhat greater difficulty. A flow reactor in which a first-order reaction with longitudinal diffusion is taking place can be described[32] by the differential equation

$$D \frac{d^2z}{d\ell^2} - u_\ell \frac{dz}{d\ell} + k(1 - z) = 0 \qquad (38)$$

where D is the diffusion coefficient, cm^2/sec

z is the conversion

ℓ is the reactor length, cm

u_ℓ is the linear gas velocity, cm/sec

k is the rate constant, sec^{-1}

When diffusional effects are neglected, Equation (38) becomes

$$u_\ell \frac{dz}{d\ell} = k(1 - z) \qquad (39)$$

Thus, a good criterion for neglecting diffusional effects is if

$$\frac{D(d^2z/d\ell^2)}{u_\ell(dz/d\ell)} \ll 1 \qquad (40)$$

At the conclusion of this study, the rate constants were fed, along with the experimental data, into an analog computer and the expressions $\frac{dz}{d\ell}$ and $\frac{d^2z}{d\ell^2}$ were easily calculated along the length of the reactor. For a typical run, the value of the fraction

in Equation (40) was approximately 1%. The diffusional effects in this work, therefore, were rightly neglected. These calculations are presented in detail in Appendix I.

IV. DISCUSSION OF EXPERIMENTAL RESULTS

The following discussion includes all of the important experimental results. The raw data for all the experimental work may be found in Appendix A, the calculated data are tabulated in Appendix B, and sample calculations are shown in Appendix K.

A. Propane Feed

1. Product Distribution

The first experimental step in this program was to determine which were the primary products of reaction in the decomposition of propane. The primary products of reaction are those products which are in appreciable concentrations at the lowest overall conversions of propane. A series of runs was made at approximately identical temperature profiles. The conversion for each run could be changed by altering either the total flow rate (and hence, the residence time) or the inlet propane mole fraction, or both. Moderate variations in temperature could be tolerated, because no quantitative results were anticipated from these runs.

For this series of runs, the conversion to each of the reaction products (as mole of that product per mole of propane reacted) was plotted against the total conversion of propane. Any carbon formed was determined by material balance.

The results of the product distribution runs are shown in Figure 11. It is seen that the primary products of reaction are methane, ethylene, propylene and hydrogen. This has been found by all

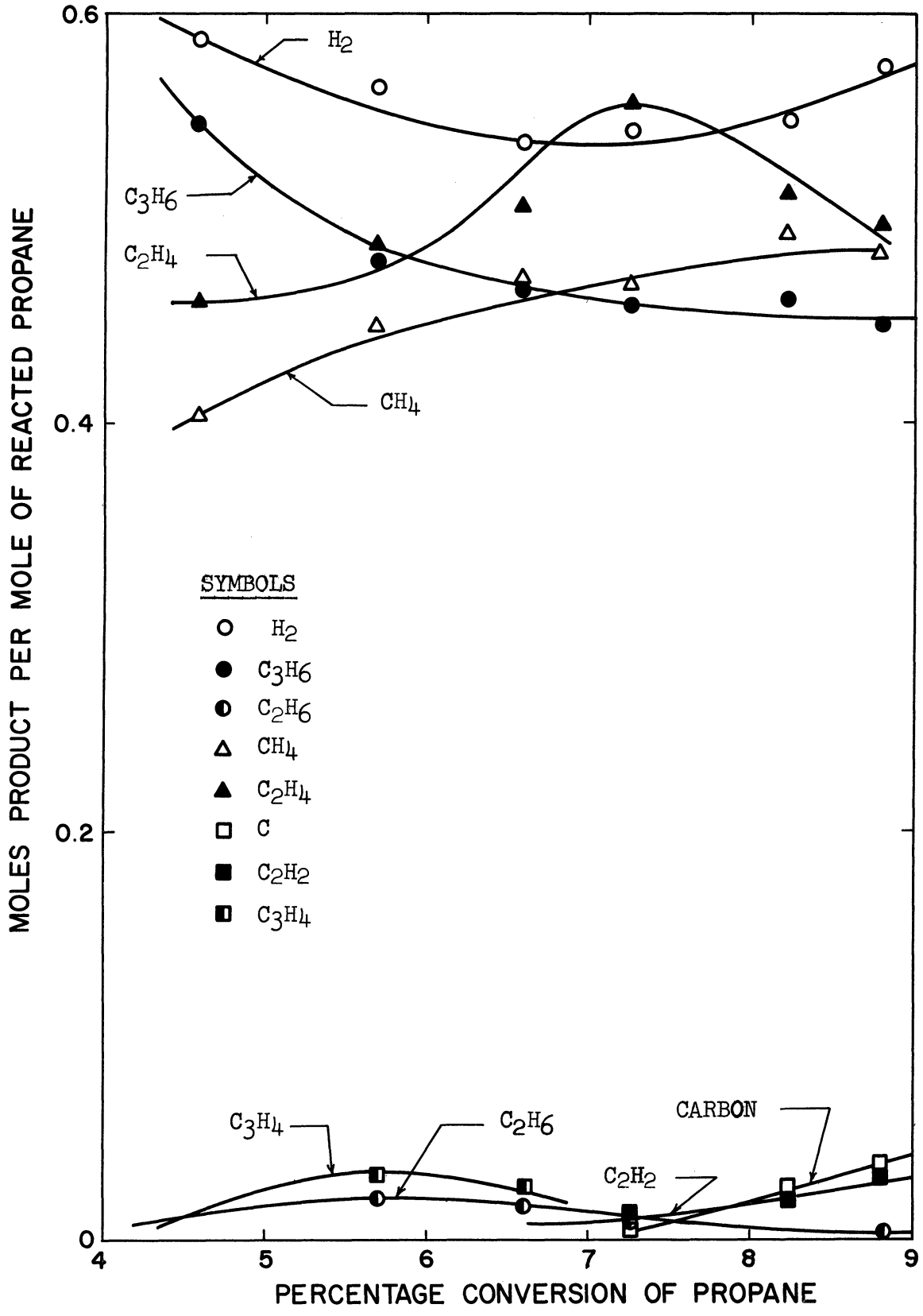

Figure 11. Propane Product Distribution, T_{max} ≈ 1514°F.

previous workers,[1,12,14,19,23,39,44] although they were working at considerably lower temperatures. Some of the minor or secondary products of reaction were ethane, methylacetylene, acetylene, carbon and butane. Each of these has been found previously by some researchers, although methylacetylene has been only rarely quoted as a reaction product.[1,48]

The stoichiometry of these major reactions may be set forth as follows:

$$C_3H_8 \rightarrow C_3H_6 + H_2$$

$$C_3H_8 \rightarrow C_2H_4 + CH_4$$

It must be realized, however, that postulation of molecular reactions is merely a convenience in representing the overall kinetic picture. As has been noted above, the decomposition is not molecular at all, but free radical in nature.

2. Orders of Reaction

Once the stoichiometric reactions are determined as above, it is possible to find the orders of reaction for the overall decomposition and for each of the individual reactions. From the theory developed in Section II-E, it is seen that a series of runs is needed in which the total flow rate and temperature profile are kept constant. Conversions were varied by changing the mole fraction of the propane in the feed. The runs were designed to hold conversions at a minimum by keeping the residence times low. A differential reaction rate could then be calculated and plotted against the average mole fraction of propane on logarithmic coordinates.

As was shown above, the slope of such a graph is the order of reaction. Figure 12 shows the results for each of the individual reactions and for the overall decomposition. The order of reaction for the overall decomposition appears to be 1.11 and those of propylene and methane formation, 1.13 and 1.17, respectively. A very important question which must be answered is, what are the experimental uncertainties in these results? In other words, if the data indicate an order of 1.13, can it be safely assumed that the reaction is either first order or 1.5 order? Or can nothing more be inferred than that the empirical order is 1.13, although there is no theoretical basis for such a result?

In answering this question, it is important to note that the theory behind the reaction order experiments (as developed above) requires a set of runs at identical temperature and pressure profiles. Since the controls were set manually, such conditions could only be approximated but never realized. For example, the maximum temperature for the set of runs varies by 3°C. Furthermore, very slight displacement of the points in Figure 12 can give rise to considerable change in the slope. With these facts taken into consideration, the uncertainty involved in the determination of orders of reaction is ± 20 to 25%.

It appears, therefore, that both the overall decomposition reaction and the individual reactions could be assumed first order. Most previous workers[6,34,36,42,58] have found the reaction to be first order, although a few[29,59] have found evidence of 1.5 order kinetics,

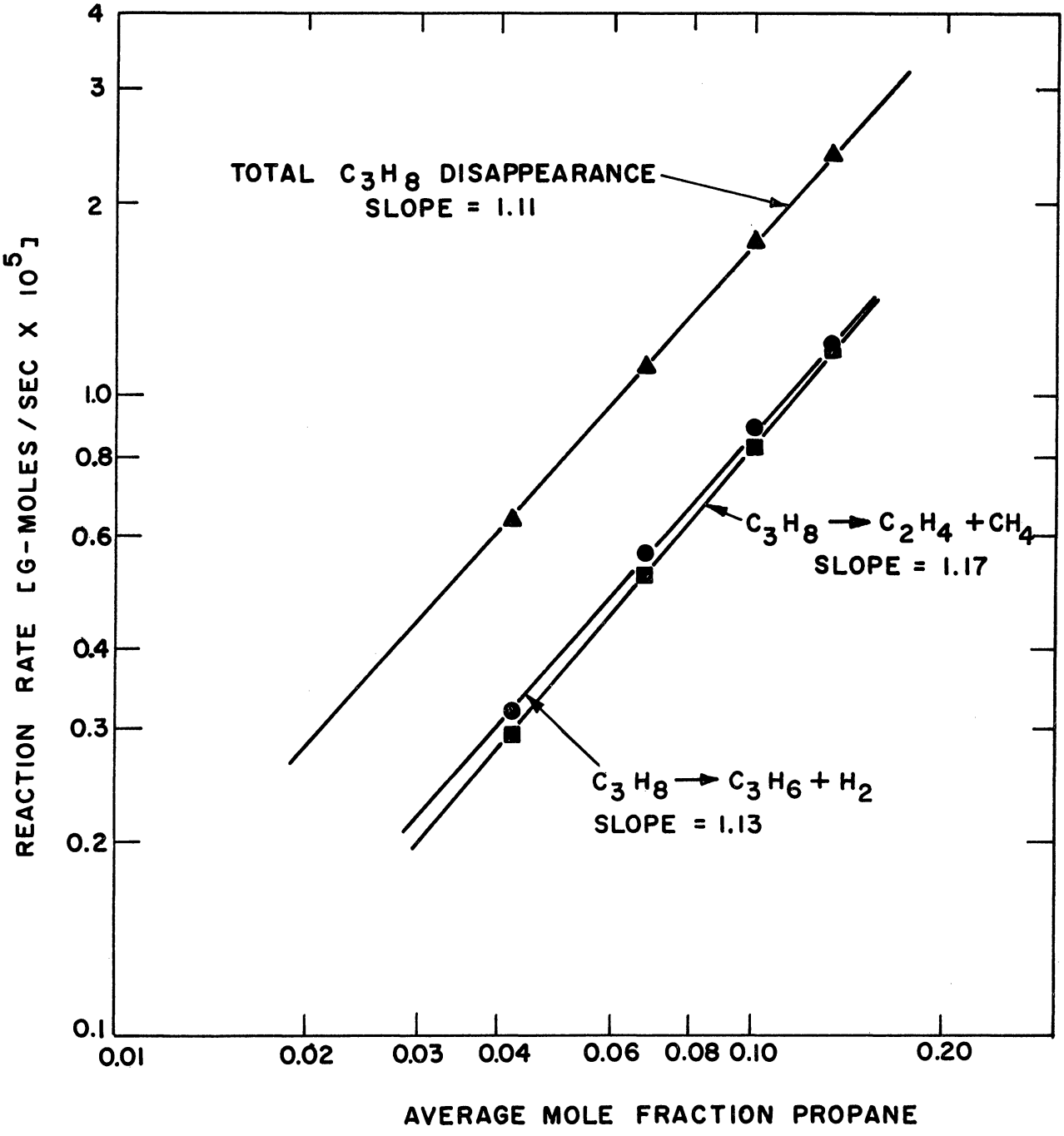

Figure 12. Order of Reaction Determination for Propane Decomposition, $T_{max} \cong 1514°F$.

at least under certain conditions of temperature and pressure. Even considering the experimental uncertainties, the results of this work can not indicate an order of 1.5.

On the other hand, Martin et al.[35] have empirically found the order to be between 1.2 and 1.3. Since these values lie within the experimental uncertainty of the data, it was decided to consider this possibility and to fit the kinetic data to a 1.25 order of reaction as well as a first order. The results are discussed in the next section.

3. Rate Constant Determination

Once the primary reactions have been determined and a reaction order has been postulated, one can conduct experiments to determine the rate constants. In actuality, since no runs were made at constant temperature, it is the parameters A and E which are determined, and not the rate constants themselves.

Other than the desirability of keeping the conversions low (to minimize secondary and reverse reactions), no limitation was placed on the experimental conditions of these runs. In fact, it would be best to have the runs cover wide ranges of temperature profiles, feed rates, nitrogen dilution, pressure profiles, etc.

The functional relationship between A and E for any run was given in Equation (18) above,

$$A = \frac{\frac{FR^n}{s}\int_0^{z_e}\left[\frac{1+No/F+z}{1-z}\right]^n dz}{\int_0^L e^{-E/RT(\ell)}\left[\frac{P(\ell)}{T(\ell)}\right]^n d\ell} \qquad (18)$$

The pressure profile, $P(\ell)$, in Equation (18) is not known experimentally throughout the length of the reactor. The only known pressures are those at the reactor inlet and outlet. In this work, a linear pressure profile was used for the entire reactor, and the justification for such an approximation is presented in detail in Appendix E.

Based upon the postulation of first order kinetics, the kinetic parameters for the overall decomposition of propane were determined first. Each experimental run was expressed in the form of Equation (18); a least squares fit of all the data generated the best values of the pre-exponential factor and activation energy.

Although the pairing of two runs was found to be an unsatisfactory method of obtaining A and E (cf. Section II-G-1), this method can be used, to a limited extent, if the paired runs were made at greatly different temperatures; then the errors introduced under these conditions are usually at a minimum. Thus, values of $k_{max} = Ae^{-E/RT_{max}}$ can be calculated and plotted against $1/T_{max}$ in the usual Arrhenius graph.

Figure 13 shows the results for the overall propane decomposition. The straight line represents the best fit of all the data by least squares methods; the points, on the other hand, are judiciously chosen results obtained by the pairing method. Only runs made under widely differing experimental conditions are paired here; inclusion of other pairs would have scattered the points considerably.

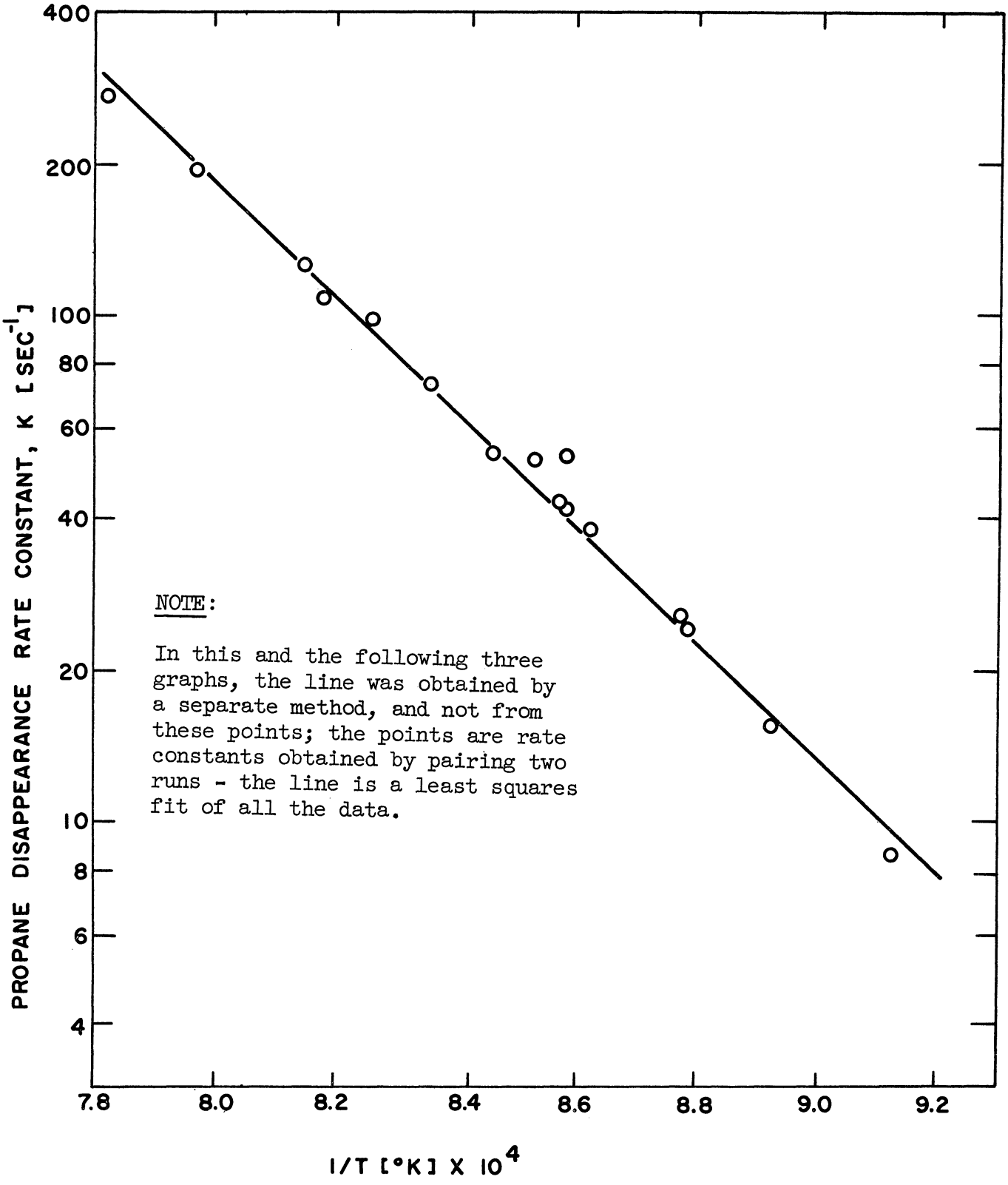

Figure 13. Rate Constants for First Order Disappearance of Propane - Arrhenius Plot.

It is seen that the line represents the paired points reasonably well, but it is not the "best" line through those points, nor should it be. It is important to remember that the line in Figure 13 is the best representation of the experimental results, and the paired points are only shown to give some idea of the scattering of the data. The same significance is attached to the lines and points in Figures 14-16 which follow.

A similar method of calculation is used in obtaining the kinetic parameters for each of the first order reactions

$$C_3H_8 \rightarrow C_3H_6 + H_2$$
$$C_3H_8 \rightarrow C_2H_4 + CH_4$$

The differences between the calculations here and for the overall decomposition reaction are slight and are illustrated in Appendix F. Figures 14 and 15 show Arrhenius plots for the formation of methane and for the formation of propylene, respectively.

As was mentioned in the previous section, it would also be consistent with the order of reaction data to postulate an order of 1.25 instead of 1.0 (although there is no theoretical basis for the former). An empirical fit of the points is possible for intermediate orders also, but would serve no important purpose. Figure 16 shows an Arrhenius plot of the log (rate constant) versus reciprocal temperature on the assumption that the order of reaction is 1.25.

Here again, the line is the least squares fit of all the data, and paired points are included to give an indication of the scatter. Comparison of Figures 13 and 16 shows perhaps slightly less scatter in

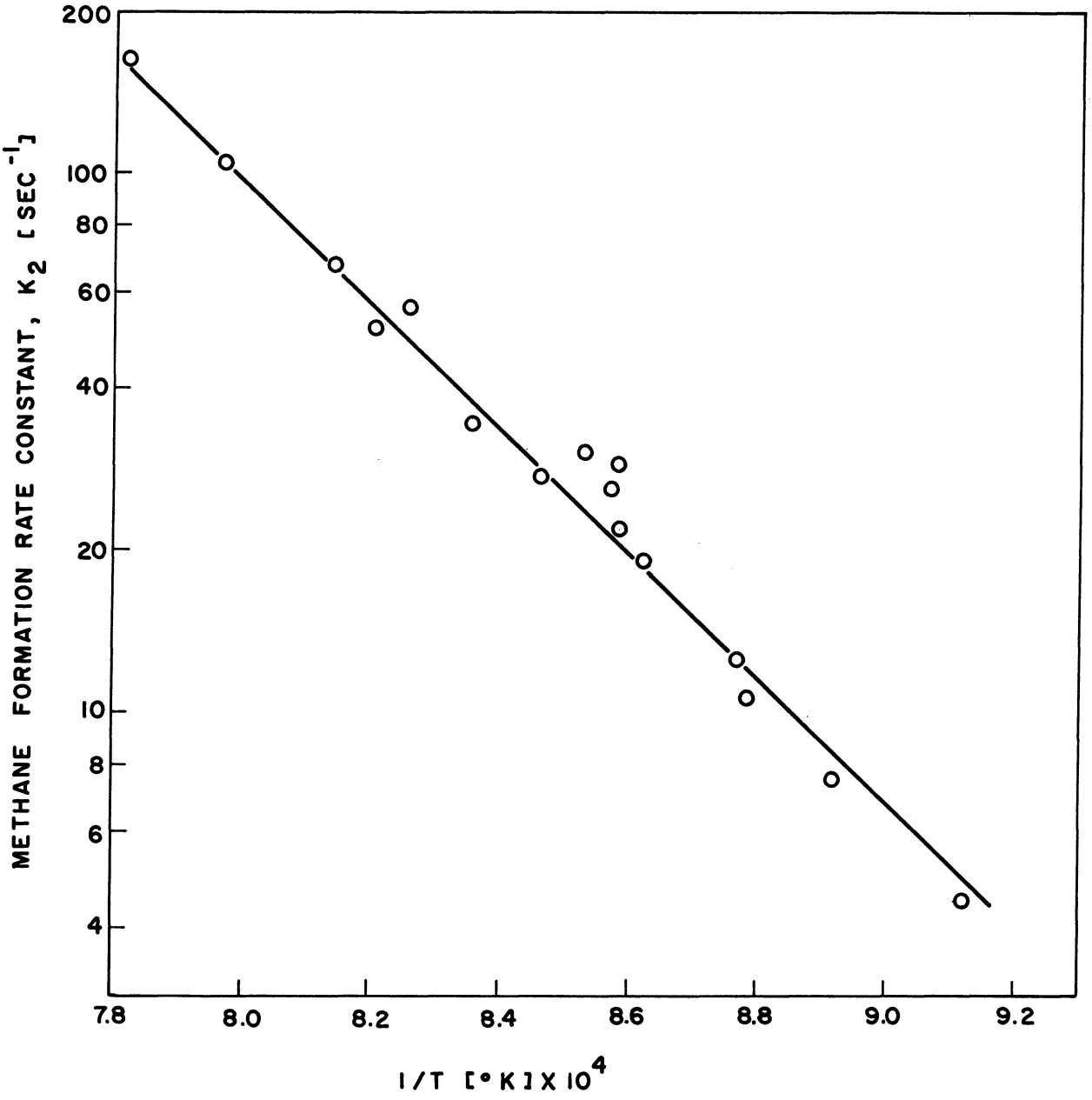

Figure 14. Rate Constants for First Order Formation of Methane from Propane - Arrhenius Plot.

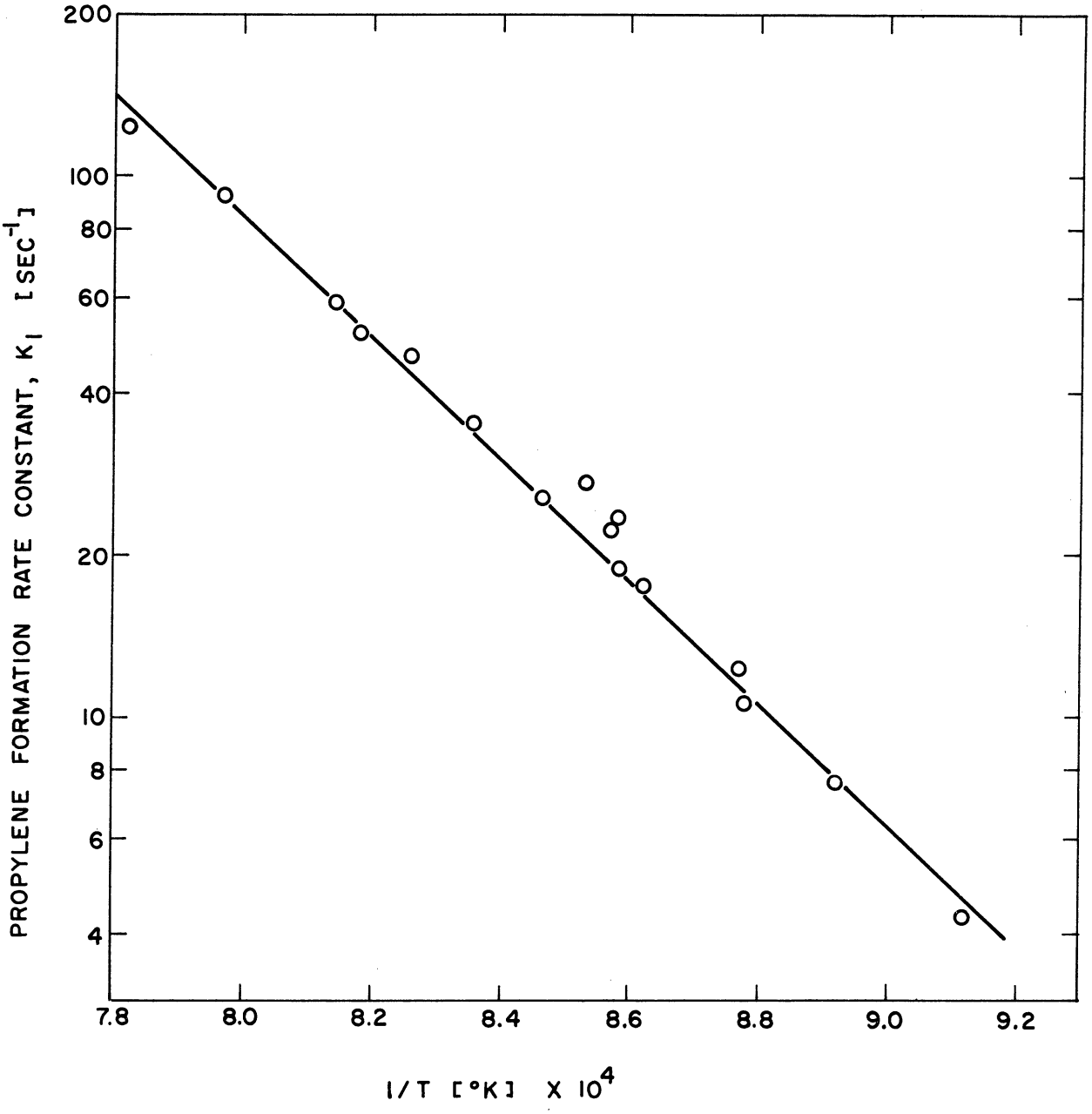

Figure 15. Rate Constants for First Order Formation of Propylene from Propane - Arrhenius Plot.

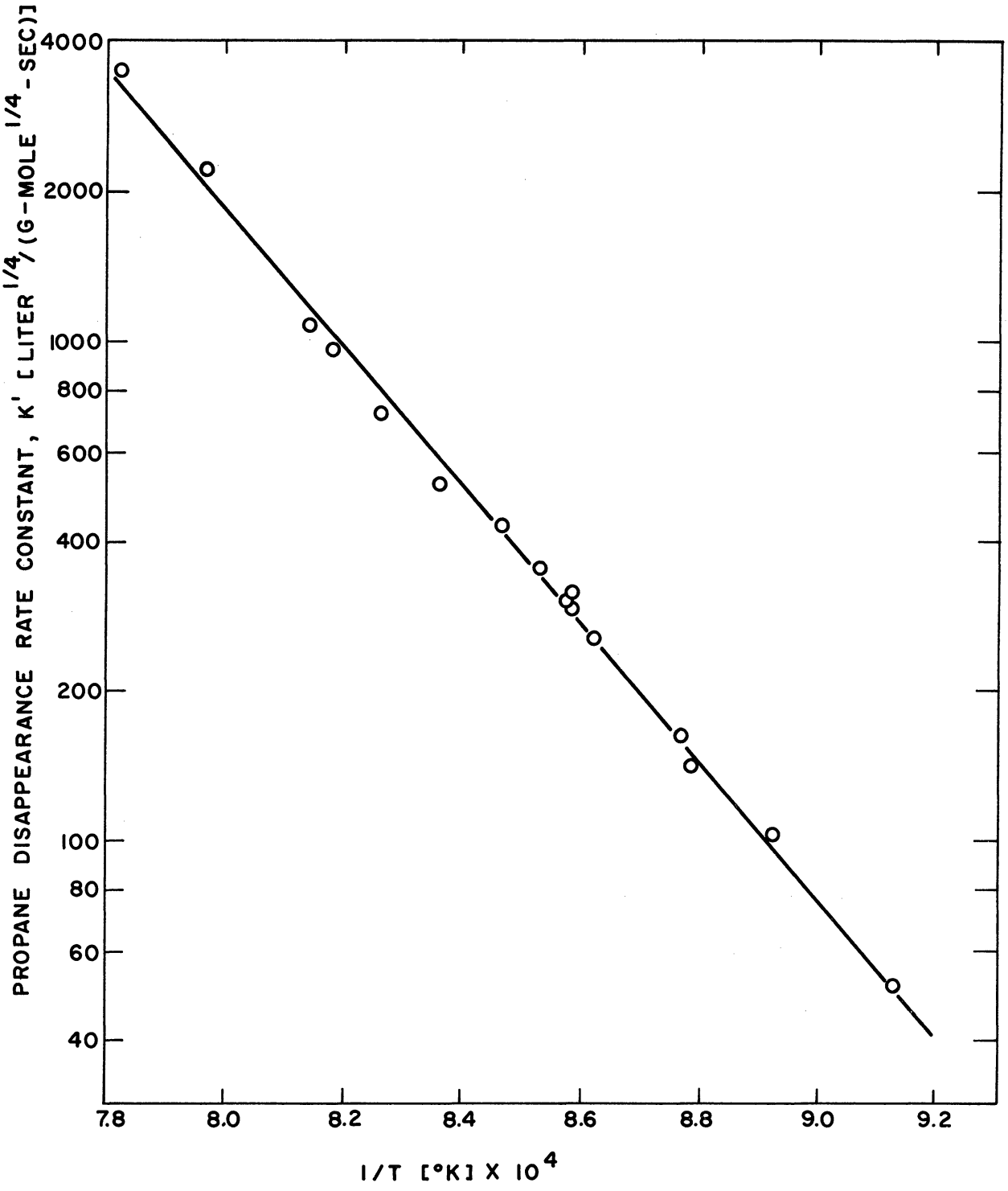

Figure 16. Rate Constants for 1.25 Order Disappearance of Propane - Arrhenius Plot.

the 1.25 order fit. But the difference is not great and it can be said that both orders of reaction (and probably all intermediate values of the order) can be used to fit the data equally well. Thus, there is no motivation for rejecting first order kinetics in favor of an empirical, fractional order fit of the data.

The values of the pre-exponential factors and activation energies as represented in Figures 13-16 are listed in Table II. In all instances, the standard deviation was ±20% for the pre-exponential factors and ±5% for the activation energies. See Appendix K for a further discussion.

TABLE II

EXPERIMENTAL VALUES OF PRE-EXPONENTIAL FACTORS AND ACTIVATION ENERGIES IN PROPANE PYROLYSIS

First Order Reaction	$A(sec^{-1})$	E(Kcal/g-mole)
Decomposition of propane	2.40×10^{11}	52.1
Formation of methane	1.52×10^{11}	52.5
Formation of propylene	9.26×10^{10}	51.7
1.25 Order Reaction	$A\left[\frac{liters^{1/4}}{g\text{-}moles^{1/4}\text{-}sec}\right]$	E(Kcal/g-mole)
Decomposition of propane	2.34×10^{14}	63.5

In comparing the results of other workers in propane decomposition, it is important to realize that all other research has been done 200° - 300°C below the temperatures of this study. Figure 17 compares all the published kinetic data for first order propane pyrolysis.

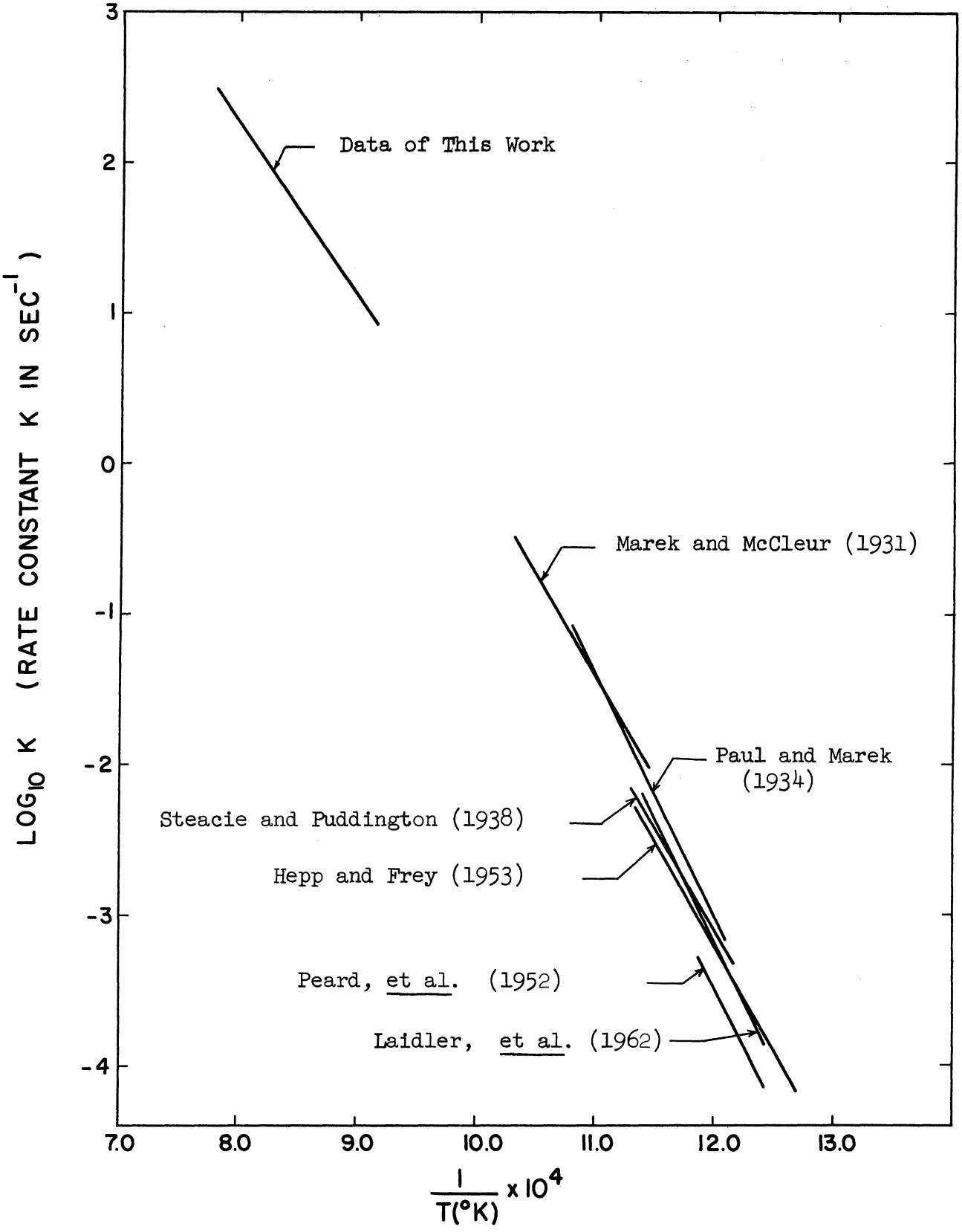

Figure 17. A Comparison with Literature Values of First Order Rate Constants for Propane Decomposition.

While it is true that the other studies have indicated higher activation energies - usually between 60 and 70 Kcal/g-mole - the discrepancies can be explained by the great temperature difference.

Several previous workers[29,35,36,61] have noted that as the temperature of hydrocarbon pyrolysis is increased, the activation energy for the reaction "appears" to decrease rather than remain constant. This is illustrated schematically in Figure 18, where the slope (activation energy) decreases with increasing temperature.

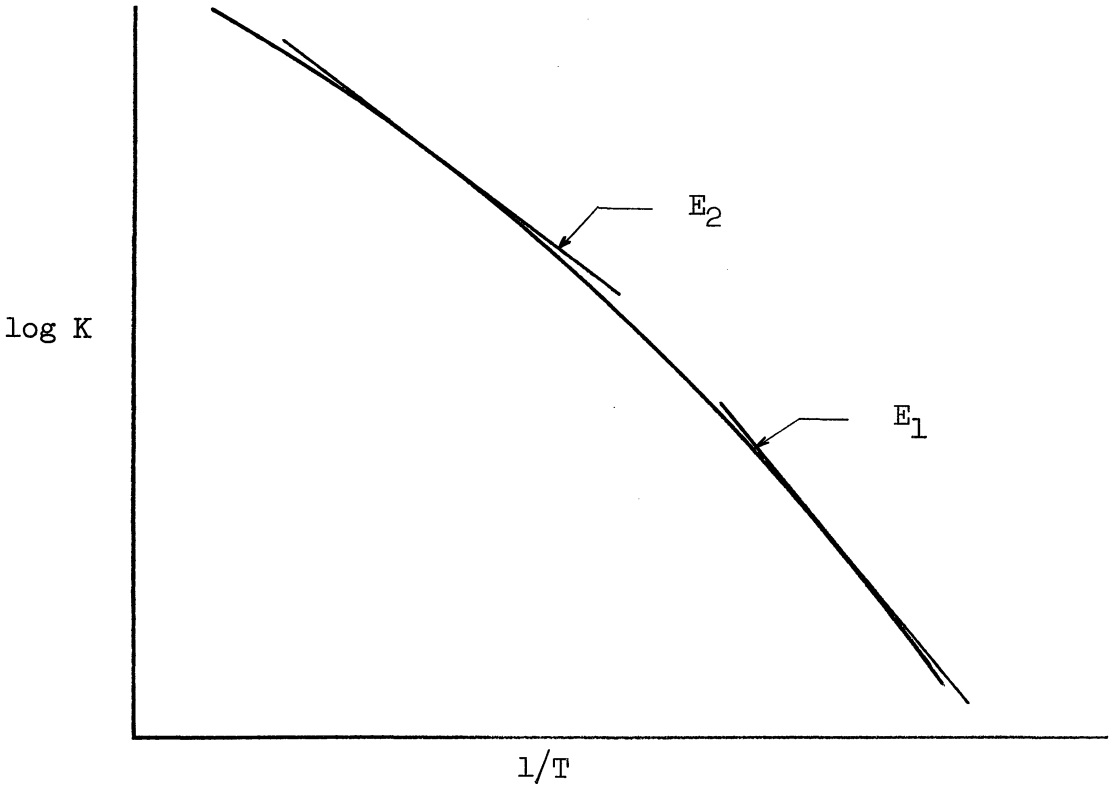

Figure 18. Apparent Decrease of Activation Energy with Temperature.

In fact, this effect can be noted even in the short temperature range of this work; Figures 13-15 show that the data might have been fit more closely by a curve (concave downward) than by the straight line.

A possible cause is a reaction rate at higher temperatures somewhat lower than the Arrhenius equation would predict, because inhibitors are formed. If it were simply a decrease in activation energy, one would expect the rate to increase correspondingly under such conditions, rather than decrease. Thus, while such an effect may be termed (as it has been by previous workers) an "apparent decrease in activation energy" with increasing temperature, it is important to realize that the true cause of this phenomenon is mechanistic. Once this point is clarified and it is stated that there is no evidence for a temperature dependence of the activation energy, the experimental results can be reported as the apparent activation energies in the range 800° - 1000°C.

An interesting sidelight of this discussion is that the data runs may be arbitrarily divided into two sets - half of which were taken above some intermediate temperature, and half below. If the identical kinetic analysis is now performed on only the lower half of the data instead of all the data, the resulting apparent activation energy is 58 Kcal/g-mole - considerably closer (in activation energy as well as in temperature) to the results of the earlier workers.

The exact nature of this inhibition effect has been discussed earlier in Section II-H. As mentioned in that section, olefins in general and propylene, in particular, are strong inhibitors of free radical reactions. While propylene is a primary product of propane decomposition at both high and low temperatures, it is much more difficult to keep the conversion low at high temperatures. Thus, the inhibition effect is magnified as the reaction temperature is increased, causing the result shown in Figure 18.

Since the individual decomposition reactions had not been studied previously, no comparison could be made for those results. However, all earlier workers had found the primary product distribution in propane pyrolysis to be approximately equal amounts of propylene, hydrogen, methane and ethylene; this study confirms those results. Hence, qualitatively, the rate constants for the two reactions

$$C_3H_8 \rightarrow C_3H_6 + H_2$$
$$C_3H_8 \rightarrow C_2H_4 + CH_4$$

should be approximately equal, and such is the case.

Furthermore, if this equal distribution is to exist at low temperatures (where the other researchers worked) as well as at high temperatures (i.e. this study), the activation energies of the two individual reactions would have to be approximately equal. Table II shows that they differ by only 1.5%.

B. Propylene Feed

The next series of runs was made with a feed of propylene diluted with nitrogen. The sole purpose of these runs was to study the product distribution of propylene pyrolysis for use in the analysis of the mixed feed (propane plus propylene) runs. The experiments were carried out at approximately equivalent temperature profiles T_{max} $\doteq$ 1815°F = 990°C). At these high temperatures, however, it became more difficult to keep the profiles constant from run to run, and the maximum temperatures varied by $\pm$ 6°C. (It was difficult to keep a constant profile because the reaction was highly endothermic. Thus,

although the total flow rate was constant, the percentage conversion changed from run to run; and the higher the conversion, the more power input required for the furnace to keep a constant temperature profile. Since the power input was controlled manually, a truly constant profile was impossible.) Since no quantitative information was desired from these runs, the resulting scatter of the data was not a serious problem.

The results of these runs are shown in Figure 19. It is seen that the primary products of decomposition are methane, hydrogen and methylacetylene, with smaller quantities of acetylene, ethylene, 1-butene and 1,3-butadiene. These results are basically in agreement with those of previous workers; at lower temperatures (500°-700°C) the primary reaction products were found to be methane, ethylene and hydrogen.[12,14,60] Ingold and Stubbs[25] had some polymerization to butene and butadiene. At higher temperatures, several workers[39,63] have detected some acetylene. This is to be expected from thermodynamic considerations as was illustrated previously (cf. Figure 1). There has been little evidence for the presence of methylacetylene, but one would not expect to find any except at the high temperatures of this work.

C. Mixed Propane and Propylene Feed

The final experimental phase of this study consisted of feeding propane with small amounts of propylene and diluted with nitrogen. A series of runs was made at constant total flow rate, temperature profile, and mole fraction propane, with varying amounts of propylene in the feed. The purpose of these runs was to note the effect of propylene, if any, on the pyrolysis of propane.

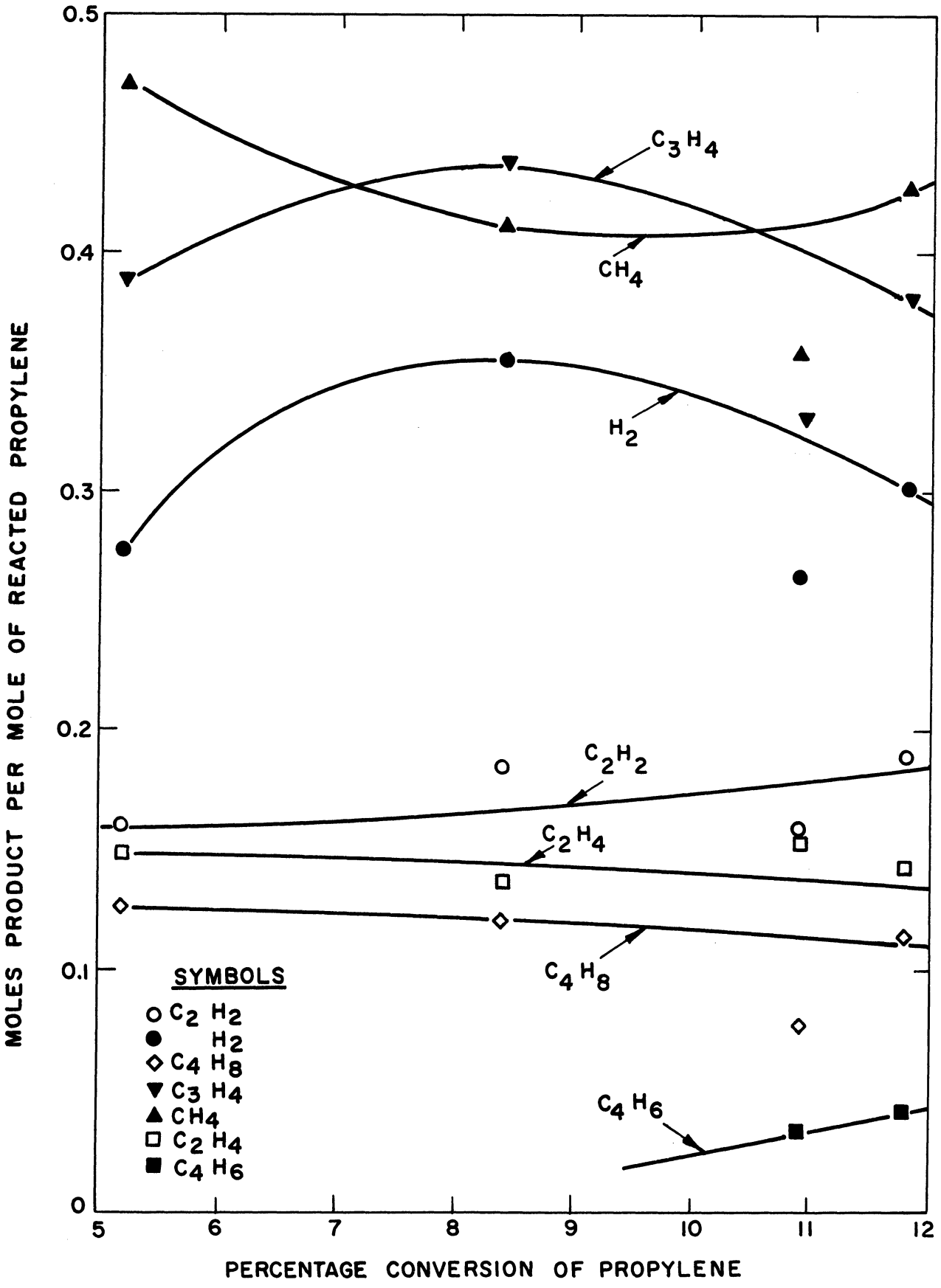

Figure 19. Propylene Product Distribution, $T_{max} \doteq 1815°F$.

Current theories (as described in Section II-H) indicate a free radical mechanism for hydrocarbon pyrolysis and note that propylene is a strong inhibitor of the reaction. Inhibition was cited above as a possible cause of the apparent curvature in the Arrhenius plot for propane decomposition.

While these runs were not designed to demonstrate the validity of mechanism hypotheses, they do point out quite clearly the extent to which propylene does inhibit propane pyrolysis. The results of these runs are shown in Figure 20, where the formation rates of propylene and methane are plotted against the average propylene-to-propane ratio in the reactor. (The formation rates of ethylene and hydrogen closely paralleled those of methane and propylene, respectively, but were omitted for clarity.) Of the two major reactions involved,

$$C_3H_8 \rightarrow C_2H_4 + CH_4$$
$$C_3H_8 \rightarrow C_3H_6 + H_2$$

note that the first does not appear to be affected by the presence of propylene, while the second is strongly inhibited.

A question might arise as to whether this is really inhibition or merely the approach to equilibrium of the reaction

$$C_3H_8 \rightleftharpoons C_3H_6 + H_2$$

However, from Figure 1 it is seen that the equilibrium constant $K_P = \frac{[C_3H_6][H_2]}{[C_3H_8]}$ at these temperatures is 100 atm. Obviously then, this is not an equilibrium effect, but actually propylene inhibition of propylene formation from propane.

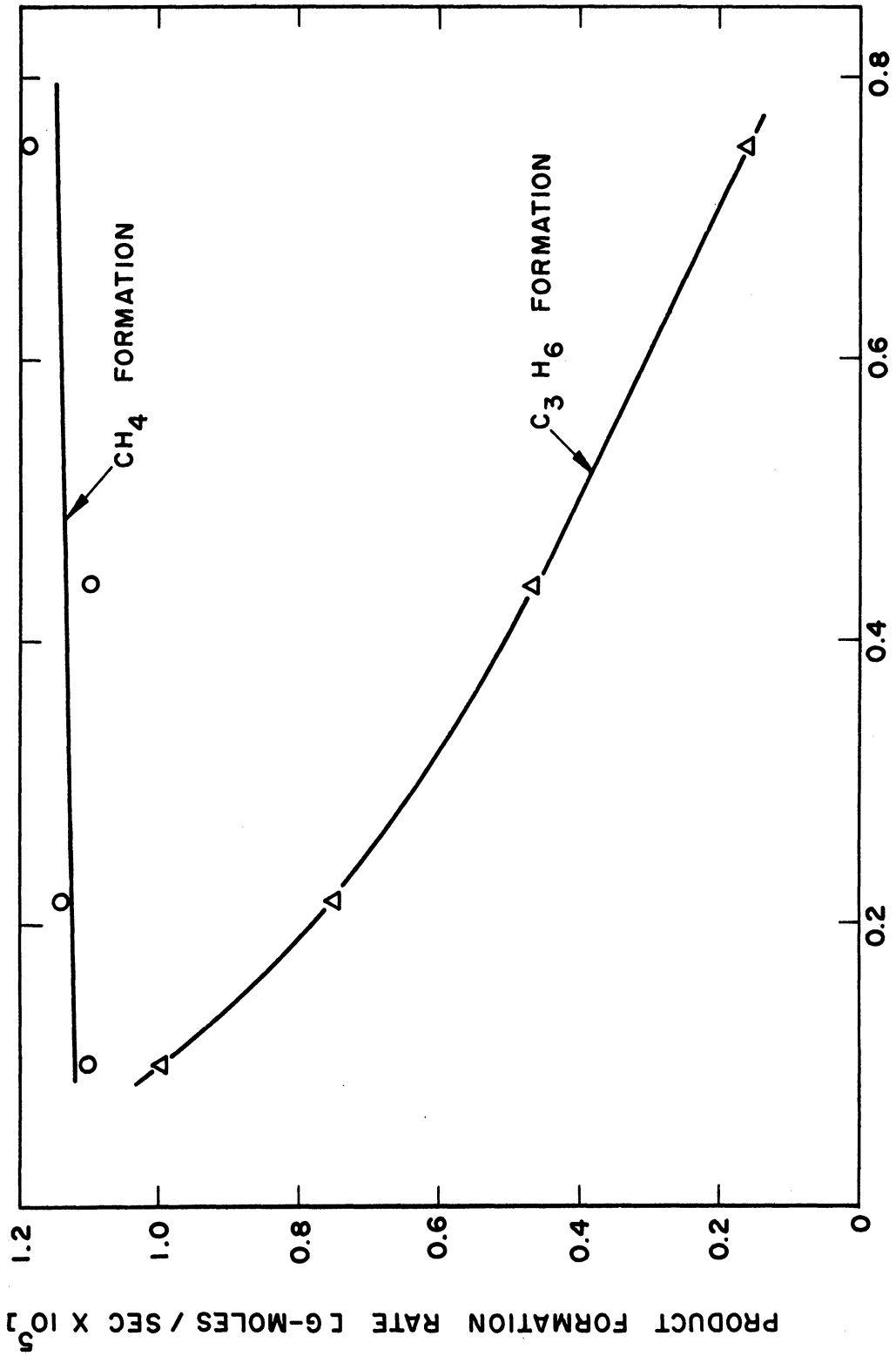

Figure 20. Propylene Inhibition of Propane Decomposition, $T_{max} = 1800°F$.

Similar results were found by Laidler and Wojciechowski[30] on propylene inhibition of hydrocarbon decomposition. Medvedeva et al.[37] note that the propylene will also enter into the reaction by decomposing to ethylene and methane. This is a possible explanation for the fact that propylene does not appear to inhibit the formation of ethylene and methane.

Figure 21 presents the overall effect of propylene inhibition in a somewhat different manner. There, the rate constant for the total disappearance of propane is plotted against the average ratio of propylene-to-propane. (In all the inhibition experiments, this average ratio was used rather than simply the ratio in the feed. It was felt that the average ratio was a more indicative parameter for inhibition than the ratio at the reactor inlet.)

It is seen that the rate constant for propane decomposition falls off very rapidly with increasing amounts of propylene present. The curve has its greatest slope at the lowest propylene-to-propane ratios; therefore, it can be inferred that even slight amounts of propylene could cause considerable reaction inhibition. Such would be the case in the pyrolysis of propane, where even at low conversions propylene is a major reaction product.

Thus, it has been shown that reaction inhibition by propylene can play an important role in the kinetics of propane pyrolysis. This lends some justification to the statements made above (Section IV-A-3) concerning the abnormalities encountered in the overall rate constants. There, propylene inhibition was cited as a possible cause for a) curvature

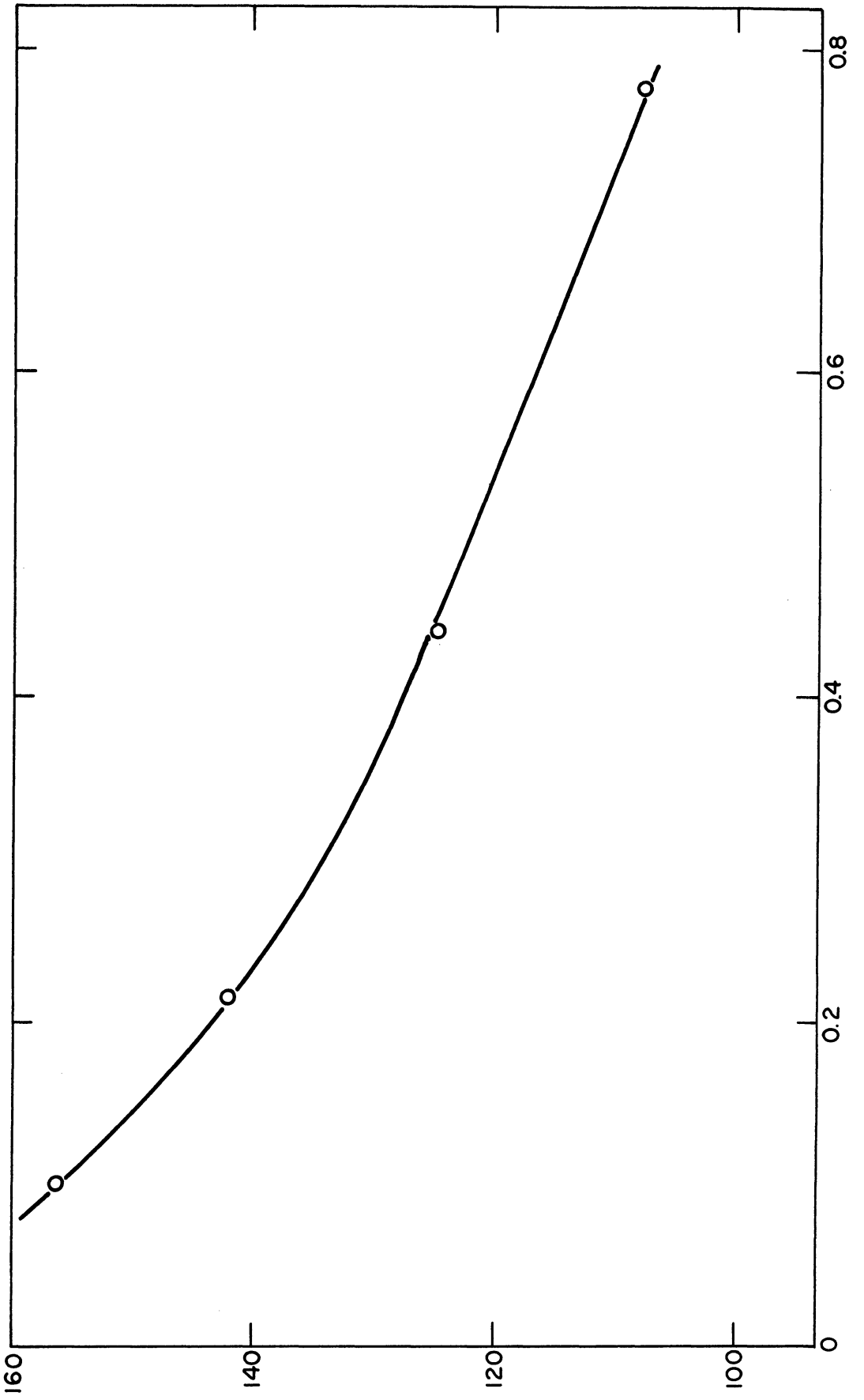

Figure 21. The Effect of Propylene on Propane Decomposition Rate Constants
T_{max} = 1800 °F.

in the Arrhenius plot (cf. Figure 13) and b) previous workers' values of the activation energy being 20% higher. In both cases, the "apparent" decrease of activation energy with increasing temperature can be explained as an effect of inhibition.

The validity of such an explanation is not necessarily proven by the inhibition experiments; however, the hypothesis is, at least, consistent with the results of those runs. The existence of the propylene inhibition also tends to indicate that a free radical mechanism is involved.

V. TEST OF THE KINETIC MODEL

When the experimental phase of this work was completed, the main results (the kinetic parameters for propane decomposition) were programmed on an analog computer. The purpose of the program was to check the validity and reproducibility of the results, and also to provide a simple means of predicting data over a wide range of experimental conditions.

The computer used was an Applied Dynamics, model number AD-2-24PB. The components available for use were 16 amplifiers, 2 function multipliers, 1 Variable Diode Function Generator; also available were a Pace Variplotter which could be used as either an X-Y plotter or a Function Generator, and several dual channel recorders.

The decomposition of propane was shown to follow Equation (16) above,

$$\frac{F}{s}\left[\frac{1 + N_o/F + z}{1 - z}\right]^n dz = \frac{A}{R^n} e^{-E/RT(\ell)}\left[\frac{P(\ell)}{T(\ell)}\right]^n d\ell \qquad (16)$$

or, for a first order reaction,

$$\frac{dz}{d\ell} = \frac{sA}{FR} e^{-E/RT(\ell)}\left[\frac{P(\ell)}{T(\ell)}\right]\left[\frac{1 - z}{1 + N_o/F + z}\right] \qquad (41)$$

Equation (41) readily lends itself to solution on an analog computer, and a flow diagram for one solution is shown in Figure 22. However,

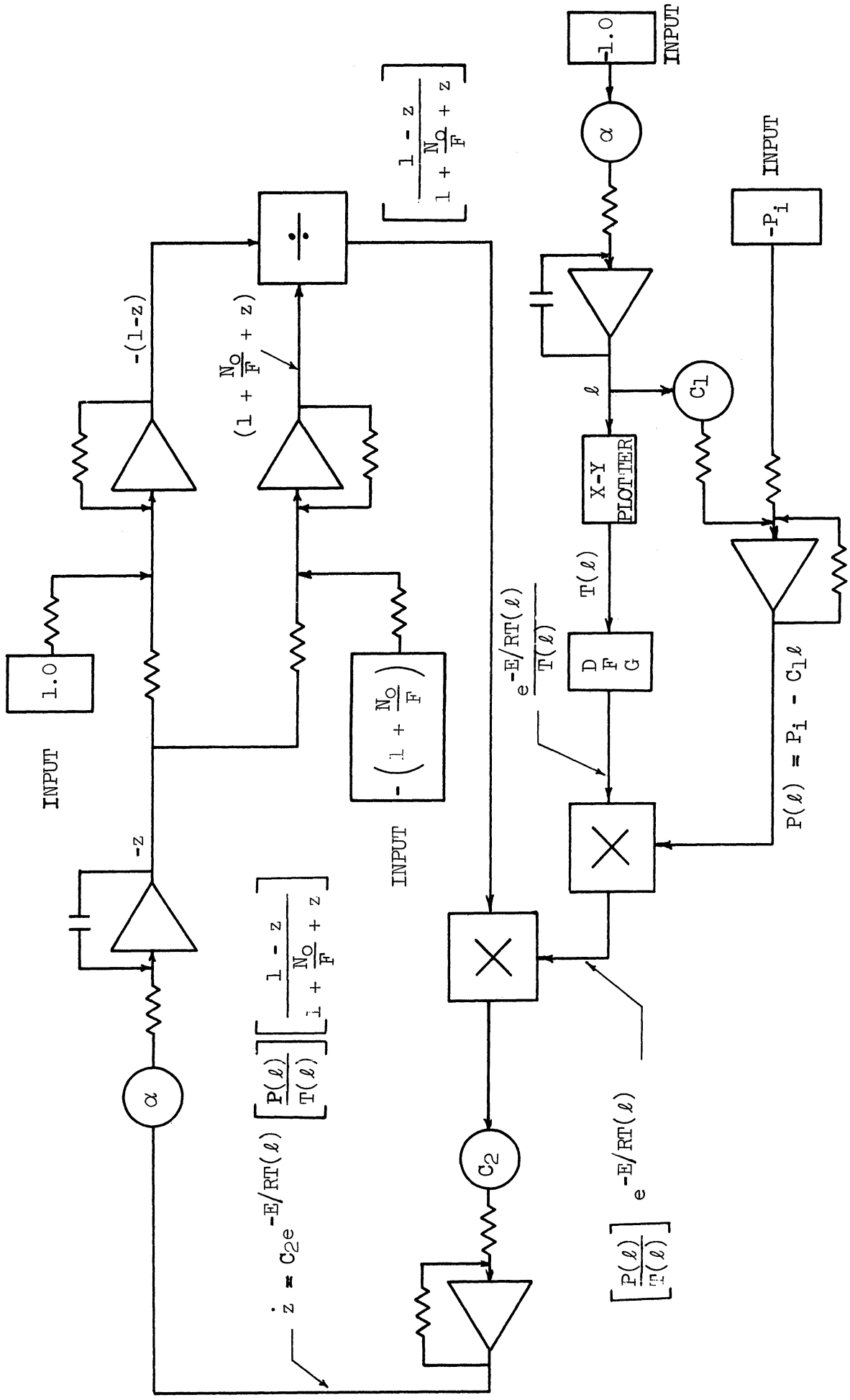

Figure 22. Analog Computer Flow Diagram (Schematic).

two problems prevented the use of that method directly: a) equipment limitations - Figure 22 calls for three function multipliers and only two were available and b) there were serious scaling problems associated with the solution. The actual method of solution is illustrated for one case in Appendix J; the differences are not great, however, and Figure 22 does present the essentials of the solution.

The computer output consists of profiles along the length of the reactor of any of the parameters of the reaction. Among these are the reaction rate, conversion rate, percentage conversion, product distribution, and, indirectly, the rate of change of the reaction rate. At the reactor exit, the percentage conversion and the mole fraction of propane can be checked against the experimental data points.

The general input to the computer consists of the overall kinetic constants and the reactor cross-section and length; in addition, for each run, the temperature and pressure profiles plus the inlet gas feed rates must be supplied.

The temperature profile is fed in through the Function Generator (X-Y plotter). For the pressure profile, the gradient can be assumed linear which makes

$$P(\ell) = P_i - \left[\frac{P_i - P_e}{L}\right] \ell$$

where P_i is the inlet pressure

P_e is the exit pressure

L is the total reactor length

The results for one set of experimental conditions (Run 47) are shown in Figures 23 and 24. Figure 23 shows profiles of the percentage conversion and mole fraction of propane. At the reactor exit are plotted the experimental values of these parameters. In Figure 24, the propane conversion rate throughout the reactor is plotted together with the experimental temperature profile, for comparison.

Programming the experimental results on the analog computer is valuable for several reasons. As mentioned above, it can serve as a check on any of the individual data points. It also serves to show the progress of the reaction in the reactor; this information is often useful and of interest. For example, it can be used to show that longitudinal diffusion effects are negligible (cf., Appendix I).

Another interesting observation is the fact that, in Figure 24, the maximum reaction rate does not coincide with the maximum temperature, but occurs approximately 1 inch before the point of maximum temperature. Although the rate constant is at its maximum at maximum temperatures, the rate of reaction is also proportional to the concentration of reactant, which decreases with length. Hence, this displacement by 1 inch is not at all surprising.

The ability of such a program to predict propane conversions over a much wider range of experimental conditions is another reason

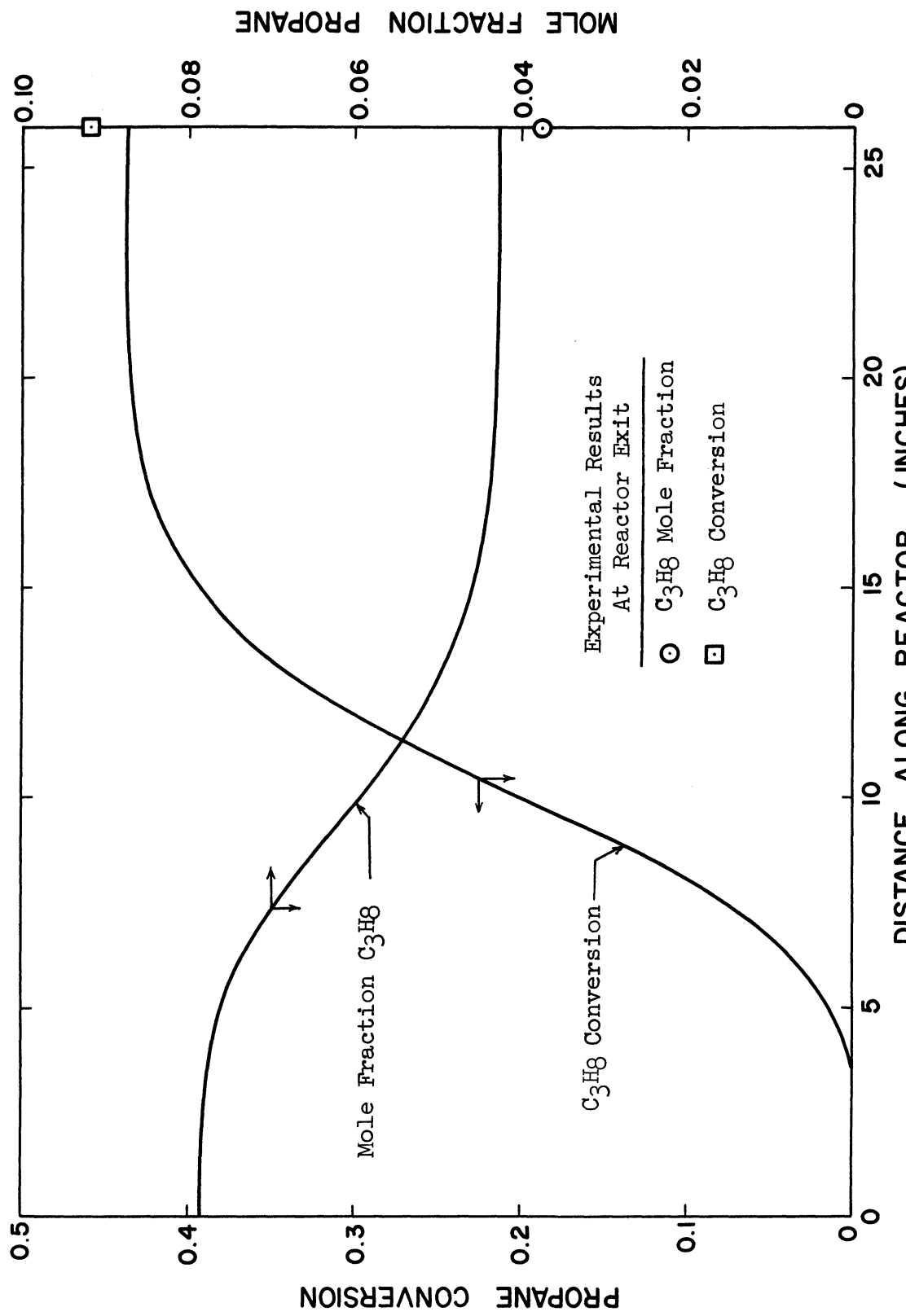

Figure 23. Calculated Propane Conversion and Mole Fraction Profiles; Analog Computer Results - Run 47.

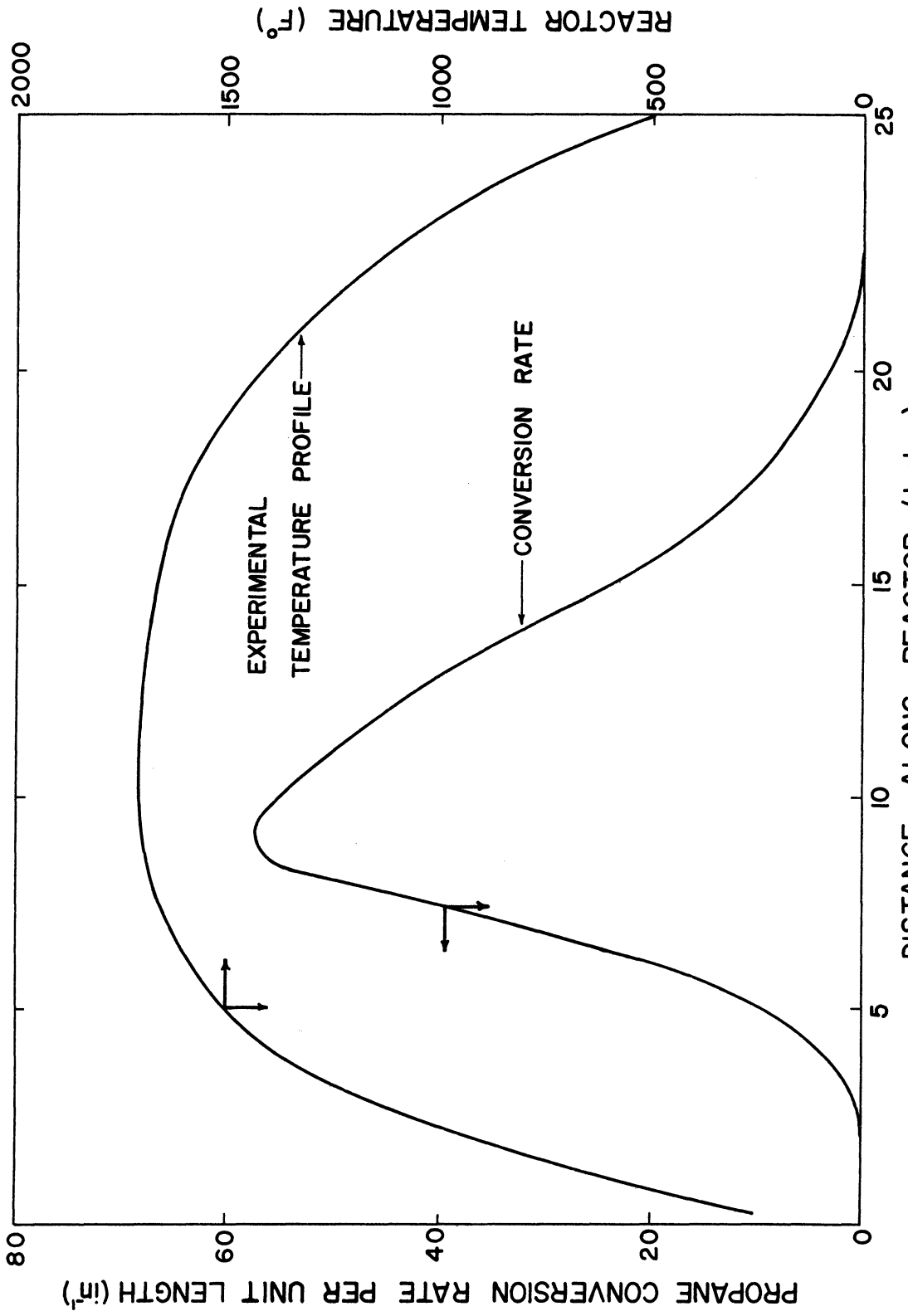

Figure 24. Temperature and Calculated Propane Conversion Rate Profiles; Analog Computer Results - Run 47.

for its importance. Parameters such as temperature, pressure, reactor dimensions, feed rates, etc. could be varied independently or simultaneously, and the effect on the overall conversion noted.

Finally, this program could be used as part of a master program for hydrocarbon pyrolysis. If a larger computer were available, a similar program could be derived to yield not only the total conversion of propane, but also the conversion to each of the desired reaction products. This would involve solving the differential equations,

$$\frac{dz}{d\ell} = \frac{sA_1}{FR\beta} e^{-E_1/RT(\ell)} \left[\frac{P(\ell)}{T(\ell)}\right] \left[\frac{1 - z}{1 + N_o/F + z}\right] \qquad (42)$$

$$\frac{dz}{d\ell} = \frac{sA_2}{FR\delta} e^{-E_2/RT(\ell)} \left[\frac{P(\ell)}{T(\ell)}\right] \left[\frac{1 - z}{1 + N_o/F + z}\right] \qquad (43)$$

Such a solution is trivial once Equation (41) is solved, in the case of propane pyrolysis; however, usually the resulting equations are not as simple as (42) and (43) and require a somewhat larger computer (additional amplifiers and function generators) for solution (cf., Appendix F).

It is then possible to consider the pyrolysis of any of the lower hydrocarbons and to investigate higher conversions, by treating an entire series of parallel and consecutive reactions. For example, upon pyrolysis, propane yields as primary products, methane, ethylene, propylene and hydrogen; further decomposition of methane

would yield carbon and hydrogen. Ethylene would react to form acetylene, hydrogen and butadiene, while propylene yields ethylene, methane, butene and methylacetylene. This chain of events may be carried as far as desired.

The resulting system of parallel, consecutive and reverse reactions presents a formidable problem for manual solution even under isothermal conditions. A large analog computer will handle the problem exactly as it did here and with no difficulty, even for the non-isothermal case. What would be needed are the kinetic parameters for each of the reactions involved in the temperature range under consideration. This study provides the parameters for the two primary reactions of propane decomposition; Towell[61,62] has given similar results for ethylene pyrolysis (in addition to pyrolysis of ethane and acetylene). Information on propylene pyrolysis would be necessary in assembling such an integrated program.

Such an application would be useful not only in checking the validity of all available data, but also to predict optimum conversions and yields in industrial operations. This would be most useful in the production of acetylene, ethylene and/or propylene from saturated hydrocarbons.

VI. CONCLUSIONS AND RECOMMENDATIONS

In this study, a method of treating non-isothermal kinetic data in a complex reaction system was developed. The technique required extensive numerical calculation, but well within the capabilities of a digital computer. Non-isothermal conditions prevailed because the reactions involved were too fast to neglect the heating up and cooling down times. Such a method should be applicable, in general, to many kinds of complicated, non-isothermal, non-isobaric experiments. In analyzing the data, several methods were developed for finding the "best" solution in a set of functional relationships between the variables.

The primary reaction studied was the pyrolysis of propane at high temperatures (800° -1000°C). The kinetics of this reaction had never before been determined at such elevated temperatures, although some product distributions and plant operation data had been published. In addition to the work with propane, some runs were made with propylene and mixtures of propane and propylene as the starting material.

Pyrolysis of propane was found to yield, as primary products, ethylene, methane, propylene and hydrogen, and to be representable stoichiometrically by two parallel reactions,

$$C_3H_8 \rightarrow C_3H_6 + H_2$$

$$C_3H_8 \rightarrow C_2H_4 + CH_4$$

The stoichiometric representation is for convenience in expressing the rate constants, and does not preclude a free radical mechanism.

The reactions were seen to be first order theoretically, and this fact was confirmed experimentally. However, it was equally possible to fit the data to an empirical 1.25 order. Arrhenius rate constants were determined for the individual reactions and the overall decomposition. Distinct curvature of the Arrhenius plot was noted at high temperatures, signifying a decrease in the rate constant. The cause of the curvature was postulated as being inhibition of the free radical reactions by propylene, one of the primary reaction products.

A set of runs was made using a mixed feed of propane and small amounts of propylene (together with nitrogen as diluent) to verify the inhibition effect. It was found that addition of small amounts of propylene inhibits the decomposition of propane quite noticeably. This pronounced effect confirmed the hypothesis that curvature in the rate constant plot was caused by reaction inhibition. It also indicated agreement with all modern theories of hydrocarbon pyrolysis that the reaction mechanism is free radical in nature.

Finally, all the experimental results were used to design a kinetic model for the pyrolysis of propane. This model was used with an analog computer to check results of any individual experiment, and to predict product distributions and conversions beyond the experimental range of this study. Such a model could be used

in an integrated program for hydrocarbon pyrolysis in general. The system would consist of several parallel, consecutive and reverse reactions which would lead to a set of simultaneous (often non-linear) differential equations, solvable on an analog computer.

This model would be able to predict conversions, product distributions, etc. without the restriction to primary reaction products and could be useful in optimization of industrial operations. Along these lines, future work might be done to investigate more fully the pyrolysis of propylene to obtain accurate rate parameters in the high temperature range.

APPENDIX A

RAW EXPERIMENTAL DATA

TABLE III

PRODUCT DISTRIBUTION AND REACTION ORDER RAW DATA

Run no.	34	35	37	38	40	42	66	67	68	69	Feed Gases	
T_{max} (°F)	1514	1514	1511	1509	1520	1517	1803	1824	1815	1802		
Hydrocarbon	C_3H_8	C_3H_8	C_3H_8	C_3H_8	C_3H_8	C_3H_8	C_3H_6	C_3H_6	C_3H_6	C_3H_6	C_3H_8	C_3H_6
Hydrocarbon Feed Rate $\left[\frac{\text{g-moles}}{\text{sec}} \times 10^4\right]$	1.07	1.69	2.43	3.06	3.06	0.67	1.67	2.19	2.56	2.92		
N_2 Feed Rate $\left[\frac{\text{g-moles}}{\text{sec}} \times 10^4\right]$	19.9	19.1	18.5	17.7	17.7	18.4	28.0	26.9	25.6	34.5		
Product Distribution Mole %												
H_2	✓0.140	0.245	0.407	0.614	0.709	0.078	0.149	0.232	0.237	0.103	—	—
CH_4	✓0.111	0.215	0.349	0.548	0.595	0.054	0.173	0.330	0.318	0.176	—	—
C_2H_6	0.005	0.008	0.004	0.010	0.003	—	—	—	—	—	0.36	0.30
C_2H_4	✓0.121	0.231	0.419	0.573	0.612	0.061	0.058	0.111	0.141	0.055	—	—
C_2H_2	—	—	0.010	0.020	0.040	—	0.078	0.146	0.142	0.060	—	—
C_3H_8	4.091	6.476	9.601	12.47	12.85	2.768	—	—	—	—	99.5	0.41
C_3H_6	0.119	0.215	0.341	0.517	0.567	0.073	4.584	5.733	7.368	6.873	—	98.7
C_3H_4	0.008	0.011	—	0.005	—	—	0.184	0.293	0.294	0.145	—	—
C_4H_{10}	—	—	—	—	0.013	0.001	—	—	—	—	0.14	—
C_4H_8	—	—	—	—	—	—	0.051	0.089	0.070	0.048	—	0.52
C_4H_6	—	—	—	—	—	—	—	0.033	0.031	0.023	—	—
C	—	—	0.003	0.025	0.045	—	—	—	—	—	—	—
N_2	95.4	92.6	88.9	85.2	84.6	97.0	94.7	93.0	91.4	92.5	—	—

TABLE IV

RATE CONSTANT RAW DATA

Run no.	24	25	26	27	29	30	31	32	35	47	52	54	57	58	59	60
C_3H_8 feed rate (g-moles/sec) x 10^4	8.80	5.30	4.26	1.93	1.85	2.69	3.57	1.72	1.69	2.33	0.93	0.80	0.82	1.01	1.31	1.42
N_2 feed rate (g-moles/sec) x 10^4	41.5	28.1	17.5	46.4	31.6	30.9	29.9	19.9	19.1	27.4	53.3	55.3	57.0	50.7	40.3	25.2
Reactor inlet pressure (mm Hg)	974	896	834	986	915	915	900	839	839	890	1013	994	1043	1001	927	854
Reactor exit pressure (mm Hg)	742	742	742	740	744	744	734	734	739	728	727	727	740	740	740	740
Product Distribution Mole %																
H_2	1.536	1.571	2.071	0.373	0.483	0.826	1.018	0.437	0.245	2.100	0.228	0.487	0.404	0.449	0.323	0.243
CH_4	1.466	1.615	2.006	0.282	0.409	0.758	0.962	0.461	0.215	1.525	0.165	0.282	0.213	0.266	0.256	0.217
C_2H_6	0.115	0.135	0.130	0.088	0.082	0.110	0.090	0.040	0.008	0.220	0.072	0.131	0.122	0.114	0.067	0.028
C_2H_4	2.114	2.279	2.801	0.188	0.474	1.151	1.399	0.259	0.231	1.930	0.075	0.537	0.295	0.303	0.148	0.019
C_2H_2	—	—	—	0.099	0.056	—	—	0.089	—	0.100	0.085	0.051	0.079	0.081	0.094	0.091
C_3H_8	11.58	9.32	12.79	2.470	3.380	5.038	7.38	5.57	6.48	3.643	1.094	0.529	0.547	1.085	2.260	4.290
C_3H_6	1.141	1.147	1.580	0.268	0.370	0.629	0.814	0.366	0.215	0.919	0.170	0.201	0.172	0.230	0.255	0.230
C_3H_4	—	—	—	0.016	0.011	0.015	0.002	0.034	0.011	0.030	—	0.011	0.011	0.009	0.002	—
C_4H_{10}	0.004	0.003	0.013	—	—	—	0.004	0.009	—	—	0.001	—	0.001	0.003	0.004	0.008
C	—	0.019	—	—	—	—	—	—	—	0.568	—	0.039	0.048	0.059	—	—
N_2	82.0	83.9	78.6	96.2	94.8	91.6	88.4	92.7	92.6	89.8	98.1	97.8	98.1	97.4	96.6	94.9
Temperature (°F) at intervals of 1.045 in.																
	340	290	280	364	462	486	443	510	233	321	182	342	396	522	516	545
	631	545	584	646	761	792	746	842	543	713	449	706	718	805	792	836
	928	820	875	962	1055	1087	1029	1116	858	1063	798	1057	972	1039	1028	1074
	1082	1057	1123	1182	1242	1273	1224	1288	1117	1316	1107	1300	1117	1151	1154	1217
	1166	1190	1264	1300	1359	1382	1335	1397	1273	1459	1268	1431	1188	1217	1234	1312
	1218	1286	1364	1374	1447	1460	1417	1474	1365	1550	1364	1504	1226	1292	1302	1384
	1279	1363	1444	1444	1518	1523	1486	1530	1433	1618	1433	1569	1408	1509	1473	1476
	1376	1442	1507	1520	1575	1578	1549	1567	1479	1671	1507	1642	1609	1619	1579	1537
	1430	1504	1552	1581	1612	1617	1593	1584	1506	1710	1588	1720	1684	1677	1629	1558
	1437	1551	1581	1617	1634	1637	1618	1589	1514	1720	1637	1749	1726	1708	1654	1558
	1456	1579	1593	1636	1637	1641	1628	1589	1514	1719	1663	1767	1751	1727	1668	1553
	1499	1598	1593	1656	1637	1641	1629	1577	1511	1716	1687	1798	1772	1741	1669	1543
	1583	1617	1591	1682	1633	1640	1629	1559	1499	1710	1711	1832	1789	1751	1667	1526
	1621	1635	1588	1693	1622	1631	1622	1533	1477	1696	1739	1843	1797	1751	1659	1502
	1638	1639	1578	1690	1602	1611	1608	1497	1449	1683	1741	1840	1797	1751	1642	1472
	1647	1637	1558	1678	1578	1587	1585	1454	1411	1654	1740	1824	1793	1739	1620	1437
	1650	1627	1534	1651	1543	1551	1551	1402	1373	1624	1723	1801	1783	1719	1592	1397
	1647	1610	1499	1619	1503	1512	1512	1350	1325	1583	1692	1771	1766	1691	1554	1349
	1623	1582	1462	1577	1449	1461	1463	1288	1276	1541	1656	1728	1737	1656	1507	1297
	1589	1548	1409	1525	1387	1403	1407	1221	1216	1479	1602	1677	1697	1609	1454	1235
	1542	1501	1351	1454	1308	1324	1329	1133	1149	1406	1539	1605	1638	1542	1381	1159
	1474	1438	1272	1367	1213	1228	1235	1020	1063	1312	1461	1517	1564	1468	1303	1073
	1412	1349	1169	1277	1123	1129	1141	920	953	1187	1358	1415	1483	1363	1207	971
	1238	1262	1082	1152	964	964	986	725	862	1081	1281	1296	1273	1101	963	742
	1070	1033	841	939	744	747	779	517	676	829	1073	1050	929	786	642	454
	873	810	604	738	526	543	573	336	489	596	879	845	682	583	455	293
	670	595	405	560	360	390	415	205	323	405	686	655	530	420	334	205

TABLE V

MIXED FEED EXPERIMENTS RAW DATA

	Run no.	72	73	74	76
$\left(\frac{\text{g-mole}}{\text{sec}} \times 10^4\right)$	C_3H_8 feed rate	0.78	0.78	0.78	0.78
	C_3H_6 feed rate	—	0.05	0.11	0.28
	N_2 feed rate	62.8	62.8	62.8	63.0
(mm Hg)	Reactor inlet pressure	1050	1050	1050	1053
	Reactor exit pressure	737	737	737	734
Product Distribution Mole %					
	H_2	0.243	0.211	0.175	0.086
	CH_4	0.145	0.153	0.175	0.152
	C_2H_6	0.058	0.058	0.077	0.079
	C_2H_4	0.152	0.170	0.170	0.147
	C_2H_2	0.072	0.070	0.082	0.058
	C_3H_8	0.661	0.693	0.704	0.738
	C_3H_6	0.132	0.220	0.395	0.777
	N_2	98.5	98.4	98.2	98.0
Temperature (°F) at intervals of 1.045 inches		412	495	375	443
		696	784	669	745
		948	1013	950	1009
		1079	1119	1111	1130
		1137	1168	1176	1180
		1178	1211	1216	1221
		1386	1451	1394	1435
		1564	1592	1581	1591
		1656	1675	1671	1676
		1708	1724	1724	1721
		1742	1752	1756	1749
		1767	1773	1777	1768
		1789	1789	1790	1782
		1800	1799	1799	1790
		1802	1797	1803	1792
		1799	1791	1804	1791
		1789	1779	1799	1778
		1768	1759	1781	1754
		1739	1729	1751	1721
		1697	1687	1711	1673
		1640	1633	1658	1614
		1574	1569	1599	1556
		1499	1480	1525	1477
		1275	1222	1316	1259
		965	917	1026	970
		750	712	791	756
		575	548	616	577

APPENDIX B

CALCULATED RESULTS

TABLE VI

PRODUCT DISTRIBUTION RESULTS —— PROPANE FEED

Run no.		34	35	37	38	40	42
T_{max}(°F)		1514	1514	1511	1509	1520	1517
Percentage Conversion		5.7	6.6	7.25	8.25	8.8	4.6
Product Distribution: (moles of product per mole of reacted propane)	H_2	0.565	0.536	0.546	0.548	0.573	0.587
	CH_4	0.448	0.471	0.465	0.489	0.481	0.405
	C_2H_6	0.020	0.018	0.005	0.009	0.002	—
	C_2H_4	0.448	0.506	0.558	0.511	0.495	0.459
	C_2H_2	—	—	0.013	0.018	0.032	—
	C_3H_6	0.480	0.470	0.455	0.461	0.458	0.549
	C_3H_4	0.032	0.024	—	0.004	—	—
	C	—	—	0.004	0.023	0.036	—

TABLE VII

RESULTS OF REACTION ORDER EXPERIMENTS

Run no.	34	35	37	38
T_{max} (°F)	1514	1514	1511	1509
Mole fraction propane:				
reactor inlet	0.0435	0.0698	0.1042	0.1375
reactor exit	0.0409	0.0648	0.0960	0.1247
average	0.0422	0.0673	0.1001	0.1311
Reaction rates ($\frac{\text{g-moles}}{\text{sec}} \times 10^5$):				
propane disappearance	0.630	1.113	1.76	2.42
propylene formation	0.320	0.562	0.880	1.19
methane formation	0.294	0.525	0.820	1.18

TABLE VIII

RESULTS OF RATE CONSTANT EXPERIMENTS

Run no.	T_{max} (°F)	$\frac{1}{T_{max}} \times 10^4$ (°K^{-1})	Rate Constant: First order fit (sec^{-1})			Rate Constant: 1.25 order fit $\left[\frac{\text{liters}^{1/4}}{\text{g-mole}^{1/4} \cdot \text{sec}}\right]$
			C_3H_8 disappearance	C_3H_6 formation	CH_4 formation	C_3H_8 disappearance
24	1650	8.53	52.2	27.5	30.7	355.
25	1639	8.58	53.0	23.4	29.0	318.
26	1593	8.77	25.7	12.6	12.5	161.
27	1693	8.36	69.6	35.3	34.2	523.
29	1637	8.58	42.2	18.8	22.0	293.
30	1641	8.57	43.2	22.1	26.0	305.
31	1629	8.62	37.8	18.4	19.0	255.
32	1589	8.78	24.0	10.6	10.5	141.
35	1514	9.12	8.6	4.3	4.5	51.9
47	1720	8.26	97.0	46.8	56.0	727.
52	1741	8.18	107.	52.0	51.5	964.
54	1843	7.82	270.	121.	161.	3520.
57	1797	7.97	193.	92.0	104.	2230.
58	1751	8.14	128.	58.4	67.3	1080.
59	1669	8.46	53.8	25.7	27.4	428.
60	1558	8.92	15.4	7.6	7.6	104.5

TABLE IX

PRODUCT DISTRIBUTION RESULTS ——

PROPYLENE FEED

Run no.		66	67	68	69
T_{max} (°F)		1803	1824	1815	1802
Percentage Conversion		8.4	11.8	10.9	5.2
Product Distribution : (moles of product per mole of reacted propylene)	H_2	0.354	0.302	0.264	0.275
	CH_4	0.412	0.430	0.354	0.471
	C_2H_4	0.138	0.144	0.156	0.148
	C_2H_2	0.186	0.190	0.158	0.160
	C_3H_4	0.438	0.382	0.327	0.388
	C_4H_8	0.121	0.116	0.078	0.128
	C_4H_6	—	0.043	0.034	0.062

TABLE X

RESULTS OF MIXED FEED EXPERIMENTS

Run no.	72	73	74	76
T_{max} (°F)	1802	1799	1804	1792
Percentage Conversion	42.7	33.6	32.5	26.0
Reaction rate $\left(\frac{\text{g-moles}}{\text{sec}} \times 10^5\right)$:				
CH_4 formation	1.10	1.14	1.31	1.19
C_3H_6 formation	1.00	0.75	0.47	0.16
Propane-to-Propylene ratio:				
Reactor inlet	0	0.114	0.318	0.501
Reactor exit	0.200	0.318	0.562	1.052
Average	0.100	0.216	0.440	0.776
Propane disappearance rate constant (sec^{-1}):				
at T_{max}	158.2	141.2	128.8	99.2
corrected to 1800°F	156.0	142.0	124.8	106.0

APPENDIX C

THE EFFECT OF REVERSE REACTIONS

In deriving the kinetic equations, it was assumed that all reactions could be considered irreversible. It will be shown here that such an assumption is completely justified from thermodynamic considerations.

The equilibrium constants for all the important reactions were presented in Figure 1 as functions of temperature. Of the two main reactions involved,

$$C_3H_8 \rightleftharpoons C_3H_6 + H_2 \qquad (1)$$

$$C_3H_8 \rightleftharpoons C_2H_4 + CH_4 \qquad (2)$$

it is seen that the second has so high an equilibrium constant that reverse reaction is out of the question. The first reaction, however, could conceivably have an appreciable amount of reversibility, especially at lower temperatures. Therefore, the data of one of the lowest temperature runs (Run 35) was examined for this effect.

The rate of formation of propylene and hydrogen from propane can be expressed as

$$\text{rate} = k_1 \left([C_3H_8] - \frac{[C_3H_6][H_2]}{K_{p_1}} \right) \qquad (44)$$

where k_1 is the rate constant, K_{p_1} is the equilibrium constant and the brackets denote the partial pressures of the components. When an irreversible reaction is assumed, the term $[C_3H_6][H_2]/K_{p_1}$ is neglected and the rate equation is simply

$$\text{rate} = k_1 [C_3H_8]$$

The reverse reaction can be neglected then, if

$$\frac{[C_3H_8]}{[C_3H_6][H_2]/K_{p_1}} \ll 1 \qquad (45)$$

at temperatures where the rate constant is appreciable.

As a first approximation, the exit gas analysis will be used in Equation (45) at the point of maximum reaction rate (i.e., maximum temperature) of Run 35.

$T_{max} = 1514°F$ $\qquad$ $x_{C_3H_8} = .06476$

$P = 789$ mm Hg $= 1.04$ atm $\qquad$ $x_{C_3H_6} = .00215$

$K_{p_1} = 10^{1.04} = 11.0$ $\qquad$ $x_{H_2} = .00245$

Therefore, the partial pressures in atmospheres are,

$$[C_3H_8] = .0672, \quad [C_3H_6] = .00223, \quad [H_2] = .00254$$

and

$$\frac{[C_3H_8]}{[C_3H_6][H_2]/K_{p_1}} = 1.3 \times 10^{-5} = 0.0013\%$$

While it is true that this ratio would be considerably higher close to room temperature, that case need not be considered since then the rate constant would be nil.

Similar results are obtained with any of the experimental runs and it is therefore concluded that the assumption of irreversible reactions is valid.

APPENDIX D

EQUIVALENT TEMPERATURES IN A NON-ISOTHERMAL KINETIC EXPERIMENT

In a non-isothermal kinetic experiment, there is a great temptation to assume some constant, "equivalent temperature" for the entire run in calculating the rate constants. Unfortunately, because of the exponential temperature dependence of the rate constants, an equivalent temperature can not be calculated by simply taking the area under the temperature profile. From the theory developed above (Section II-F) it is seen that the temperature dependence of the reaction rate is

$$\text{rate} \quad \alpha \quad \frac{e^{-E/RT(\ell)}}{T(\ell)^n}$$

or, for a first order reaction,

$$\text{rate} \quad \alpha \quad \frac{e^{-E/RT(\ell)}}{T(\ell)}$$

Thus, an equivalent temperature, T_{eq}, is one for which

$$\frac{e^{-E/RT_{eq}}}{T_{eq}} \Delta\ell = \int_0^L \frac{e^{-E/RT(\ell)}}{T(\ell)} \, d\ell$$

Two such equivalent temperatures are shown in Figure 25 -- one for the entire length and one for a portion of the reactor. The method of calculation is to choose a profile A or B in Figure 25b which has the same area under it as the experimental profile; then the profile can be transformed to temperature units in Figure 25a. Obviously, the activation energy E (which is one of the results of the kinetic study)

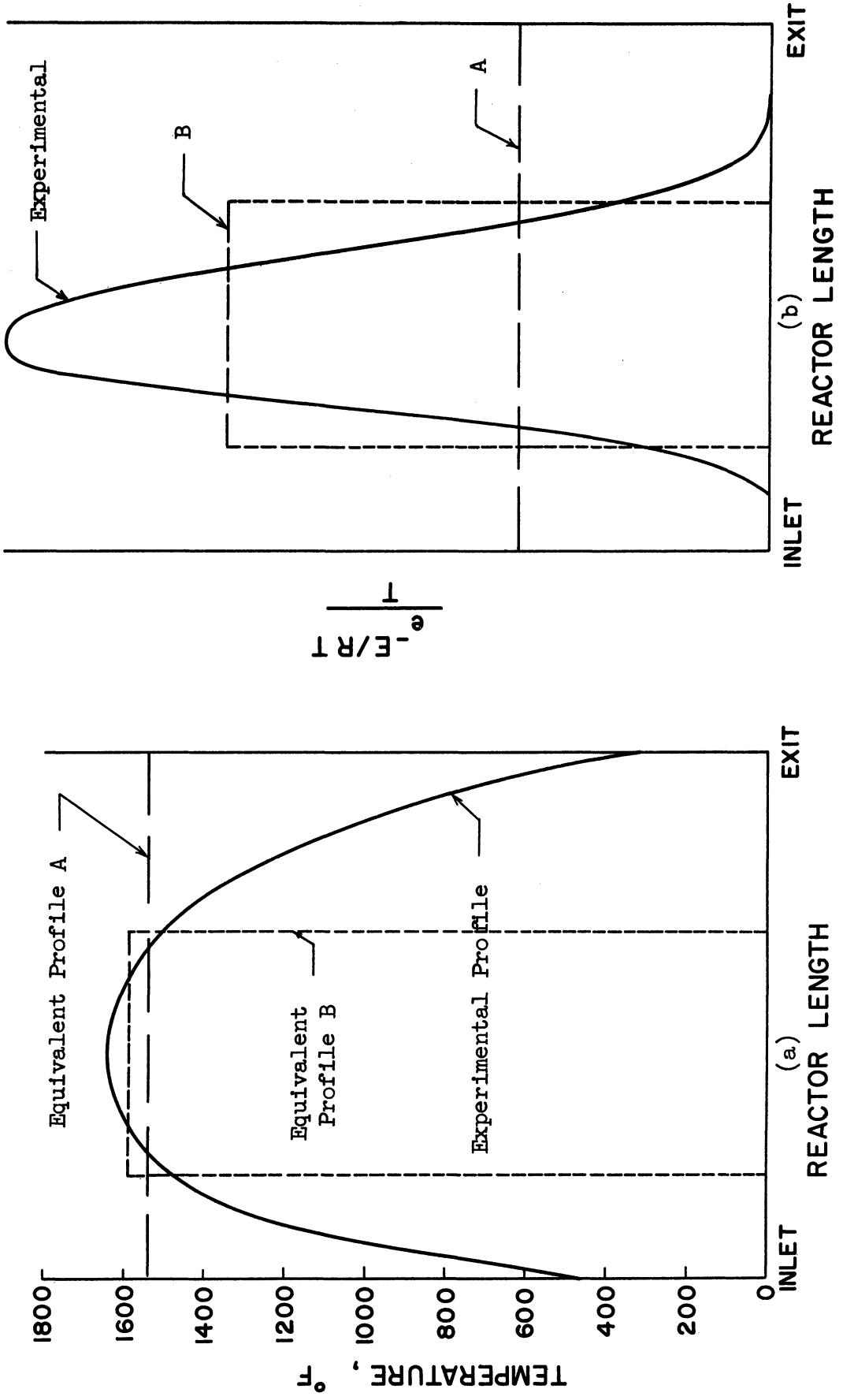

Figure 25. Equivalent Temperature Profiles - Run 29.

must be known to perform this operation, and a trial and error process is necessary in finding an equivalent temperature.

A fair approximation to T_{eq} can be obtained if the general order of magnitude of E is known; however, such a method would offer no advantage over the direct approach developed in the theoretical section of this paper.

APPENDIX E

DETERMINATION OF THE PRESSURE PROFILE, $P(\ell)$

Solution of the rate equation for this system requires knowledge of the pressure profile, $P(\ell)$, along the length of the reactor. Known experimentally are the pressures at the inlet and exit of the reactor for each run. A linear profile was used in the calculations and its use will be justified here.

First, for one particular run the pressure profile was calculated step-by-step through the reactor. The equations describing the pressure drop are:

$$\frac{\Delta P}{\Delta L} = \frac{2fG^2}{g_c D_e \rho} = \varphi_1(f, G, D_e, \rho) \tag{46}$$

$$f = \varphi_2(D_e, G, \mu) \tag{47}$$

$$\mu = \varphi_3(T) \tag{48}$$

$$\rho = \frac{P}{RT} \cdot \overline{MW} = \varphi_4(P, T) \tag{49}$$

where

f is the friction factor

G is the mass flow rate [lb/hr-ft^2]

D_e is the equivalent reactor diameter [ft]

ρ is the gas density [lb/ft^3]

μ is the gas viscosity [lb/hr-ft]

and the functions in Equations (47) and (48) are available in graphical form.

Thus, if the inlet pressure to the reactor and the entire temperature profile are known for any run, the pressure profile can be calculated by a stepwise progression through the reactor. The result of such an analysis is shown by the curve in Figure 26 labeled "Actual Pressure Profile;" the results for all other experimental runs are similar. Note that the pressure gradient, $dP/d\ell$, is at a maximum near the center of the reactor, as would be expected, since the temperature is highest there.

It was unnecessary to perform such an analysis for every run because it was then shown that assumption of a linear profile introduces virtually no error. The calculation of rate constants was performed on a set of experimental runs in which first a linear pressure profile was assumed, and then the actual profile was used. The difference in the final results was barely measurable; in fact, even a mean, constant pressure could have been used with no appreciable error. This is true because at the center of the reactor, where the rate is highest, the three profiles in Figure 26 give approximately the same pressure.

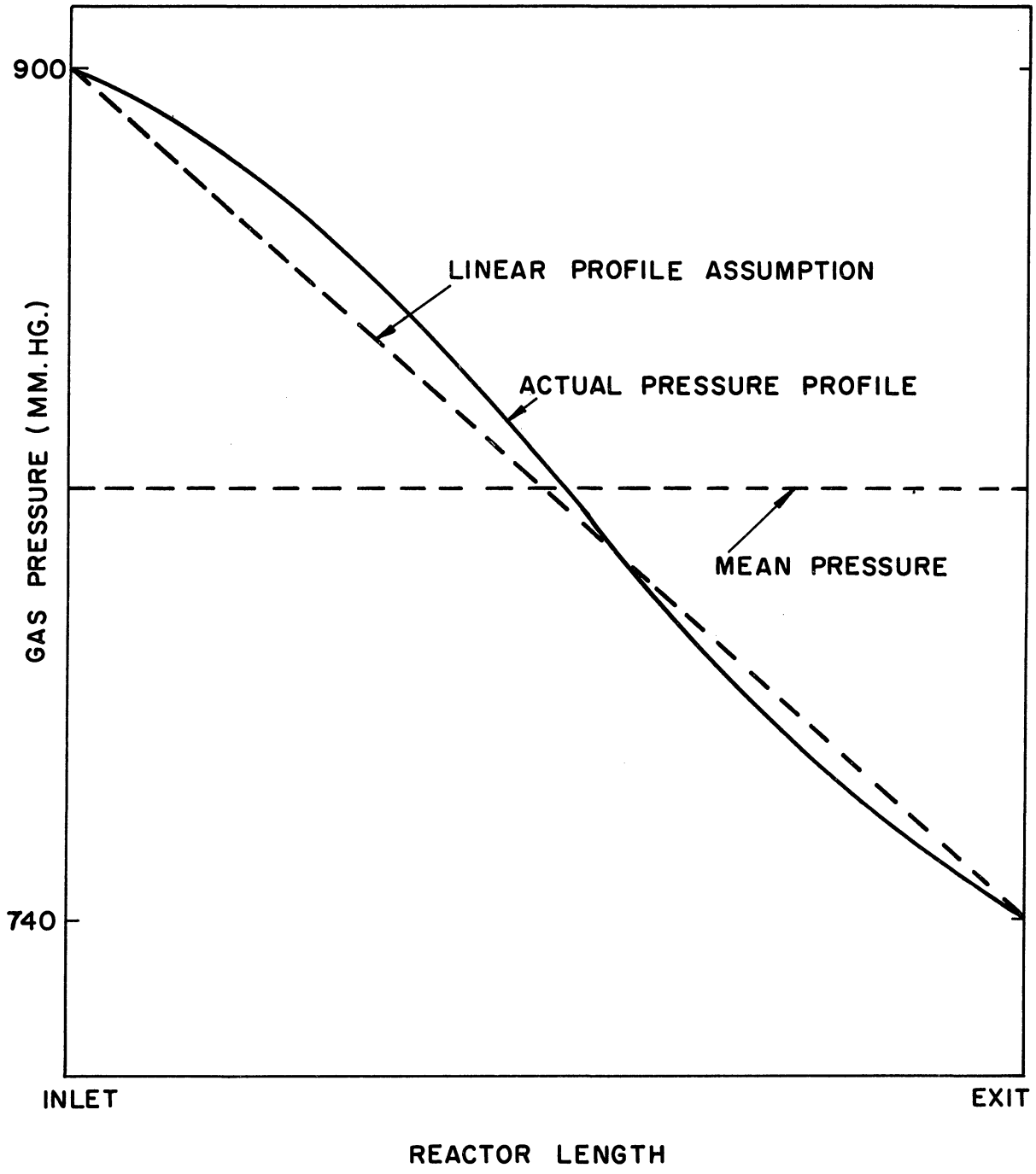

Figure 26. Determination of Pressure Profiles along the Reactor.

APPENDIX F

MODIFICATIONS FOR SIMULTANEOUS REACTIONS

The rate equations, as developed in Section II-F, were derived for the case of decomposition of the form

$$C_3H_8 \rightarrow B + C$$

and led to the relationship between the parameters

$$A = \frac{\frac{FR^n}{s}\int_o^{z_e}\left[\frac{1 + N_o/F + z}{1 - z}\right]^n dz}{\int_o^L e^{-E/RT(\ell)}\left[\frac{P(\ell)}{T(\ell)}\right]^n d\ell} \tag{18}$$

Consider, now, the more general case of two simultaneous reactions with an arbitrary number of reaction products

$$A \xrightarrow{k_1} B + C + \ldots \quad \text{(u products)}$$

$$A \xrightarrow{k_2} D + E + \ldots \quad \text{(v products)}$$

If the overall conversion of A is z, then let the conversion to B, C, ... be βz and to D, E, ... be δz, where β and δ are fractions whose sum is unity.

Then, for the first reaction, Equation (9) is replaced by

$$\frac{dm_1}{sd\ell} = A_1 e^{-E_1/RT(\ell)}\left[\frac{xP(\ell)}{RT(\ell)}\right]^{n_1} \tag{50}$$

where m_1 is the flow rate of material B or C or ... $\left[\frac{\text{g-moles}}{\text{sec}}\right]$

Now,

$$m_1 = F(\beta z)$$

and

$$dm_1 = \beta F dz \tag{51}$$

From the stoichiometry of the reaction,

$$x = \frac{F(1 - z)}{F(1 - z + u\beta z + v\delta z) + N_o}$$

$$= \frac{1 - z}{1 + N_o/F + (u\beta + v\delta - 1)z} \qquad (52)$$

Substituting (51) and (52), in Equation (50)

$$\frac{\beta F}{s}\left[\frac{1 + N_o/F + (u\beta + v\delta - 1)z}{1 - z}\right]^{n_1} dz = \frac{A_1}{R^n} e^{-E_1/RT(\ell)}\left[\frac{P(\ell)}{T(\ell)}\right]^{n_1} d\ell$$

and integrating along the length of the reactor,

$$A_1 = \frac{\frac{FR^{n_1}}{s}\beta \int_o^{z_e}\left[\frac{1 + N_o/F + (u\beta + v\delta - 1)z}{1 - z}\right]^{n_1} dz}{\int_o^{L} e^{-E_1/RT(\ell)}\left[\frac{P(\ell)}{T(\ell)}\right]^{n_1} d\ell} \qquad (53)$$

Similarly, for the second reaction,

$$A_2 = \frac{\frac{FR^{n_2}}{s}\delta \int_o^{z_e}\left[\frac{1 + N_o/F + (u\beta + v\delta - 1)z}{1 - z}\right]^{n_2} dz}{\int_o^{L} e^{-E_2/RT(\ell)}\left[\frac{P(\ell)}{T(\ell)}\right]^{n_2} d\ell} \qquad (54)$$

Treatment of the data to find the best values of A_1, E_1, A_2, E_2 is exactly analogous to the treatment of Equation (18) for the case of one reaction. The important fact is that the pre-exponential factor A_1 or A_2 can still be expressed linearly as

$$\log A_1 = u_i + v_i E$$

or

$$\log A_2 = u_j + v_j E$$

The remainder of the analysis follows Section II-G.

APPENDIX G

DERIVATION OF AVERAGING TECHNIQUES

In Section II-G, three methods were developed for determining the best values of the constants A and E which are functionally related by

$$\begin{array}{rcl} \log A &=& u_1 + v_1 E \\ \vdots & & \vdots \\ \log A &=& u_i + v_i E \\ \vdots & & \vdots \\ \log A &=& u_N + v_N E \end{array} \qquad (55)$$

Each of Equations (55) above represents the data of a single experimental run. Such a set was illustrated schematically in Figure 6.

The center of gravity method states that the best point (E, log A) is that point from which the sum of the squares of the distances to all the intersection points is a minimum. It will be shown that this corresponds to the center of gravity of the intersection points.

The square of the distance between a point (x, y) and one of the intersection points (x_i, y_i) is

$$\begin{aligned} s_i^2 &= (x - x_i)^2 + (y - y_i)^2 \\ &= x^2 + y^2 - 2xx_i - 2yy_i + x_i^2 + y_i^2 \end{aligned}$$

and the sum of the squares of the distances to all the intersection points is

$$\Sigma s_i^2 = N'x^2 + N'y^2 + \Sigma x_i^2 + \Sigma y_i^2 - 2x\Sigma x_i - 2y\Sigma y_i$$

where N' is the number of intersection points.

The point (x, y) for which this sum is a minimum is obtained by setting

$$\frac{\partial \Sigma s_i^2}{\partial x} = \frac{\partial \Sigma s_i^2}{\partial y} = 0 .$$

The results are:

$$x = \frac{\Sigma x_i}{N'} ; \quad y = \frac{\Sigma y_i}{N'}$$

or, the best point is simply the center of gravity of the intersection points.

Since the intersection of any two lines,

$$\log A = u_1 + v_1 E$$

$$\log A = u_2 + v_2 E$$

is

$$E = \frac{u_2 - u_1}{v_1 - v_2} ; \quad \log A = \frac{v_2 u_1 - v_1 u_2}{v_2 - v_1}$$

the best values of E and $\log A$ by this method are

$$E = \frac{2}{N(N-1)} \sum_{i=1}^{N} \sum_{j=i+1}^{N} \frac{u_j - u_i}{v_i - v_j} \tag{28}$$

$$\log A = \frac{2}{N(N-1)} \sum_{i=1}^{N} \sum_{j=i+1}^{N} \frac{v_j u_i - v_i u_j}{v_j - v_i} \tag{29}$$

where N is the number of runs (lines) and $N(N-1)/2$ is the number of intersection points.

Alternatively, the minimum distance method states that the best point $P(x, y)$ is that one for which the sum of the squares of the distances to all the lines $(y = u_i + v_i x)$ is a minimum. The distance squared between a point (x,y) and a line $(y = u_i + v_i x)$ is given

$$s_i^2 = \frac{(v_i x - y + u_i)^2}{v_i^2 + 1}$$

The sum of the squares of the distances to all the lines is then

$$\sum s_i^2 = x^2 \sum_{i=1}^{N} \frac{v_i^2}{v_i^2+1} + 2x \sum_{i=1}^{N} \frac{u_i v_i}{v_i^2+1} - 2xy \sum_{i=1}^{N} \frac{v_i}{v_i^2+1}$$

$$- 2y \sum_{i=1}^{N} \frac{u_i}{v_i^2+1} + y^2 \sum_{i=1}^{N} \frac{1}{v_i^2+1} + \sum_{i=1}^{N} \frac{u_i^2}{v_i^2+1} \qquad (56)$$

$\sum s_i^2$ can be minimized by setting the derivatives $\frac{\partial \sum s_i^2}{\partial x}$ and $\frac{\partial \sum s_i^2}{\partial y}$ equal to zero, which yields two equations

$$x \sum_{i=1}^{N} \frac{v_i^2}{v_i^2+1} - y \sum_{i=1}^{N} \frac{v_i}{v_i^2+1} + \sum_{i=1}^{N} \frac{u_i v_i}{v_i^2+1} = 0$$

$$x \sum_{i=1}^{N} \frac{v_i}{v_i^2+1} - y \sum_{i=1}^{N} \frac{1}{v_i^2+1} + \sum_{i=1}^{N} \frac{u_i}{v_i^2+1} = 0$$

Solving,

$$x = \frac{\sum_{i=1}^{N} \frac{v_i}{v_i^2+1} \sum_{i=1}^{N} \frac{u_i}{v_i^2+1} - \sum_{i=1}^{N} \frac{u_i v_i}{v_i^2+1} \sum_{i=1}^{N} \frac{1}{v_i^2+1}}{\sum_{i=1}^{N} \frac{v_i^2}{v_i^2+1} \sum_{i=1}^{N} \frac{1}{v_i^2+1} - \left(\sum_{i=1}^{N} \frac{v_i}{v_i^2+1} \right)^2}$$

$$y = \frac{\sum_{i=1}^{N} \frac{v_i^2}{v_i^2+1} \sum_{i=1}^{N} \frac{u_i}{v_i^2+1} - \sum_{i=1}^{N} \frac{v_i}{v_i^2+1} \sum_{i=1}^{N} \frac{u_i v_i}{v_i^2+1}}{\sum_{i=1}^{N} \frac{v_i^2}{v_i^2+1} \sum_{i=1}^{N} \frac{1}{v_i^2+1} - \left(\sum_{i=1}^{N} \frac{v_i}{v_i^2+1} \right)^2}$$

The point (x,y) is, of course, equivalent to the point of best fit (E, log A).

Finally, an overall least squares fit of the data is possible. The Equations (55) are rearranged to

$$\begin{aligned} u_1 &= \log A + (-E)\, v_1 \\ &\vdots \\ u_i &= \log A + (-E)\, v_i \\ &\vdots \\ u_N &= \log A + (-E)\, v_N \end{aligned} \tag{57}$$

Note that this is precisely the form in which a set of experimental data, u as a function of v, would be put in order to determine their functional relationship by fitting two constants, log A and E. The fact that this is an artificial function is of no consequence.

Log A and E can easily be deduced from Equations (57) by defining the deviation

$$\Delta^2 = [u_i - (\log A + (-E)\, v_i)]^2 \tag{58}$$

for any particular run and taking the sum over all the runs. For a summation over N runs,

$$\sum \Delta^2 = \sum_{i=1}^{N} u_i^2 + N(\log A)^2 + E^2 \sum_{i=1}^{N} v_i^2 - 2(\log A) \sum_{i=1}^{N} u_i + 2E \sum_{i=1}^{N} u_i v_i - 2(\log A)\, E \sum_{i=1}^{N} v_i$$

The optimum values of E and log A are obtained by setting the derivatives $\frac{\partial \sum \Delta^2}{\partial E}$ and $\frac{\partial \sum \Delta^2}{\partial \log A}$ equal to zero. Then,

$$E = \frac{\sum_{i=1}^{N} u_i \sum_{i=1}^{N} v_i - N \sum_{i=1}^{N} u_i v_i}{N \sum_{i=1}^{N} v_i^2 - \left(\sum_{i=1}^{N} v_i \right)^2}$$

$$\log A = \frac{\sum_{i=1}^{N} u_i \sum_{i=1}^{N} v_i^2 - \sum_{i=1}^{N} u_i v_i \sum_{i=1}^{N} v_i}{N \sum_{i=1}^{N} v_i^2 - \left(\sum_{i=1}^{N} v_i \right)^2}$$

A closer look at Equation (58) points out a minor, but interesting fact. What is actually being minimized in this program is (under the guise of a least squares analysis) simply the square of the vertical distance between a point and the experimental lines,

$$\Delta^2 = [\log A - (u_i + v_i E)]^2$$

This is certainly why the overall least squares method gave results so much in agreement with those of the minimum distance method.

APPENDIX H

DEVELOPMENT OF RATE EQUATIONS FROM FREE RADICAL REACTIONS

The individual free radical reactions for propane pyrolysis, as postulated by Laidler, Sagert and Wojciechowski[29] are:

$$M + C_3H_8 \xrightarrow{k_1} CH_3 + C_2H_5 + M \qquad \text{(I)}$$

$$C_2H_5 + C_3H_8 \xrightarrow{k_2} C_2H_6 + C_3H_7 \qquad \text{(II)}$$

$$H + C_3H_8 \xrightarrow{k_3} C_3H_7 + H_2 \qquad \text{(III)}$$

$$CH_3 + C_3H_8 \xrightarrow{k_4} C_3H_7 + CH_4 \qquad \text{(IV)}$$

$$C_3H_7 \xrightarrow{k_5} CH_3 + C_2H_4 \qquad \text{(V)}$$

$$C_3H_7 \xrightarrow{k_6} H + C_3H_6 \qquad \text{(VI)}$$

$$M + C_3H_7 + CH_3 \xrightarrow{k_7} CH_4 + C_3H_6 + M \qquad \text{(VII)}$$

$$\text{OR} \quad M + 2CH_3 \xrightarrow{k_8} C_2H_6 + M \qquad \text{(VIII)}$$

In these reactions, M represents another body necessary for the reaction to take place. Ordinarily, this would be another molecule of propane.

Reactions (VII) and (VIII) represent alternate methods of chain termination. It will be shown that (VII) leads to first order kinetics and (VIII) leads to 1.5 order kinetics.

The theoretical order for this, or any, model is obtained by using the steady-state approximation. That is, at steady-state the rate of change of any of the free radicals with time is zero. For example,

from the system of free radical reactions above with termination via reaction (VII),

$$\frac{d[H]}{dt} = k_6[C_3H_7] - k_3[H][C_3H_8] = 0$$

$$\frac{d[C_3H_7]}{dt} = k_2[C_2H_5][C_3H_8] + k_3[H][C_3H_8] + k_4[CH_3][C_3H_8]$$

$$- k_5[C_3H_7] - k_6[C_3H_7] - k_7[CH_3][C_3H_7][C_3H_8] = 0$$

$$\frac{d[CH_3]}{dt} = k_1[C_3H_8]^2 - k_4[C_3H_8][CH_3] + k_5[C_3H_7]$$

$$- k_7[CH_3][C_3H_7][C_3H_8] = 0$$

$$\frac{d[C_2H_5]}{dt} = k_1[C_3H_8]^2 - k_2[C_3H_8][C_2H_5] = 0$$

These four equations can be solved for the four steady-state radical concentrations

$$[H]_{ss} = \frac{k_6}{k_3}\sqrt{\frac{k_4k_1}{k_5k_7}}$$

$$[C_3H_7]_{ss} = \sqrt{\frac{k_4k_1}{k_5k_7}}\,[C_3H_8]$$

$$[CH_3]_{ss} = \sqrt{\frac{k_1k_5}{k_4k_7}}$$

$$[C_2H_5]_{ss} = \frac{k_1}{k_2}[C_3H_8]$$

From these concentrations it can be shown that

$$-\frac{d[C_3H_8]}{dt} = (k_5 + k_6)\sqrt{\frac{k_4k_1}{k_5k_7}}\,[C_3H_8] \qquad (59)$$

Equation (59) shows, therefore, that such a model predicts first order kinetics.

If, on the other hand, reaction (VIII) is chosen as the chain termination step, a steady-state analysis yields for the radical concentrations

$$[H]_{ss} = \frac{k_4 k_6}{k_3 k_5}\sqrt{\frac{2k_1}{k_8}}\,[C_3H_8]^{1/2}$$

$$[C_3H_7]_{ss} = \frac{k_4}{k_5}\sqrt{\frac{2k_1}{k_8}}\,[C_3H_8]^{3/2}$$

$$[CH_3]_{ss} = \sqrt{\frac{2k_1}{k_8}}\,[C_3H_8]^{1/2}$$

$$[C_2H_5]_{ss} = \frac{k_1}{k_2}\,[C_3H_8]$$

Again, the total disappearance rate of propane can then be calculated, and

$$-\frac{d[C_3H_8]}{dt} = \frac{k_4}{k_5}\sqrt{\frac{2k_1}{k_8}}\,(k_5 + k_6)\,[C_3H_8]^{3/2} \qquad (60)$$

Thus, it is seen that chain termination via reaction (VIII) leads to 3/2 order kinetics.

The dependence of the overall order of reaction upon the chain initiation and termination steps has been presented, in general, by Goldfinger et al.[21] They consider two kinds of free radicals: unimolecular, denoted by μ and bimolecular, denoted by β. A μ-type free radical can react by itself, while a β-type can not. Looking at reactions (I) through (VIII) above, it is seen that C_3H_7 is a μ-type free radical (reactions (V) and (VI)) while CH_3 is a β-type (reaction (IV)).

Also possible are two kinds of chain terminations: simple —— where two free radicals simply react, and third body —— where the presence of a third body of some kind, denoted by M, is required for the reaction to take place. Similarly, in chain initiation, a molecule may decompose to two free radicals, or it may require the presence of some other molecular species (for collision purposes) in order to react.

Table XI gives the resulting overall order of reaction for all possible combinations of μ-type and β-type radical terminations, simple and third body terminations, and first order and second order initiations.

TABLE XI

OVERALL REACTION ORDER DEPENDENCE

First order initiation		Second order initiation		
Simple Termination	Third body Termination	Simple Termination	Third body Termination	Overall Order
-	-	ββ	-	2
ββ	-	βμ	ββM	3/2
βμ	ββM	μμ	βμM	1
μμ	βμM	-	μμM	1/2
-	μμM	-	-	0

Note that Table XI agrees with the derivations presented above for two cases of propane decomposition. The first postulated mechanism was second order initiation and third body termination through reaction (VII) —— βμM —— and this led to an overall first order reaction. The

other mechanism was second order initiation and third body termination through reaction (VIII) —— $\beta\beta M$ —— and this led to an overall 3/2 order reaction.

The kinetic parameters for each of the free radical reactions (I) through (VIII) have been previously estimated and these results, tabulated by Laidler et al.,[29] are presented in Table XII.

TABLE XII

KINETIC PARAMETERS FOR FREE RADICAL REACTIONS

Reaction	A	E	$k_{600°C}$
I	9×10^{17}	67.2	13.3
II	1×10^{12}	10.0	3.2×10^{9}
III	1×10^{12}	8.2	8.85×10^{9}
IV	1×10^{13}	8.5	7.45×10^{10}
V	8×10^{13}	32.	1.39×10^{6}
VI	1.3×10^{14}	37.	7.12×10^{4}
VII	-	-	1.3×10^{19}
VIII	-	-	$1. \times 10^{18}$

Units of A and k are [sec^{-1}] and [$m\ell$/mole-sec] for first and second order reactions, respectively.

APPENDIX I

THE EFFECTS OF LONGITUDINAL DIFFUSION

The general differential equation for a first order reaction in a flow reactor with possible longitudinal diffusion is expressible, in one form, as

$$D \frac{d^2z}{d\ell^2} - u_\ell \frac{dz}{d\ell} + k(1-z) = 0 \qquad (38)$$

The equation used to describe the reaction kinetics in this study was equivalent to (at least for small conversions):

$$u_\ell \frac{dz}{d\ell} = k(1-z) \qquad (61)$$

Thus, the term describing the effect of diffusion, $D \frac{d^2z}{d\ell^2}$, has been neglected. If it can be shown that this term is negligible when compared to either of the terms in Equation (61), the omission of the diffusional term is justified.

Evaluation of these terms is simplified by the use of the reaction model as programmed on the analog computer. Figures 23 and 24 (in Section IV) illustrated the profiles of several important parameters along the length of the reactor for a typical run. The diffusional effect, if any, would tend to be greatest when $d^2z/d\ell^2$ is large (cf. Equation 38), so the profiles were examined at a point somewhat removed from the maximum temperature of the reactor.

At such a point (approximately 13 - 15 inches from the reactor inlet),

$$dz/d\ell \doteq 0.014 \text{ cm}^{-1} \; ; \; d^2z/d\ell^2 \doteq 0.002 \text{ cm}^{-2}$$

Levenspiel[32] has correlated the dimensionless group, $D/u_\ell D_e$ as a function of Reynolds number, where D_e is the equivalent diameter of the annular reactor.

For the conditions at this point,

$$Re \doteq 4500; \quad u_\ell \doteq 4000 \text{ cm/sec}; \quad D_e \doteq 0.08 \text{ cm}$$

and the diffusion coefficient $D \doteq 300 \text{ cm}^2/\text{sec}$.

Therefore, the ratio

$$\frac{D(d^2z/d\ell^2)}{u_\ell(dz/d\ell)} \doteq 0.01$$

and neglecting longitudinal diffusion introduces an error of only 1%.

APPENDIX J

COMPUTER PROGRAMS

It was shown that for a single reaction, the kinetic parameters were related by Equation (18)

$$A = \frac{\frac{FR^n}{s}\int_o^{z_e}\left[\frac{1 + N_o/F + z}{1 - z}\right]^n dz}{\int_o^L e^{-E/RT(\ell)}\left[\frac{P(\ell)}{T(\ell)}\right]^n d\ell} \qquad (18)$$

The upper integral in Equation (18) can be evaluated exactly for values of $n = 1.0, 1.5, 2.0$. However, it was simpler to evaluate it numerically by Simpson's rule (three point, parabolic fit).

Since the temperature profile was only known graphically, the lower integral had to be evaluated numerically. The profile was divided into a number of sections from which the recorded temperatures could be read easily, and a linear pressure profile was assumed (see Appendix E). Simpson's rule was then used for this integral also.

Flow diagrams for the several digital computer programs are shown in Figure 27. Figure 27a illustrates the program for Simpson's rule. The function SIMP. has four arguments: the two limits of the integral, the number of equidistant steps, and the function to be integrated.

$$\text{SIMP.}(\alpha,\beta,\gamma,\varphi) = \int_\alpha^\beta \varphi(t)dt$$

$$= \frac{\Delta}{3}\left[\varphi_o + 4\varphi_1 + 2\varphi_2 + 4\varphi_3 + 2\varphi_4 + \ldots + 4\varphi_{\gamma-1} + \varphi_\gamma\right]$$

where

$$\Delta = \text{step size} = \frac{|\beta - \alpha|}{\gamma}$$

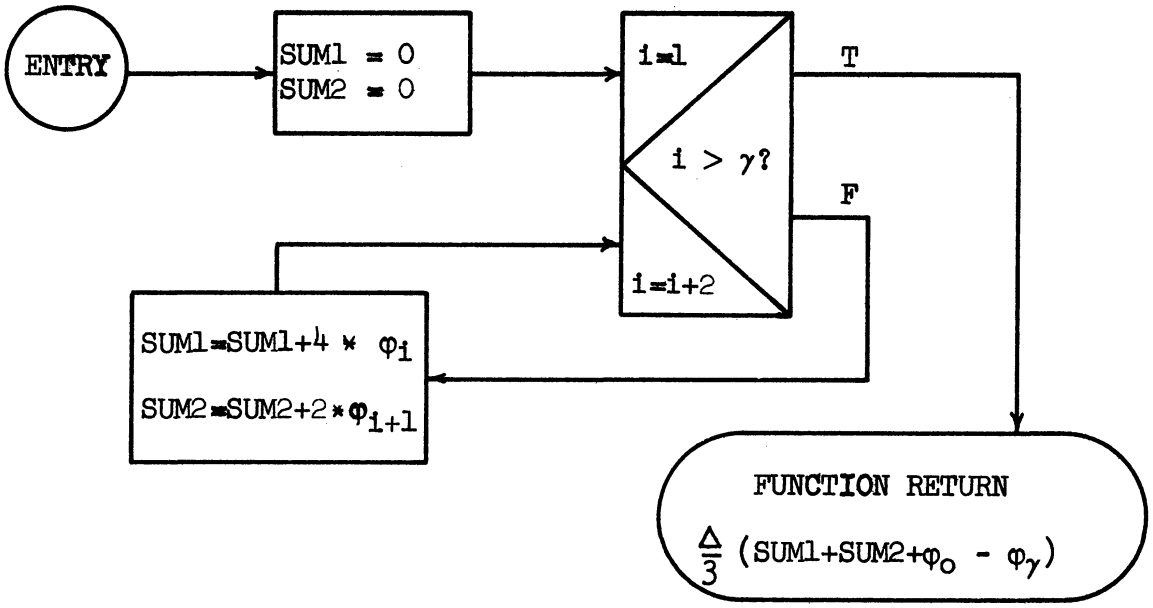

Figure 27a. Digital Computer Flow Diagram - Simpson's Rule

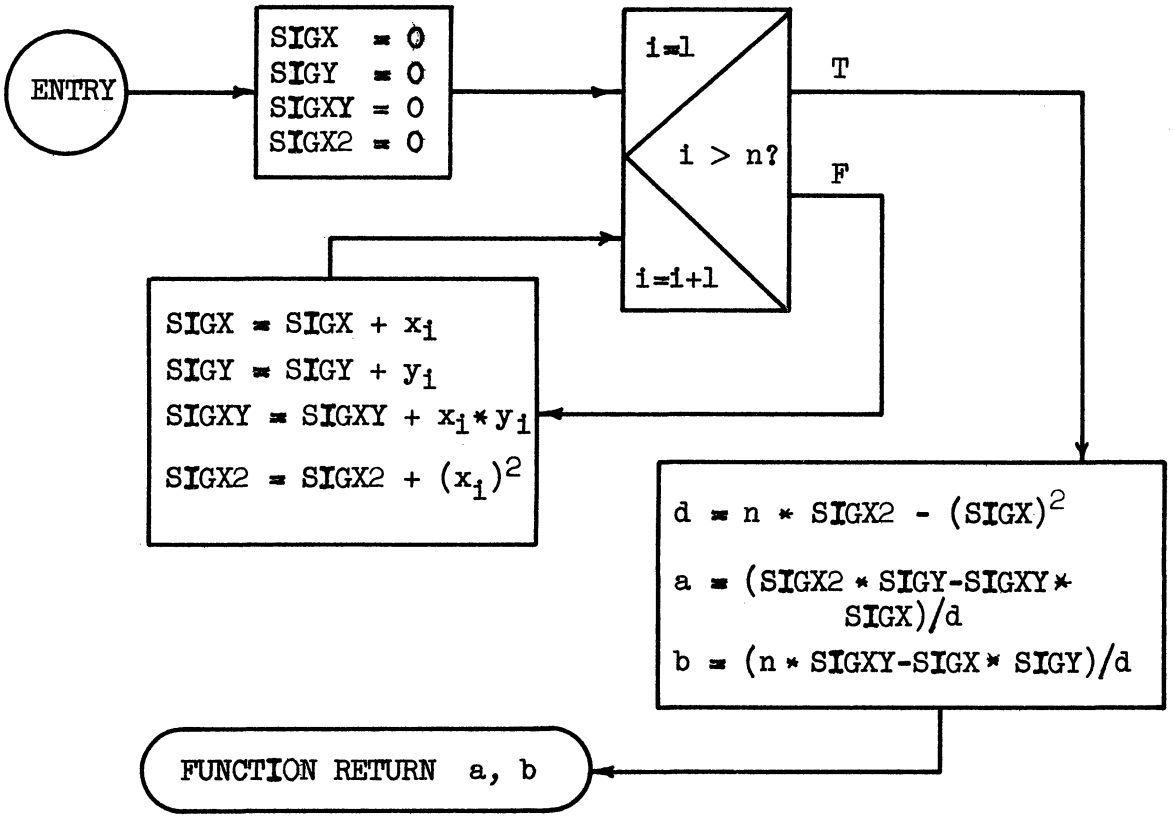

Figure 27b. Digital Computer Flow Diagram - Least Squares.

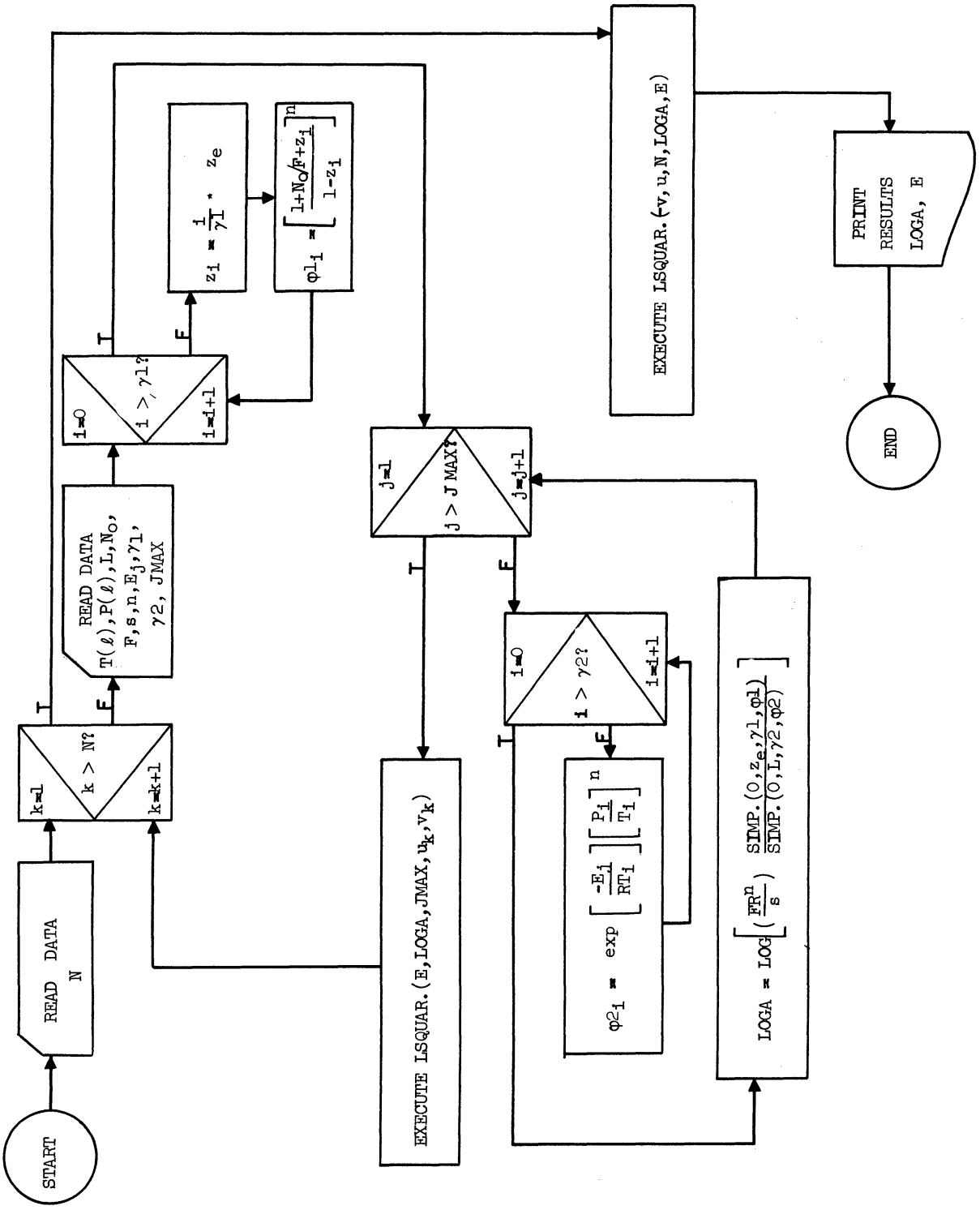

Figure 27c. Digital Computer Flow Diagram - Main Program.

Figure 27b represents the program for least squares analysis. The function LSQUAR. (x, y, n, a, b) gives, for a set of n data points (x_i, y_i), the best values of the constants a and b for a linear fit $y = a + bx$.

Figure 27c shows the main program, which evaluates A as a function of E from Equation (18). For each run, J_{max} values of E are assumed, the corresponding values of A are calculated, and the data are expressed as $\log A = u + vE$. Then, a least squares analysis is performed on all the runs simultaneously to yield the best values of A and E. Simpson's rule is used in the evaluation of both integrals in Equation (18); the number of steps used in the upper and lower integrals is represented by γ_1 and γ_2, respectively.

The analog computer program of the kinetic model was illustrated, in general form, in Figure 22. Equipment limitations and scaling problems prevented the use of that flow diagram exactly as shown. The method by which scaling problems were solved is given here for one run (Run 47) and the actual flow diagram is shown in Figure 28.

The differential equation to be solved was

$$\frac{dz}{d\ell} = \frac{sA}{FR} e^{-E/RT(\ell)} \left[\frac{P(\ell)}{T(\ell)}\right] \quad \left[\frac{1 - z}{1 + N_o/F + z}\right] \qquad (41)$$

Because of a lack of function multipliers, the term $e^{-E/RT(\ell)} \left[\frac{P(\ell)}{T(\ell)}\right]$ had to be calculated separately on a digital computer and was then fed in to the analog computer through the function generator (X-Y plotter). Substituting the experimental data, the unscaled equation becomes

$$\frac{dz}{d\ell} = 1.20 \times 10^8 \left[\frac{P(\ell)\ e^{-E/RT(\ell)}}{T(\ell)}\right] \quad \left[\frac{1 - z}{12.75 + z}\right]$$

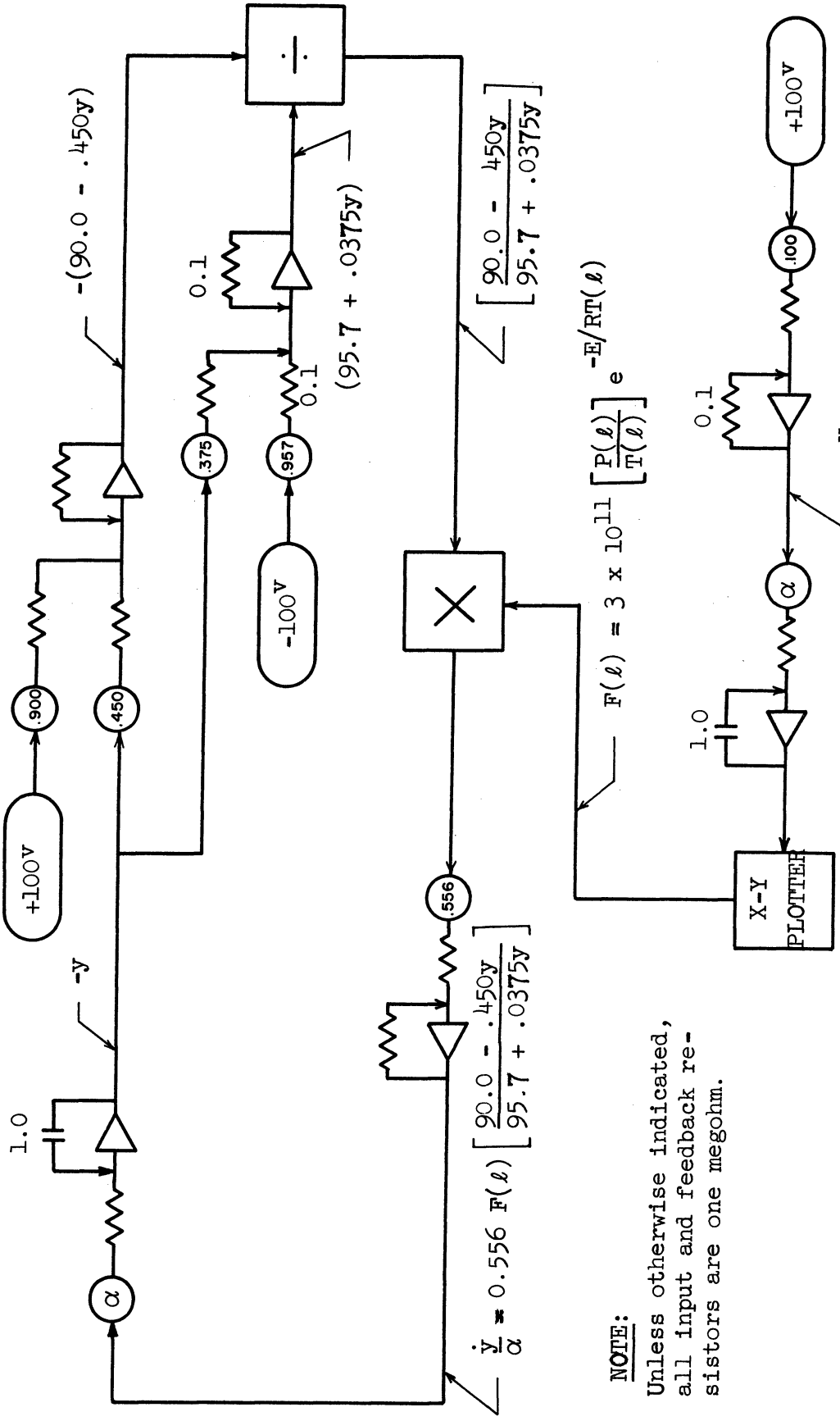

Figure 28. Analog Computer Flow Diagram - Run 47.

or

$$\frac{dz}{d\ell} = 0.0004 \left[3 \times 10^{11} \frac{P(\ell)\, e^{-E/RT(\ell)}}{T(\ell)} \right] \left[\frac{1 - z}{12.75 + z} \right]$$

where the first bracketed term in now in the range 0 - 100 volts. The anticipated exit conversion is approximately 0.4, so letting $y = 200\, z$,

$$\frac{dy}{d\ell} = 0.08 \left[3 \times 10^{11} \frac{P(\ell)\, e^{-E/RT(\ell)}}{T(\ell)} \right] \left[\frac{1 - 0.005\, y}{12.75 + 0.005\, y} \right]$$

$$= 0.08 \left[3 \times 10^{11} \frac{P(\ell)\, e^{-E/RT(\ell)}}{T(\ell)} \right] \left[\frac{7.5 - 0.0375\, y}{95.7 + 0.0375\, y} \right]$$

In setting the voltage scale on the X-Y plotter, it is convenient to make a change in independent variable consistent with the units and size of the generating graph. Letting $\tau = \ell/83.4$

$$\frac{dy}{d\tau} = 0.556 \left[3 \times 10^{11} \frac{P(\ell)\, e^{-E/RT(\ell)}}{T(\ell)} \right] \left[\frac{90.0 - 0.450\, y}{95.7 + 0.0375 y} \right] \quad (62)$$

The flow diagram for the solution of Equation (62) is shown in detail in Figure 28, although some of the sign changers used in conjunction with the function multipliers are omitted. In this program one unit is taken as 1 volt (not 100 volts, as is commonly done). The circles represent variable potentiometers with their settings for solution of Equation (62) in the centers of the circles; all input and feedback resistors are 1 megohm unless otherwise noted; the value of α can be varied at will —— only the speed of solution is affected.

APPENDIX K

SAMPLE CALCULATIONS

In this appendix, a sample calculation will be outlined for each of the important steps in the data analysis. These calculations will indicate how the calculated data (as tabulated in Appendix B) were obtained from the raw experimental data (Appendix A).

1) Product Distribution

The data of Run 35 will be used to illustrate the calculation of the product distribution (moles of product formed per mole of reacted propane) from the exit gas analysis.

The exit gas analysis for this run is shown in Table XIII.

TABLE XIII

PRODUCT DISTRIBUTION SAMPLE CALCULATIONS

Component	Exit Gas Analysis mole %	Material Balance		Moles of Product per Mole of Reacted Propane
		C	H	
H_2	0.245	-	0.490	0.536
CH_4	0.215	0.215	0.860	0.448
C_2H_6	0.008	0.016	0.048	0.020
C_2H_4	0.231	0.462	0.924	0.448
C_3H_8	6.476	-	-	-
C_3H_6	0.215	0.645	1.290	0.480
C_3H_4	0.011	0.033	0.044	0.032
N_2	92.6	-	-	-
		1.371	3.656	

A material balance performed on the products of decomposition shows that the ratio $H/C = \frac{3.656}{1.371} = 2.67$, as it is for pure propane $(8/3 = 2.67)$. Thus, no free carbon was formed in the pyrolysis and, on the basis of 100 moles of exit gas, the amount of reacted propane is $\frac{3.656}{8} = \frac{1.371}{3} = 0.457$ moles. Then, the number of moles of each product formed per mole of reacted propane can be calculated; for example, the production of hydrogen is $\frac{0.245}{0.457} = 0.536$. The percentage conversion of propane is $\frac{0.457}{6.476 + 0.457} = 6.6\%$.

These results may be found in Figure 11.

2) Order of Reaction Determination

In the determination of the orders of reaction, the differential reaction rates were plotted against the average propane mole fraction. Using Run 35 as an example once again, the rate of propane disappearance equals the number of moles of propane reacting per second —— or the inlet flow rate of propane minus the exit flow rate of propane. This may be easily calculated as

$$\text{rate} = \left[\frac{\text{moles of reacted } C_3H_8}{\text{moles of } C_3H_8 \text{ feed}}\right] \times \left[\frac{\text{moles of } C_3H_8 \text{ feed}}{\text{sec}}\right]$$

$$= z \times F$$

Where

z is the conversion of propane

and

F is the propane feed rate (see Table III)

Substituting the appropriate values,

$$\text{rate} = 0.066 \times (1.69 \times 10^{-4}) = 1.113 \times 10^{-5} \ \frac{\text{g-moles}}{\text{sec}}$$

The propane mole fraction at the reactor exit is read directly from the gas analysis (0.06476) and the inlet mole fraction is

$$X_{in} = \frac{6.476 + 0.457}{6.476 + 0.457 + 92.6} = 0.0698$$

The average mole fraction is 0.0673. This data point may be found in Figure 12.

3) Determination of Rate Parameters

For any experimental run, the kinetic parameters A and E are related by

$$A = \frac{\frac{FR^n}{s}\int_o^{z_e}\left[\frac{1 + N_o/F + z}{1 - z}\right]^n dz}{\int_o^L e^{-E/RT(\ell)}\left[\frac{P(\ell)}{T(\ell)}\right]^n d\ell} \qquad (18)$$

One method of determining the parameters is to solve Equation (18) simultaneously for two experimental runs. If Runs 58 and 60 are paired the important data are:

	Run 58	Run 60
F (g-moles/sec)	50.7×10^{-4}	1.01×10^{-4}
N_o (g-moles/sec)	25.2×10^{-4}	1.42×10^{-4}
z_e	0.386	0.086
P_i (mm Hg)	1001.	854.
P_e (mm Hg)	740.	740.
n	1.0	1.0
s (meters^2)	0.743×10^{-5}	0.743×10^{-5}
L (mm)	620	620
T_{max} (°K)	1228.3	1121.1

The temperature profiles are given in Table VIII and the pressure profiles are assumed to be linear.

The integrals in Equation (18) are evaluated by Simpson's rule and A is calculated for a series of values of E. It is found empirically that for each run, a linear relationship exists between log A and E.

Thus, for Run 58

$$\log A = 1.9448 + 0.18099\ E$$

and for Run 60,

$$\log A = 0.98464 + 0.19867\ E$$

Solving simultaneously,

$$A = 5.95 \times 10^{11};\quad E = 54.3$$

The rate constant ($k_{max} = Ae^{-E/RT_{max}}$) may be calculated at the maximum temperature of each run and plotted against that temperature on Arrhenius coordinates (log k vs. 1/T).

For Run 58, $k_{max} = 128.$

For Run 60, $k_{max} = 15.4$

These points can be found in Figure 13.

The best values of log A and E are obtained by an overall least squares analysis. The experimental data of each run is linearized in the form $\log A = u_i + v_i E$, as was done with Runs 58 and 60 above. A least squares analysis on u as a function of v yields,

$$\log A = 11.380,\quad E = 52.1$$

as the best values of the parameters over the entire temperature range. The equation $\log k = 11.380 - \frac{52.1}{2.3\ RT}$ represents the line in Figure 13.

4) Mixed Feed Runs

In the mixed feed runs, calculation of product distribution per mole of reacted propane was more difficult than in the single feed runs. This was true because propylene was fed in with the propane and the formation rates had to be calculated by material balance. In all these calculations, the ratio of propylene to propane in the feed could not be obtained by simply reading the rotameters because proportionally large errors would be introduced.

The data for Run 73 and some of the calculations are shown in Table XIV.

TABLE XIV

MIXED FEED SAMPLE CALCULATIONS

Component	Exit Gas Analysis mole %	Material Balance		Moles of Product per Mole of Reacted Propane
		C	H	
H_2	0.211	-	0.422	0.601
CH_4	0.153	0.153	0.612	0.436
C_2H6	0.058	0.116	0.348	0.165
C_2H_4	0.170	0.340	0.680	0.485
C_2H_2	0.070	0.140	0.140	0.199
C_3H_8	0.693	-	-	-
C_3H_6	0.220	0.660	1.320	0.286
N_2	98.4	-	-	-
		1.409	3.522	

Depending upon the ratio of propylene to propane in the feed, the material balance will yield a value of H/C between 2.00 and 2.67. In this case,

H/C = 2.50. Therefore, on a basis of 100 moles of gas leaving the reactor, if F_1 is the amount of propylene (C_3H_6) in the feed,

$$\frac{3.522 - 6F_1}{1.409 - 3F_1} = 2.67$$

and

$$F_1 = 0.119$$

Therefore, the propylene formed by propane decomposition is $0.220 - 0.119 = 0.101$.

On this basis, then, the amount of reacted propane is $\frac{3.522 - 6F_1}{8} = 0.351$, and the percentage conversion of propane is $\frac{0.351}{0.693 + 0.351} = 33.6\%$. Once the amount of reacted propane has been determined, the formation of each of the products per mole of reacted propane can be calculated. The results are shown in the last column of Table XIV and are plotted in Figure 20.

The rate constants for these runs were obtained by pairing each run independently with one of the low temperature runs —— Run 35.

Since there was wide variation in the maximum temperatures of these runs, the rate constants were all corrected to 1800°F = 1255.6°K. For example, T_{max} for Run 76 is 1792°F = 1251.1°K and $k_{max} = 99.2$ sec^{-1} . If the approximate value of the activation energy E is known,

$$\frac{k_1}{k_2} = e^{\frac{E}{R}\left(\frac{1}{T_2} - \frac{1}{T_1}\right)}$$

Therefore

$$k_{1800°} = k_{max} \exp\left[\frac{E}{R}\left(\frac{1}{T_{max}} - \frac{1}{T_{1800°}}\right)\right]$$

$$= 99.2 \exp\left[\frac{52.0}{1.987}\left(\frac{1}{1251.1} - \frac{1}{1255.6}\right)\right]$$

$$= 106.0$$

5) Miscellaneous Calculations

Many situations in this study called for the integration of an arbitrary function, and Simpson's rule was used in all cases. Simpson's rule is a three-point, parabolic integration; it states that if the value of a function, $\varphi(z)$, is known at three equidistant points, $\varphi(z_1)$, $\varphi(z_2)$, $\varphi(z_3)$, then

$$\int_{z_1}^{z_3} \varphi(z)dz = \frac{\Delta z}{3} [\varphi(z_1) + 4\varphi(z_2) + \varphi(z_3)]$$

where Δz is the spacing of points in the z-direction. All the numerical integrations were programmed for the digital computer.

The calculation of Reynolds numbers was important in determining pressure profiles and diffusional effects. For gas flowing through an annulus, the Reynolds number is

$$Re = \frac{D_e G}{\mu}$$

where

D_e is the equivalent diameter

For non-circular cross-sections, the equivalent diameter is 4 x (cross-sectional area)/(wetted perimeter). In an annulus with inner diameter D_1 and outer diameter D_2

$$D_e = \frac{4\pi(D_2^2 - D_1^2)/4}{\pi(D_2 + D_1)} = D_2 - D_1$$

Because of the variation of viscosity with temperature, the Reynolds number was not constant throughout the reactor for any run. For an intermediate temperature, 1600°F, of Run 57,

$$D_e = \frac{1}{32}'' = 0.0026 \text{ ft.}$$

$$s = \frac{\pi}{4}(D_2^2 - D_1^2) = \frac{\pi}{4}\left[\left(\frac{1}{4}\right)^2 - \left(\frac{7}{32}\right)\right]^2 \quad in^2$$

$$= 8 \times 10^{-5} \quad ft^2$$

$$G = \frac{[57.0(28) + 0.82(44)] \times 10^{-4} \frac{g}{sec} \times \frac{3600}{454}}{8 \times 10^{-5} \quad ft^2}$$

$$= 16{,}200 \quad \frac{lb}{hr \quad ft^2}$$

$$\mu = 0.045 \text{ cp} = 0.109 \frac{lb}{hr \text{ ft}}$$

and

$$Re = \frac{D_e G}{\mu} = \frac{0.0026(16{,}200)}{0.109} = 3900$$

Over the range of flow rates and temperatures in this study, Reynolds numbers usually were between 3500 and 7000.

When the rate parameters were obtained by an overall least squares fit of the data, the standard deviations of the pre-exponential factors were calculated. For the i-th run, the deviation Δ_i = Log A - $(u_i + v_i E)$ where u and v are the empirically fit linear constants for any run. For each of the reactions studied the standard deviation over all the runs was $\pm$20%.

Then, on an Arrhenius plot, the effect of a 20% change in the intercept of the line (pre-exponential factor) upon the slope of the line (activation energy) was noted. In all cases the deviation was $\pm$5% and that was taken as the activation energy standard deviation.

APPENDIX L

THE COMPENSATION EFFECT

In solving the rate equations, it was found that for any experimental run, log A was a linear function of E. That is, the rate equation was satisfied by infinite combinations of activation energies and pre-exponential factors and no single solution could be obtained; however, all these combinations were linearly related.

This phenomenon has often been observed previously, primarily in the area of heterogeneous kinetics. There, log A is a linear function of the activation energy for a given reaction over a wide range of catalysts; even more surprising, it is also observed for a given catalyst over an entire family of reactions.[9] Although this effect can likewise take place in homogeneous reactions, the instances are not as plentiful because variation of one of the experimental parameters is not as easily achieved.

A very brief description of the consequences of the compensation effect will be given here; a good review along with some possible explanations has been presented by Bond.[7] Although very many explanations have been offered, no satisfactory basis for this effect has been found. Indeed, many feel that there is no single general explanation for this behavior.

The compensation effect (also known as the Theta Rule) gets its name from the fact that if log A increases linearly with E, there can be very large variations of both the activation energy and the pre-exponential factor with relatively small changes in the rate

constant, $k = Ae^{-E/RT}$. Furthermore, there is always one temperature for which compensation is so complete, that no matter what value of E (and corresponding value of A), the rate constant does not change.

If $\log A = u + vE$, let u be replaced by $\log A_o$ and v by $\frac{1}{2.3\ R\Theta}$, where A_o and Θ are arbitrary constants. Then, the rate constant $k = Ae^{-E/RT}$ becomes

$$k = A_o e^{-\frac{E}{R}\left(\frac{1}{T} - \frac{1}{\Theta}\right)}$$

Thus, at temperature $T = \Theta$, the rate constant is no longer a function of the activation energy E or the pre-exponential factor A. At temperatures in the vicinity of $T = \Theta$, variation of A and E still change the rate constant only slightly.

Many attempts have been made to explain this strange behavior. One interpretation assumes that in the catalysis, the active surface is itself heterogeneous; that is, the activation energy is not constant across the surface. Such an assumption leads to a rate constant in which the pre-exponential factor is a function of the activation energy. However, the original assumption of a heterogeneous surface is of questionable validity.

A second possible explanation is that the true activation energies and pre-exponential factors are temperature dependent. They are then related to the apparent parameters by

$$E_{APP} = RT \text{ Ln } A_{APP} + (E_{TRUE,T} - RT \text{ Ln } A_{TRUE,T})$$

From this hypothesis, it can be shown that the apparent pre-exponential factor is the required function of activation energy to produce compensation. However, there is no physical indication that the true parameters are actually temperature dependent.

For heterogeneous catalysis, a third explanation which has been offered is that compensation arises because of a relationship between the enthalpies and entropies of adsorption. This then causes the dependence of log A upon E.

All of these theories are outlined in greater detail by Bond.[7] He also gives additional references to these and other aspects of the compensation effect.

Observation of the compensation effect in hydrocarbon cracking was made by Boudart[8] in analyzing the data of Franklin and Nicholson.[17] They had studied the cracking of propane, iso-butane, iso-pentane, etc., on a silica-alumina catalyst.

NOMENCLATURE

A	Pre-exponential factor (liters^{n-1}/g-mole^{n-1} · sec) where n is the order of reaction
C	Concentration (g-moles/cm^3)
D	Diffusion coefficient (cm^2/sec)
D_e	Equivalent diameter (cm)
E	Activation energy (Kcal/g-mole)
ΔF_f^o	Standard state free energy of formation (Kcal/g-mole)
F	Hydrocarbon feed rate (g-moles/sec)
f	Friction factor
G	Mass flow rate (lb/hr-ft^2)
ΔH_f^o	Standard state heat of formation (Kcal/g-mole)
I	Intensity of mass spectrometer peak (divisions)
K_p	Equilibrium constant, pressure units
k	Rate constant (same units as A)
k_{max}	Rate constant at maximum temperature (same units as A)
L	Total reactor length (mm)
ℓ	Reactor length (mm)
$\overline{MW}$	Average molecular weight
m	Flow rate of any component (g-moles/sec)
N	Number of experimental runs
N_o	Feed rate of diluent (g-moles/sec)
n	Order of reaction
P	Pressure (mm Hg)
P_i	Reactor inlet pressure (mm Hg)
P_e	Reactor exit pressure (mm Hg)

R	Gas constant $\left(\frac{\text{liters - mm Hg}}{\text{g-mole - °K}}\right)$ or (Kcal/g-mole - °K)
Re	Reynolds number
ΔS_f^o	Standard state entropy of formation (cal/g-mole - °K)
s	Reactor cross-sectional area (meters^2)
T	Temperature (°K)
T_{max}	Maximum temperature (°K)
T_{eq}	Reactor equivalent temperature (°K)
t	Time (sec)
u_ℓ	Linear Velocity (cm/sec)
u_i	Empirical constant
V	Reactor volume (liters)
v_i	Empirical constant
x	Mole fraction
$\bar{x}$	Average mole fraction
y	Fractional conversion
z	Fractional conversion
z_e	Reactor exit fractional conversion
β, δ	Fraction of total conversion to specific products
Δ	Deviation
Θ	Temperature (°K)
μ	Partial pressure in mass spectrometer samples (microns)
μ	Viscosity (lb/hr-ft)
ρ	Density (lb/ft^3)
σ	Sensitivity of components in mass spectrometer (divisions/micron)
τ	Analog computer time (sec) or (volts)
φ, ψ	Arbitrary functions

BIBLIOGRAPHY

1. Akin, G. A., T. F. Reid, and R. J. Schrader, Chem. Eng. Prog., 54, No. 1, 41 (1958).

2. API Research Project No. 44, Catalog of Mass Spectral Data, Carnegie Institute of Technology, 1959.

3. ASTM Technical Publication No. 109A, Physical Constants of Hydrocarbons C_1 to C_{10}, ASTM, Philadelphia.

4. Benson, S. W., The Foundations of Chemical Kinetics, McGraw-Hill, New York, 1960.

5. Bixler, G. H. and C. W. Coberly, Ind. Eng. Chem., 45, 2596 (1953).

6. Blackmore, D. R. and C. N. Hinshelwood, Proc. Roy. Soc. (London), A268, 36 (1962).

7. Bond, G. C., Catalysis by Metals, Academic Press, New York, 1962.

8. Boudart, M., Advances in Catalysis, IX, 636 (1957).

9. Boudart, M., Chem. Eng. Prog., 57, No. 8, 33 (1961).

10. Calderbank, P. H., V. P. Hovnanian and I. D. Talbot, J. Appl. Chem., 7, 425 (1957).

11. Deansley, R. M. and C. H. Watkins, Chem. Eng. Prog., 47, 134 (1951).

12. Dunsten, A. E., ed., The Science of Petroleum, Section 30: "Gas Pyrolysis and Polymerization," Oxford Press, London (1938).

13. Eastwood, S. C. and A. E. Potas, Pet. Eng., 19, 43 (Aug., 1948).

14. Egloff, G., Reactions of Pure Hydrocarbons, Reinhold, New York, 1939.

15. Eltenton, G. C., J. Chem. Phys., 15, 465 (1947).

16. Farnsworth, J. F., M. Manes, G. V. McGurland, and G.M. Bretz, Ind. Eng. Chem., 47, 1517 (1955).

17. Franklin, J. L. and D. E. Nicholson, J. Phys. Chem., 60, 59 (1959).

18. Frey, F. E. and W. F. Huppke, Ind. Eng. Chem., 25, 54 (1933).

19. Frey, F. E. and D. F. Smith, Ind. Eng. Chem., 20, 948 (1928).

20. Frost, A. and R. Pearson, Kinetics and Mechanism, 2nd ed., Wiley, New York, (1961).

21. Goldfinger, P., M. Letort and M. Niclause, 1948, Volume Commémoratif Victor Henri: Contribution à l'Etude de la Structure Moléculaire, p. 283, Liège: Desoer.

22. Greene, E. F., R. L. Taylor and W. L. Patterson, J. Phys Chem., 62, 238 (1958).

23. Hepp, H. J. and F. E. Frey, Ind. Eng. Chem., 45, 410 (1953).

24. Hobbs, J. E. and C. N. Hinshelwood, Proc. Roy. Soc. (London), A167, 447 (1938).

25. Ingold, K. U. and F. J. Stubbs, J. Chem. Soc., p. 1749 (1951).

26. Kinney, R. E. and D. J. Crowley, Ind. Eng. Chem., 46, 258 (1946).

27. Kistiakowsky, G. B. and A. G. Nickle, Disc. Far. Soc., 10, 175 (1951).

28. Kossiakoff, A. and F. O. Rice, J. Am. Chem. Soc., 65, 590 (1943).

29. Laidler, K. J., N. H. Sagert and B. W. Wojciechowski, Proc. Roy. Soc. (London), A270, 242 (1962).

30. Laidler, K. J. and B. W. Wojciechowski, Proc. Roy. Soc. (London), A259, 257 (1960).

31. Lee, E. H. and G. D. Oliver, Ind. Eng. Chem., 51, 1351 (1959).

32. Levenspiel, O., Chemical Reaction Engineering, Wiley, New York, 1962.

33. Linden, H. R. and R. E. Peck, Ind. Eng. Chem., 47, 2470 (1955).

34. Marek, L. F. and W. B. McCleur, Ind. Eng. Chem., 23, 878 (1931).

35. Martin, R., M. Dzierzynski and M. Niclause, J. Chimie Physique, 61, 286 (1964).

36. Medvedeva, N. I., M. B. Neiman, E. S. Torsueva and I. P. Kravchuk, Russ. J. Phys. Chem., 34, 1307 (1960).

37. Medvedeva, N. I., M. B. Neiman and E. S. Torsueva, Russ. J. Phys. Chem., 36, 529 (1962).

38. Miller, I. F., University of Michigan Industry Program, Report IP-392, October 1959 (Ph.D. Thesis, University of Michigan).

39. Myers, P. S. and K. M. Watson, Nat. Pet. News, 38, R388 (1946).

40. Neiman, M. B., Int. J. Appl. Radiation Isotopes, 3, 20 (1958).

41. Partington, R. G., Disc. Far. Soc., 2, 114 (1947).

42. Paul, R. E. and L. F. Marek, Ind. Eng. Chem., 26, 454 (1934).

43. Peard, M. G., F. J. Stubbs and C. N. Hinshelwood, Proc. Roy. Soc. (London), A214, 471 (1952).

44. Pease, R. N., J. Am. Chem. Soc., 50, 1779 (1928).

45. Peirce, B. and R. Foster, A Short Table of Integrals, 4th ed., Ginn and Co., Boston, 1956.

46. Poltorak, V. A. and V. V. Voevodskii, Doklady Akad. Nauk, S.S.S.R., 91, 589 (1953).

47. Poltorak, V. A., L. Y. Leitis and V. V. Voevodskii, Russ. J. Phys. Chem., 33, 379 (1959).

48. Pretsch, H., Erdöl u. Kohle, 10, 666 (1957).

49. Reid, J. M. and H. R. Linden, Chem. Eng. Prog., 56, 47 (1960).

50. Rice, F. O. and K. F. Herzfeld, J. Am. Chem Soc., 56, 285 (1934).

51. Rice, F. O. and O. L. Polly, J. Chem. Phys., 6, 273 (1938).

52. Rice, F. O. and O. L. Polly, Trans. Far. Soc., 35, 850 (1939).

53. Rice, F. O. and E. Teller, J. Chem. Phys., 6, 489 (1938).

54. Rice, F. O. and R. E. Varnerin, J. Am. Chem. Soc., 76, 324 (1954).

55. Rossini, F. D., ed., API Research Project No. 44, Selected Values of Physical and Thermodynamic Properties of Hydrocarbons and Related Compounds, Carnegie Press, 1953.

56. Schutt, H. C., Chem. Eng. Prog., 55, 68 (Jan., 1959).

57. Steacie, E. W. R. and N. A. D. Parlee, Trans Far. Soc., 35, 854 (1939).

58. Steacie, E. W. R. and I. E. Puddington, Can. J. Res., B16, 411 (1938).

59. Stubbs, F. J. and C. N. Hinshelwood, Proc. Roy. Soc. (London), A200, 458 (1950); A201, 18 (1950); A203, 486 (1950).

60. Szwarc, M., J. Chem. Phys., 17, 284 (1949).

61. Towell, G. D., University of Michigan Industry Program, Report IP-454, September 1960 (Ph.D. Thesis, University of Michigan).

62. Towell, G. D. and J. J. Martin, A.I.Ch.E. Journal, 7, 693 (1961).

63. Tropsch, H., C. I. Parrish and G.Egloff, Ind. Eng. Chem., 28, 581 (1936).

64. Voevodsky, V. V., Trans. Far. Soc., 55, 65 (1959).

65. Wojciechowski, B. W. and K. J. Laidler, Can. J. Chem., 38, 1027 (1960).

UNIVERSITY OF MICHIGAN
3 9015 03023 8623

THE UNIVERSITY OF MICHIGAN

DATE DUE